8-2016

# DEFINING THE FUNCTIONS OF USP22 AND USP44 IN REGULATION OF H2BUB1 LEVELS

xianjiang Lan

**DEFINING THE FUNCTIONS OF USP22 AND USP44 IN REGULATION OF H2BUB1 LEVELS**

**BY**

**Xianjiang Lan, Ph.D. Candidate**

**APPROVED:**

_____

Sharon Y.R. Dent, Ph.D., Supervisory Professor

_____

Rick A. Finch, Ph.D.

_____

Mark T. Bedford, Ph.D.

_____

Xiaobing Shi, Ph.D.

_____

Taiping Chen, Ph.D.

APPROVED:

_____

Dean, The University of Texas
Graduate School of Biomedical Sciences at Houston

# DEFINING THE FUNCTIONS OF USP22 AND USP44 IN REGULATION OF H2BUB1 LEVELS

A

Dissertation

Presented to the Faculty of

The University of Texas Health Science Center at Houston

And

The University of Texas M.D. Anderson Cancer Center

Graduate School of Biomedical Sciences

in Partial Fulfillment

of the Requirements

for the degree of

DOCTOR OF PHILOSOPHY

By

Xianjiang Lan, Ph.D. Candidate

Houston, Texas

Aug 2016

## DEDICATION

This dissertation is dedicated to the following individuals:

My parents for giving me unlimited support and love

My wife for giving me unlimited understanding and care

My daughter for giving me unlimited motivation

**ACKNOWLEDGEMENTS**

First of all, I would like to thank my mentor, Dr. Sharon Dent, for giving me the opportunity to join her lab as a graduate student, spending time on training me and greatly helping me achieve my scientific goals. She teaches me how to critically think about science, how to address scientific questions and issues, and how to succeed in graduate school. I also thank her in every possible way for her precious time in helping with my project, answering my questions and polishing my scientific manuscript, dissertation and many write-ups during the course of my Ph.D.

I also want to thank my advisory committee members, Dr. Mark Bedford, Dr. Taiping Chen, Dr. Rick Finch, Dr. Xiaobing Shi and Dr. Donna Kusewitt who provided important suggestions and comments for my projects. I particularly want to thank Dr. Mark Bedford and Dr. David Johnson for providing me the opportunities to rotate in their labs, where I learned a lot of experimental skills under the great guidance of Dr. Yanzhong Yang and Dr. Renier Velez-Cruz. Dr. Taiping Chen who I treat more as a friend, gave me a lot of help not only for research but also for life.

My success in graduate school would not have happened without the help and support of my lab members. Dr. Evangelia Koutelou taught me a lot of experimental skills and helped me a lot with my projects. Dr.Boyko Atanassov, another excellent post-doc in the lab, provided me a lot of help and suggestions for my projects. I also would like to thank Andria Schibler for teaching me the molecular biology basics during my first lab rotation in the Dent lab. Andrew Salinger, Amanda Martin and Xianghong Kuang helped me a lot with my mouse project. Wenqian Li, Aimee Farria and Li Wang gave me a lot of help for exams, projects and life.

I also would like to thank all Chinese folks and Basketball teammates, who made my life more relaxed.

Finally, I want to thank my family without whose support, I could not have succeed for my Ph.D.

**DEFINING THE FUNCTIONS OF USP22 AND USP44 IN REGULATION OF H2BUB1 LEVELS**

Xianjiang Lan, Ph.D. Candidate

Supervisory Professor: Sharon Dent, Ph.D.

Aberrant levels of histone ubiquitination are involved in various human diseases including neurodegenerative disorders and cancers. Particularly, Histone H2B monoubiquitination (H2Bub1) is highly associated with gene regulation in both normal cells and diseases. Many deubiquitinases (mainly USPs) are defined to regulate global H2Bub1 levels. However, how these USPs are regulated and how they contribute to diseases are not well understood.

USP22, part of the deubiquitination module (DUBm) in the SAGA complex, is a well-defined regulator of H2Bub1 levels. ATXN7, another crucial subunit of the SAGA DUBm, is involved in a neurodegenerative disease, spinocerebellar ataxia type 7 (SCA7), due to a polyglutamine (polyQ) expansion in its N-terminal region. Given the allosteric regulation of USP22 DUB activity within the DUBm, whether and how the polyQ expansion in ATXN7 affects SAGA DUB activity was not known. To address this question, we reconstituted the SAGA DUBm in vitro with wild type ATXN7 or the ATXN7polyQ mutant. We found that the DUBm has minimal activity in the absence of ATXN7. ATXN7-92Q, which corresponds to a pathogenic form of the protein, is largely insoluble unless it is incorporated into the DUBm. Importantly, we demonstrated that ATXN7-92Q enhances DUB activity to a similar extent as WT ATXN7. Consistent with these in vitro results, co-overexpression of DUBm components in human astrocytes promotes the solubility of ATXN7-92Q, and greatly inhibits its aggregation into nuclear inclusions that sequester other DUBm components including ATXN7L3, leading to global increases in H2Bub levels. Co-overexpression of ATXN7L3 and ENY2 with ATXN7-92Q reverses this effect. Finally, we found that global H2Bub levels are increased in

cerebellums taken from a SCA7 mouse model, consistent with reduced DUB activity in the presence of ATXN7 polyQ mutant. Taken together, our study suggests that ATXN7-polyQ expansions do not change the biochemical activity of the DUBm, but they likely contribute to SCA7 by initiating aggregate formation that sequesters DUBm components away from H2B and other substrates. To further study the contribution of the DUB activity of USP22 to SCA7 disease, we also planned to delete USP22 in Purkinje cells and Bergman glia, both of which are involved in the pathogenesis of SCA7 disease, through establishing a FloxP-Usp22 mouse model. We generated Usp22FloxFRT mice by in vitro fertilization using sperm obtained from the Knock Out Mouse Project (KOMP). After crossing with FLpase mice, we obtained the Usp22Flox mouse model. Currently, we are crossing Usp22Flox mice with Pcp2-Cre and GFAP-Cre mice, which will specifically delete Usp22 in Purkinje cells and Bergman glia, respectively. We will analyze the potential “Ataxia” phenotypes of the mice with Usp22 deletion in Purkinje cells or Bergman glia.

Similar to USP22, USP44 is also involved in H2Bub1 regulation. The USP44 deubiquitinase is implicated in various biological processes including ES cell differentiation, DNA damage repair, and cancer development. However, USP44 alone is not active, and whether USP44 directly deubiquitinates histone H2B and what other partners are required for its DUB activity are not known. Using tandem affinity purification and Multidimensional Protein Identification Technology (MudPIT), we identified USP44 as an integral subunit of the Nuclear receptor co-repressor complex (N-CoR complex). As part of N-CoR, USP44 deubiquitinates H2B in vitro and in vivo. Depletion of USP44 impairs the repressive activity of N-CoR complex targeted to a chromatinized luciferase reporter. ChIP-qPCR experiments indicate that USP44 is recruited to the promoter of luciferase reporter, leading to decreased H2Bub levels. These data indicate that USP44 and HDAC3 work together within N-CoR, to repress

transcription of target genes. Furthermore, USP44 expression is higher, and H2Bub1 levels are lower, in MDA-MB-231 triple negative breast cancer cells than in MCF-10A cells. Depletion of USP44 impairs invasiveness of MDA-MB-231 cells in vitro and leads to an increase of global H2Bub1 levels, as does depletion of another essential subunit of NCoR, TBL1XR1. Together, our findings indicate that USP44 and N-CoR may contribute to metastatic behaviors of triple negative breast cancer cells.

In summary, both USP22 and USP44 participate in multiple biological processes through modulating H2Bub1 levels and defective activity of these DUBs likely contributes to various human diseases. Our data highlight the importance of appropriate DUB activity and H2Bub1 levels for normal cell growth and behavior.

## TABLE OF CONTENTS

**APPROVAL PAGE**

**TITLE PAGE**

**DEDICATION** i

**ACKNOWLEDGEMENTS** ii

**ABSTRACT** iv

**TABLE OF CONTENTS** vii

**LIST OF FIGURES** xi

**LIST OF TABLES** xiii

**LIST OF ABBREVIATIONS** xiv

**Chapter 1: Introduction** ..... **1**

**1.1 DUBs** ..... **1**

1.1.1 USP22 and USP44 ..... 1

**1.2 Histone modifications** ..... **4**

**1.3 PolyQ diseases** ..... **6**

1.3.1 SCA7 disease and SAGA complex ..... 8

1.4 H2Bub1 and Cancer ..... 11

**Chapter 2: Materials and Methods** ..... **13**

**2.1 Plasmids** ..... **13**

**2.2 Antibodies** ..... **14**

**2.3 Cell lines** ..... **14**

**2.4 Baculovirus expression system** ..... **17**

**2.5 Protein purification from Baculovirus system** ..... **17**

**2.6 Gel filtration ..... 18**

**2.7 In vitro deubiquitination assay ..... 19**

**2.8 Preparation of cell lysates ..... 19**

**2.9 Immunoprecipitation (IP) ..... 20**

**2.10 Western blot analyses ..... 21**

**2.11 Nuclear extract preparation, affinity purification for gel filtration, deubiquitination assay or MudPIT analysis ..... 21**

**2.12 *In vitro* binding assay ..... 24**

**2.13 Histone purification from ATXN7 Wild-type and mutant adult mouse cerebellums ..... 24**

**2.14 Immunofluorescence microscopy ..... 25**

**2.15 Transfection and lentiviral infection ..... 25**

**2.16 Stable cell lines generation ..... 25**

**2.17 Subcellular fractionation ..... 26**

**2.18 Quantitative RT-PCR analysis ..... 27**

**2.19 ChIP-qPCR ..... 27**

**2.20 Luciferase activity assay ..... 29**

**2.21 Transwell invasion assay ..... 30**

**2.22 Mice ..... 30**

**Chapter 3: PolyQ expansions in ATXN7 affect solubility but not activity of the SAGA deubiquitinating module ..... 33**

**3.1 Solubility of ATXN7 polyQ is increased by incorporation into the DUBm ..... 33**

**3.2 ATXN7 enhances DUB activity *in vitro* ..... 39**

**3.3 PolyQ ATXN7 does not impair the assembly or activity of the DUBm *in vitro* ..... 47**

**3.4 ATXN7-92Q aggregates sequester DUBm components *in vivo* .....54**

**3.5 Increased solubility of ATXN7-92Q rescues DUB activity *in vivo* .....58**

**3.6 Conclusions.....63**

**3.7 Discussion .....63**

3.7.1 Nuclear aggregates caused by polyQ expansions are cytotoxic.....64

3.7.2 Associations with other subunits of DUBm improves the solubility of ATXN7-92Q .....65

3.7.3 Nuclear aggregates caused by ATXN7-polyQ sequester both enzymatic subunits of SAGA complex .....66

**Chapter 4: Defining the role of *Usp22* in SCA7 disease through establishing a *Usp22* conditional knockout mouse model .....68**

**4.1 Establishment of *USP22* conditional knockout mouse.....68**

**4.2 Future directions .....69**

**Chapter 5: USP44 is an integral component of N-CoR that contributes to target gene repression by modulating H2Bub1 levels .....73**

**5.1 USP44 is a subunit of the N-CoR complex .....73**

**5.2 USP44 interacts directly with WD40 repeats in TBL1X and TBLXR1 .....80**

**5.3 USP44 deubiquitinates H2Bub1 as part of N-CoR.....83**

**5.4 USP44 enhances the repressive activity of N-CoR .....87**

**5.5 USP44-N-CoR complex links H2Bub1 to invasiveness of triple negative breast cancer cells .....90**

**5.6 Conclusions.....95**

**5.7 Discussion and future directions .....95**

5.7.1 USP44-NCOR1 complex is a multiple enzymatic subunits containing complex .....96

5.7.2 USP44-NCOR1 complex is involved in the regulation of breast cancer development....98

**Chapter 6: Discussion ....100**

**Chapter 7: Future studies ....102**

**7.1 Identifying the role of Usp22 in SCA7 disease using *Usp22* conditional knock-out mouse....102**

**7.2 Identifying the USP44-N-CoR complex gene targets involved in breast cancer aggressiveness ....103**

**8. References....105**

**9. Vita ....115**

## LIST OF ILLUSTRATIONS

Figure 1: Phylogenetic analysis of human DUBs. ..... 3

Figure 2: Histone post-translational modifications. ..... 5

Figure 3: SAGA complex is very conserved from yeast to mammals. ..... 10

Figure 4: Ubiquitin ligases and deubiquitinating enzymes responsible for monoubiquitination of histones H2A and H2B. ..... 12

Figure 5: Reconstitution of the mammalian DUBm. ..... 36

Figure 6: In vitro binding assay shows USP22 directly interacts with ATXN7 or ATXN7L3, but not with ENY2 ..... 38

Figure 7: Reconstitution of mammalian DUBm sub-complex. ..... 41

Figure 8: ATXN7-24Q NT promotes robust DUB activity of the DUBm *in vitro*. ..... 44

Figure 9: Both ATXN7L3 and ENY2 are required for the activation of DUB activity of USP22 and ATXN7 further stimulates the DUB activity of DUBm. ..... 45

Figure 10: Increased incorporation of ATXN7-92Q into DUBm promotes DUBm activity. ..... 49

Figure 11: ATXN7-92Q NT is not defective in promoting DUBm activity. ..... 51

Figure 12: Overexpression of ATXN7L3 and ENY2 prevents sequestration of ATXN7L3 into aggregates with ATXN7-92Q in vivo. ..... 56

Figure 13: Solubility of ATXN7-92Q *in vivo* correlates with DUB activity. ..... 60

Figure 14: Establishment of *Usp22* conditional knockout mouse. ..... 71

Figure 15: Recombinant USP44 alone is not active and interaction with CETN2 does not affect the DUB activity of USP44. ..... 76

Figure 16: USP44 associates with N-CoR complex. ..... 77

Figure 17: USP44 mainly associates with chromatin in the nucleus, together with N-CoR subunits. ..... 79

Figure 18: WD40 repeats of TBL1X/R1 are required for the association of USP44 with N-CoR complex. ..... 81
Figure 19: Recombinant USP44 interaction with TBL1X and/or TBL1XR1, and/or PSMC5 does not affect the DUB activity of USP44. ..... 82
Figure 20: USP44-N-CoR complex deubiquitinates H2B in vivo and in vitro. ..... 84
Figure 21: FH-TBL1X-N-CoR complex purification from 293T cells. ..... 86
Figure 22: USP44 facilitates the repressive activity of N-CoR complex through deubiquitinating H2B. ..... 88
Figure 23: USP44 regulates the invasiveness of breast cancer cells. ..... 91
Figure 24: Ablation of TBL1XR1 impairs the invasiveness of MDA-MB-231 cells. ..... 93
Figure 25: Model of the function of USP44-N-CoR complex in cells. ..... 94

## LIST OF TABLES

Table 1: Polyglutamine diseases ..... 7

Table 2: Antibodies used in this study ..... 16

Table 3: Primers used for PCR ..... 32

Table 4: Primers used for RT-qPCR and ChIP-qPCR ..... 32

## LIST OF ABBREVIATIONS

| | |
|---|---|
| DMEM | Dulbecco's Modified Eagle Medium |
| DRPLA | Dentatorubral-pallidoluysian atrophy |
| DTT | Dithiothreitol |
| DUB | Deubiquitinase |
| DUBm | Deubiquitinase module |
| EGF | Epidermal growth factor |
| ES | Embryonic Stem |
| FBS | Fetal bovine serum |
| HAT | Histone acetyltransferase |
| HD | Huntington's Disease |
| IP | Immunoprecipitation |
| kDa | Kilodalton |
| $\alpha$-MEM | Minimum Essential Medium alpha |
| MJD | Machado-Joseph Disease Protein Domain Protease |
| MudPIT | Multidimensional Protein Identification Technology |
| NE | Nuclear Extract |
| OTU | Ovarian Tumor Protease |
| PBS | Phosphate-buffered saline |
| PI | Protease inhibitors |
| PMSF | Phenylmethylsulfonyl fluoride |
| PolyQ | polyglutamine tract |
| PTM | Post translational modification |
| qPCR | Quantitative polymerase chain reaction |

| | |
|---|---|
| RIPA | Radioimmunoprecipitation assay |
| SAGA | Spt-Ada-Gcn5-Acetyltransferase |
| SBMA | Spinal and Bulbar Muscular Atrophy |
| SCA | Spinocerebellar ataxia |
| TCA | Trichloroacetic acid |
| Ub-AMC | Ubiquitin–7-amido-4-methylcoumarin |
| Ub-VS | Ubiquitin vinyl sulfone |
| UCH | Ubiquitin C-Terminal Hydrolase |
| USP | Ubiquitin-Specific Proteases |
| WCEs | Whole-cell extracts |
| ZnF | Zinc finger |

# Chapter 1: Introduction

## 1.1 DUBs

There are around 95 deubiquitinating enzymes (DUBs) encoded by the human genome (Nijman et al., 2005). These DUBs are grouped into five major classes according to sequence homology: Ubiquitin-Specific Proteases (USPs), Ubiquitin C-Terminal Hydrolases (UCHs), Machado-Joseph Disease Protein Domain Proteases (MJDs), Ovarian Tumor Proteases (OTUs), and JAMM Motif Proteases (Figure 1) (Sowa et al., 2009). USP class represents the major DUBs in human genome. As the names indicate, all the USPs contain USP domain which possesses two short and well-conserved motifs, called Cys and His boxes, where the critical residues for catalysis locate (Sowa et al., 2009). USP22 and USP44 belong to the USP class. Both of USP22 and USP44 have been shown to regulate H2Bub1 levels, however, the molecular mechanism of USP22 and USP44 involved in diseases through modulating H2Bub1 remains to be known.

### 1.1.1 USP22 and USP44

USP22, an enzymatic subunit of the DUB module in the SAGA complex, functions to deubiquitinate histone H2Bub1 and other non-histone substrates including TRF1, FBP1 and Sirt1 (Atanassov and Dent, 2011; Atanassov et al., 2009; Lin et al., 2012; Zhang et al., 2008; Zhao et al., 2008). Importantly, recombinant USP22 alone is not active. Associations with other components of the DUB module including ATXN7,

ATXN7L3 and ENY2 are required for its full DUB activity (Lan et al., 2015; Lang et al., 2011).

The USP44 deubiquitinase also belongs to USP class. USP44 plays important roles in ES cell differentiation, DNA damage repair, cell cycle regulation and cancer development (Fuchs et al., 2012; Liu et al., 2015; Mosbech et al., 2013; Stegmeier et al., 2007; Zhang et al., 2012). USP44 was reported to regulate centrosome positioning through interaction with CETN2 (Centrin2) (Zhang et al., 2012). Previous studies also indicated a major role for USP44 in regulation of the H2Bub1 levels during ES cells differentiation (Fuchs et al., 2012). However, similar to USP22, recombinant USP44 by itself is not active toward histone H2Bub1 in vitro. What are the other partners required for the activation of USP44 DUB activity is not known.

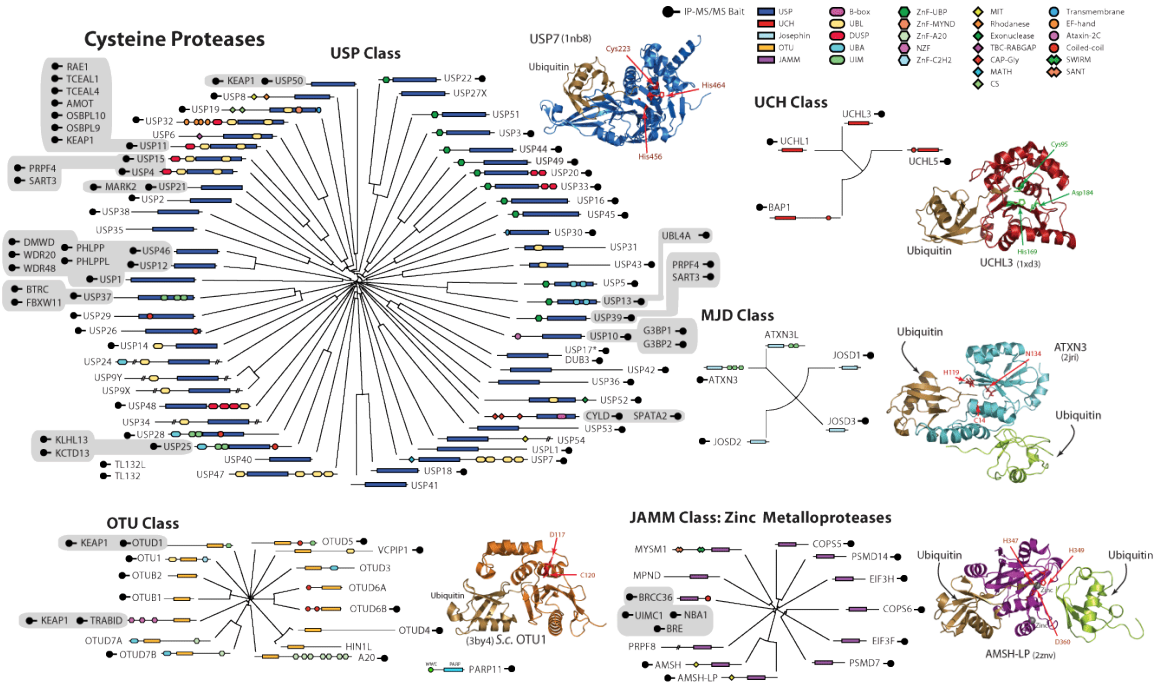


**Figure 1: Phylogenetic analysis of human DUBs.**

The human genome encodes ~95 DUBs in five major classes. They are USPs, UCHs, OTUs, MJDs and JAMMs (see main text introduction for details).

Figure 1 is adapted from Sowa, M.E., Bennett, E.J., Gygi, S.P., and Harper, J.W. (2009). Defining the human deubiquitinating enzyme interaction landscape. Cell *138*, 389-403.

*Permission has been acquired from the journal to use this figure.*

## 1.2 Histone modifications

Nucleosomes, consisting of the four core histone proteins (H2A, H2B, H3 and H4), are the basic functional units in eukaryotic chromatin. Histones undergo multiple post-transcriptional modifications including methylation, acetylation, ubiquitylation, phosphorylation, butyrylation, formylation, citrullination, proline isomerization, ADP ribosylationsumoylation, propionylation, and crotonylation (Kouzarides, 2007; Tan et al., 2011) (Figure 3). Enzymes that catalyze such modifications are named as “writers”; enzymes that remove a modification are named as “erasers”, and proteins that bind the modified histones are named as “readers” (Plass et al., 2013). Different modification states of the histones contribute to regulation of various biological processes, and dysregulation of histone modifications contribute to multiple human diseases (Cole et al., 2015).

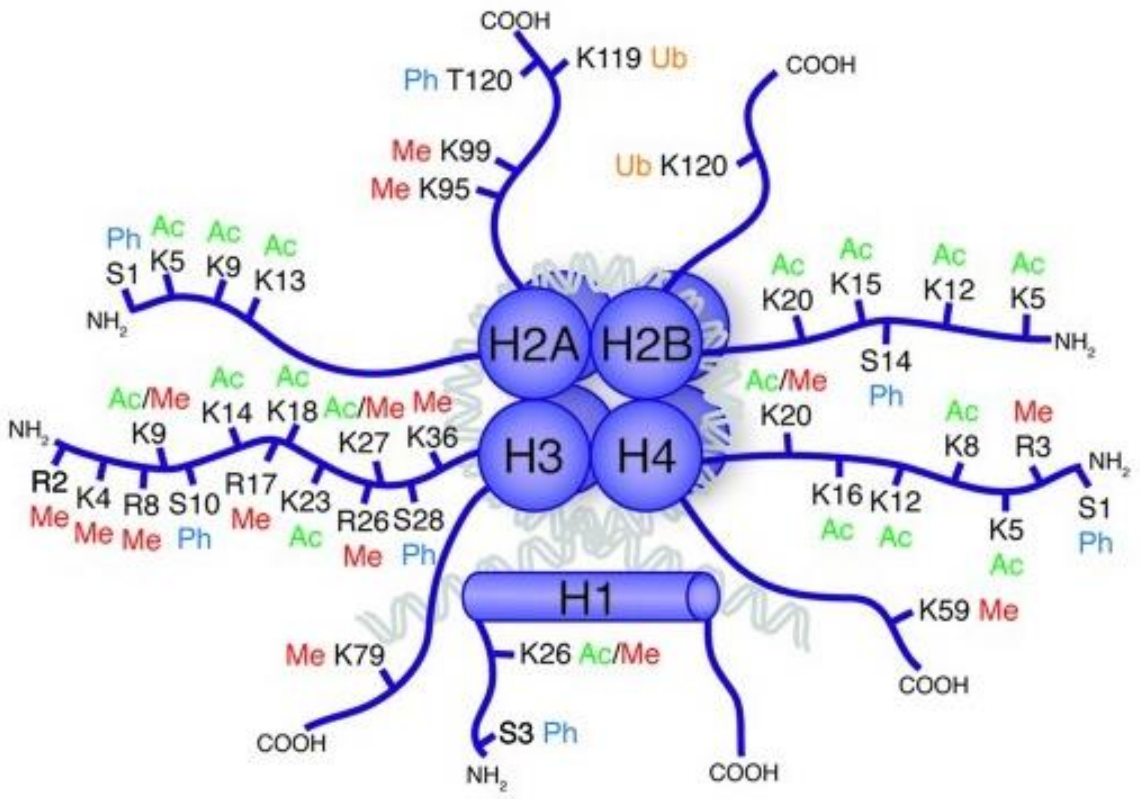


**Figure 2: Histone post-translational modifications.**

Schematic drawing of a nucleosome with the four canonical histones (H2A, H2B, H3 and H4) and the linker histone H1. The covalent PTMs [methylation (Me), acetylation (Ac), ubiquitination (Ub), and phosphorylation (Ph)] are highlighted on the N- and C-terminal tails of each histone.

Figure 2 is adapted and modified from Tollervey, J.R., and Lunyak, V.V. (2012). Epigenetics: judge, jury and executioner of stem cell fate. Epigenetics *7*, 823-840.

*Permission has been acquired from the journal to use this figure.*

### 1.3 PolyQ diseases

There are nine neurologic disorders caused by a number of CAG repeat expansions, typically in coding regions of different proteins. During translation, the expanded CAG repeats are encoded into a series of glutamine residues called polyglutamine tract (polyQ). These diseases include Huntington's Disease (HD), Spinal and Bulbar Muscular Atrophy (SBMA), Dentatorubral-pallidoluysian atrophy (DRPLA), and the spinocerebellar ataxia (SCA) types 1, 2, 3, 6, 7 and 17 (Table 1) (Todd and Lim, 2013). The polyQ tracts tend to form aggregates (Wetzel, 2012), which are the hallmark of many neurodegenerative diseases. However, what the role of these aggregates is in the pathogenesis of these diseases is highly debated. Although this group of neurodegenerative diseases is caused by the polyQ expansions in different unrelated proteins, they share a common symptom, ataxia, characterized by a progressive degeneration of nerve cells (Todd and Lim, 2013). Moreover, The longer the expanded glutamine tract is, the earlier the symptoms start and the more severe the diseases develop (David et al., 1998).

| Disease Name | Protein | Wildtype Q length | Expanded Q length | Affected tissues | Inclusion Location | Clinical Features |
|---|---|---|---|---|---|---|
| Huntington's Disease (HD) | Huntingtin (HTT)   | 6-35 | 36-121 | Striatum (caudate nucleus, putamen), globus pallidus, Cerebral cortex | Nucleus and Cytoplasm | Chorea, dystonia, cognitive deficits, psychiatric problems |
| Spinal and Bulbar Muscular Atrophy (SBMA) | Androgen Receptor (AR) 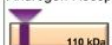  | 6-36 | 38-62 | Motorneurons of the Anterior Horn and Bulbar Regions, Dorsal Root Ganglia, Skeletal Muscle | Nucleus and Cytoplasm | Proximal and bulbar muscle weakness, atrophy and fasticulation, mild androgen insensitivity |
| Dentatorubral-pallidoluysian Atrophy (DRPLA) | Atrophin-1 (ATN1)   | 3-38 | 49-88 | Cerebellum (dentate nucleus), cerebral cortex, globus pallidus, basal ganglia | Nucleus | Ataxia, epilepsy/seizures, myoclonus, choreoathetosis, dementia |
| Spinocerebellar Ataxia Type 1 (SCA1) | ATAXIN-1 (ATXN1)   | 6-34 | 39-83 | Cerebellum (Purkinje cells and dentate nucleus), inferior olive, pons, anterior horn cells and pyramidal tracts | Nucleus | Ataxia, dysarthia, cognitive impairments, progressive motor deterioration |
| SCA2 | ATAXIN-2 (ATXN2) 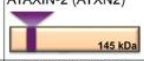  | 15-32 | 32-200 | Cerebellum (Purkinje cells), inferior olive, pons, substantia nigra, frontotemporal lobes | Nucleus | Ataxia, decreased reflexes, dysarthia, Parkinsonian rigidity, sensory disturbance, mental deterioration |
| Machado-Joseph Disease (MJD)/SCA3 | ATAXIN-3 (ATXN3)   | 12-40 | 61-86 | Globus pallidus, cerebellum (molecular layer), pons, substantia nigra, anterior horn cells | Nucleus | Ataxia, dystonia, Parkinsonism, amotrophy, eyelid retraction and vision problems, faciolingual fasciculation, dysphagia, weight loss |
| SCA6 | α1A subunit of the voltage-gated $Ca^{2+}$ channel CACNA1A   | 4-19 | 21-33 | Cerebellum (Purkinje cells, molecular and granular layers), inferior olive | Cytoplasm | Ataxia, dysarthria, oculomotor disorders, incontinence, peripheral neuropathy |
| SCA7 | ATAXIN-7 (ATXN7) 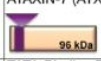  | 4-35 | 37-306 | Cerebellum (Purkinje cells, molecular and granular layers), pons, inferior olive, visual cortex | Nucleus | Ataxia, retinal degeneration, dysphagia, dysarthria, changes in reflexes or sensation |
| SCA17 | TATA-Binding Protein (TBP)   | 25-43 | 45-63 | Cerebelllum (Purkinje cells), inferior olive | Nucleus | Ataxia, cognitive decline/dementia, epilepsy/seizures, psychiatric problems |

**Table 1: Polyglutamine diseases**

There have been nine polyglutamine diseases identified to date. The human protein mutated in each disease is noted, along with a schematic of its relative size and glutamine (Q) expansion location (purple box and triangle). The approximate size of the wildtype protein is noted in kilodaltons (kDa). Polyglutamine-expanded protein size can vary depending on the length of the CAG repeat. The tissues principally affected in each disease, as well as the clinical output and the cellular locations of the inclusions are listed.

This table is adapted from Todd, T.W., and Lim, J. (2013). Aggregation formation in the polyglutamine diseases: protection at a cost? Mol Cells *36*, 185-194.

*Permission has been acquired from the journal to use this table.*

### 1.3.1 SCA7 disease and SAGA complex

Spinocerebellar ataxia type 7 (SCA7) is one of nine polyQ diseases correlated with progressive neurodegeneration (Lebre and Brice, 2003; Todd and Lim, 2013). SCA7 is dominantly inherited and is caused by polyQ expansions within the N-terminal region of ATXN7. Wild type ATXN7 contains 4 to 35 glutamine (Q) residues, whereas mutant ATXN7 contains from more than 36 to up to 300 Q repeats (Todd and Lim, 2013). SCA7 not only leads to progressive spinocerebellar neurondegeneration, but also a unique symptom of retinal degeneration. SCA7 patients display dysarthria, abnormal gait, uncoordinated movements and visual loss, usually followed by early death (Johansson et al., 1998). Although it is broadly agreed that aggregation of the expanded glutamine stretch plays an important role in neurotoxicity, the detailed molecular mechanism of toxicity remains to be known.

ATXN7 is a subunit of the deubiquitinase module (DUBm) in the conserved SAGA complex (Figure 3), which regulates gene expression via modulating histone ubiquitination and acetylation (Koutelou et al., 2010). ATXN7 in itself has no enzymatic activity. It resides within the DUB submodule of SAGA and serves to anchor this module to the main complex. The PolyQ expansions in ATXN7 could affect either or both of the enzymatic activities. Previous studies provided conflicting evidence regarding the effects of ATXN7-polyQ on the activity of Gcn5, the catalytic component of the histone acetyltransferase (HAT) module in SAGA complex (Helmlinger et al., 2006; McMahon et al., 2005; Palhan et al., 2005). In a SCA7 mouse model, the deletion of Gcn5 facilitates cerebellar Purkinje cell and retinal degeneration, indicating that Gcn5 is involved in SCA7 disease progression (Chen et al., 2012). However, specific deletion of *Gcn5* in Purkinje cells is not enough to cause severe ataxia, indicating that other SAGA functions may also contributes to SCA7 development (Chen et al., 2012). Given that ATXN7 is a

subunit of the DUB module in SAGA, polyQ expansions might affect the deubiquitinating activity of SAGA.

In Saccharomyces cerevisiae, the SAGA DUB module consists of Ubp8, Sgf11, Sus1, and Sgf73 (homologs of USP22, ATXNL3, ENY2, and ATXN7, respectively, in humans) (Figure 3) (Helmlinger et al., 2004; Lee et al., 2005; Zhao et al., 2008). Sgf73/ATXN7 functions both to bridge the DUBm to SAGA through its central domain and to form an integral part of the DUBm through its N-terminal domain (Kohler et al., 2008). However, Ubp8 alone is not active and other subunits of DUBm are required for its DUB activity. The crystal structure of the yeast DUBm provides a molecular interpretation about how these associations with other DUBm components are required to activate Ubp8 (Kohler et al., 2010; Samara et al., 2010). Similarly, the DUB activity of the mammalian catalytic subunit USP22 is also allosterically regulated through multiple interactions with human SAGA DUBm components (Lang et al., 2011). The zinc finger (ZnF) domain of ATXN7 is required for association with the DUBm (Lang et al., 2011). However, whether and how the polyQ-expanded ATXN7 affect DUBm activity or integrity has not been directly addressed.

Although other substrates for USP22 have been identified in mammalian cells (Atanassov and Dent, 2011; Atanassov et al., 2009), the best-characterized substrate is histone H2B (Zhang et al., 2008). Genome-wide analyses by ChIP-seq in human cells show that H2Bub1 signal is enriched in the gene body of highly expressed genes (Minsky et al., 2008), but this modification is involved in both gene repression and activation (Shema et al., 2008). For example, expression of reelin, an important factor for the development and maintenance of Purkinje cells, is highly downregulated in SCA7 astrocytes, and this downregulation leads to an increase of H2Bub1 levels at the *reelin* gene promoter (McCullough et al., 2012). Together, these data suggest that the DUB

activity of USP22 may be defective in SCA7 tissues, causing dysregulation of crucial target genes, which contribute to SCA7 disease.

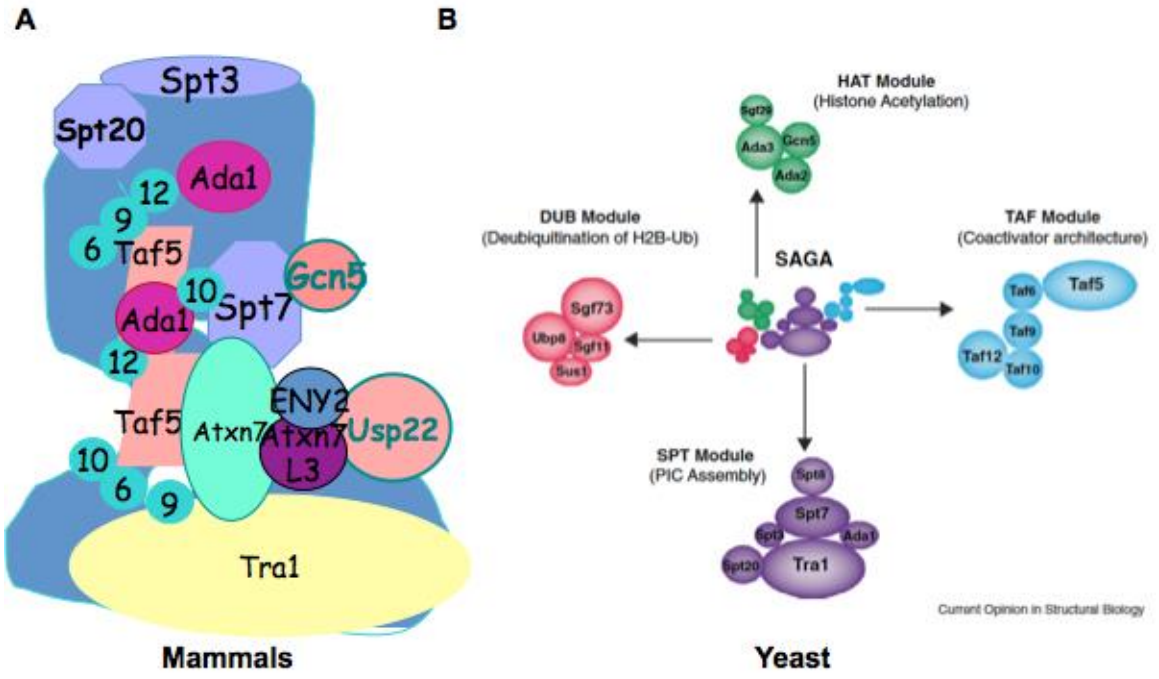


**Figure 3: SAGA complex is very conserved from yeast to mammals.**

SAGA complex contains both HAT module and DUB module where Gcn5 and USP22/Ubp8 serve as the enzymatic subunits, respectively. HAT module consists of Ada3, Ada2, Sgf29 and Gcn5. The DUB module consists of Sgf11, Sgf73, Sus1 and Ubp8.

Figure 3A is adapted and modified from Wu, P.Y., Ruhlmann, C., Winston, F., and Schultz, P. (2004). Molecular architecture of the S. cerevisiae SAGA complex. Mol Cell *15*,199-208.

Figure 3B is adapted from Samara, N.L., and Wolberger, C. (2011). A new chapter in the transcription SAGA. Curr Opin Struct Biol *21*, 767-774.

*Permissions have been acquired from the journals to use these figures.*

### 1.4 H2Bub1 and Cancer

Histone H2B is monoubiquitinated on lysine 123 in yeast and the corresponding lysine 120 in mammals (H2Bub1). H2Bub1 appears to contribute to creation of open and accessible chromatin structures (Fierz et al., 2011), as it has been reported to play important roles in transcriptional initiation and elongation (Henry et al., 2003; Pavri et al., 2006; Xiao et al., 2005), mRNA 3'-end processing (Pirngruber et al., 2009), DNA damage response (Moyal et al., 2011), DNA replication (Trujillo and Osley, 2012) and maintenance of stem cell multipotency (Fuchs et al., 2012; Karpiuk et al., 2012). H2Bub1 is required in yeast and human cells for histone H3 methylation on lysine 4 (H3K4) and lysine 79 (H3K79) (Briggs et al., 2002; Ng et al., 2002; Sun and Allis, 2002; Wu et al., 2011), which further contributes to transcriptional activity.

H2Bub1 levels are governed by a balance in the activities of specific ubiquitin E3 ligases, such as RNF20/40 (Kim et al., 2005), and deubiquitinases that target this modification (Figure 4). Several deubiquitinases including USP22 (Zhang et al., 2008; Zhao et al., 2008), USP27X, USP51 (Atanassov et al., 2016), USP3 (Nicassio et al., 2007), and USP49 (Zhang et al., 2013) can remove ubiquitin from histone H2B. USP44 has also been implicated in H2Bub1 deubiquitylation (Fuchs et al., 2012), but USP44 alone is not active. The importance of H2Bub1 to human health is emphasized by several studies that indicate H2Bub1 levels are low to absent in many aggressive cancers including colorectal cancer, metastatic breast cancer, testicular seminoma, parathyroid cancer, and lung cancer (Cao and Yan, 2012; Fuchs and Oren, 2014).

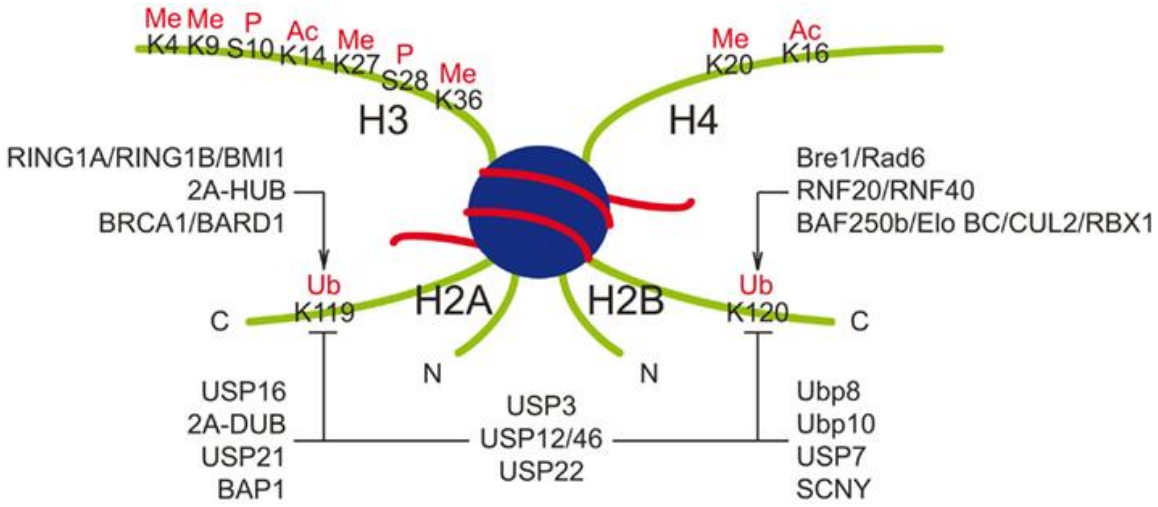


**Figure 4: Ubiquitin ligases and deubiquitinating enzymes responsible for monoubiquitination of histones H2A and H2B.**

Major post-transcriptional modifications on histone H3 and H4 tails are shown. An E1 ubiquitin (ub)-activating enzyme engages ATP to activate free ubiquitin, which is transferred to the active site of an E2 ubiquitin-conjugating enzyme, two of which have been reported to be associated with H2Bub1. E3 ubiquitin ligases work with E2 to transfer ubiquitin to the target protein. Four E3s, most of them appearing in RING finger complexes, have been identified in the H2Bub1 cascade; however, it is unclear how, or if, they function together for the monoubiquitination of histone H2B. Deubiquitinating (DUB) enzymes, of which seven have been reported to be associated with H2Bub1, cleave ubiquitin from its substrate. Ac, acetylation; Me, methylation; P, phosphorylation. Figure 4 is adapted from Cao, J., and Yan, Q. (2012). Histone ubiquitination and deubiquitination in transcription, DNA damage response, and cancer. Front Oncol *2*, 26

*Permission has been acquired from the journal to use this figure.*

## Chapter 2: Materials and Methods

Contents of this chapter are partially based on Lan, X*., Koutelou, E*., Schibler, A.C., Chen, Y.C., Grant, P.A., and Dent, S.Y. (2015). Poly(Q) Expansions in ATXN7 Affect Solubility but Not Activity of the SAGA Deubiquitinating Module. *Mol Cell Biol 35*, 1777-1787. (* Equal contribution authors)



### 2.1 Plasmids

USP22 cDNA was acquired from Open Biosystems. ATXN7L3 and ENY2 cDNAs were a gift from Didier Devys. USP22, ATXN7L3, and ENY2 were subcloned into the 2.1-TOPO vector by PCR, sequenced, and then cloned into the NruI and NotI sites of the baculovirus expression vector pBacPAK8 (Clontech). A hemagglutinin (HA) tag was introduced into pBacPAK8 in BamHI and NruI, and a Flag tag was introduced into pBacPAK8 in KpnI and NruI. Mutation of USP22 cysteine 185 to serine was introduced using a site-directed mutagenesis kit (Agilent Technologies). Full-length Flag–ATXN7-24Q and Flag–ATXN7-92Q in the pSDM vector were provided by Patrick A. Grant. The cDNAs of human ATX7L3 and ENY2 were gifts from Didier Devys. The N termini of Flag–ATXNT7-24Q NT and Flag–ATXN7-92Q NT were subcloned into NheI and PstI of pBacPAK8.3. Packaging vectors (psPAX2 and pMD2G) and transfer vectors containing full-length Flag–ATXN7-24Q or Flag–ATXN7-92Q, which were used for production of recombinant lentivirus, were provided by Patrick A. Grant. The full-length Flag or V5-tagged ATXN7L3 and ENY2 expression constructs were generated in pSDM101 with MluI and NdeI by using a PCR cloning strategy with pBacPAK8-ATXN7L3 and pBACPAK8-ENY2 as the templates, respectively. pINTO-NFH vector and pINTO-GAL4

vector were gifts from Dr. Danny Reinberg lab as described previously (Gao et al., 2014; Gao et al., 2012). pCAG-C-FH vector was a gift from Dr. Taiping Chen lab. USP44 cDNA was a gift from Dr. Paul J. Galardy lab. CETN2, TBL1X and TBL1XR1 cDNAs were purchased from Open Biosystems (GE Healthcare). These cDNAs were further subcloned into pINTO-NFH, pINTO-GAL4 or pCAG-C-FH vectors. For truncated GAL4-TBL1XR1, PCR was used to amplify the fragments of interest before insertion to the pINTO-GAL4 vector. For protein expression in insect cells, cDNAs of interest were subcloned into pBacPAK8.3 vectors, Production of recombinant viruses and Sf21 cell infection were performed following the manufacturer's protocols (BD Biosciences).

**2.2 Antibodies**

The details of all the antibodies used in this study are described in table 1

**2.3 Cell lines**

Primary human astrocytes (N7805-100; Life Technologies) were grown in Dulbecco modified Eagle medium (DMEM) supplemented with 1% N-2 supplement and 10% fetal bovine serum (FBS) (Life Technologies). Artificially immortalized human astrocytes were provided by Patrick A. Grant and grown in alpha minimal essential medium (Life Technologies) supplemented with 10% FBS (Life Technologies). 293T, 293T-REx-luciferase and MDA-MB-231 cells were maintained in high-glucose Dulbecco's Modified Eagle Medium (DMEM-H) (Thermo Scientific) supplemented with 10% Fetal Bovine Serum (FBS) (HyClone, Cat. # SH30910.03) and 1% penicillin-streptomycin (Thermo Scientific). MCF10A cells were provided by Dr. Khandan Keyomarsi and were grown in 1:1 mixture of alpha-Medium (Minimum Essential Medium

alpha (Corning, Cat. # 15-012-CV) and Ham's F-12 medium (Corning, Cat. # 10-080-CV) supplemented with 1% FBS, 10mM HEPES, 2 mM glutamine, 1 μg/ml hydrocortisone, 12.5 μg/ml epidermal growth factor (EGF), 1 μg/ml insulin, 35 μg/ml bovine pituitary extract (BPE), 10 μg/ml ascorbic acid, 0.2 nM β-estradiol, 2.5 ng/ml Na selenite, 6.65 ng/ml triiodothryonine III, 0.0006% ethanolonine, 14.1 μg/ml phosphoethanolanine (PE), and 10 μg/ml transferrin. Cells were maintained in $CO_2$ incubator at 37°C and 5% $CO_2$. Sf21 insect cells were grown in Sf-900™ II SFM (Life Technologies, Cat. # 10902-096) supplemented with 1% penicillin-streptomycin. Cells were maintained in flasks (Corning, 250 mL Cat. # 431144 or 500 mL Cat. # 431145) on an orbital shaker at 120 rpm, 27 °C.

| Antibody | Suppliers | Cat. # | Applications |
|---|---|---|---|
| Anti-TBL1X | Proteintech | 13540-1-AP | WB/IP |
| Anti-TBL1XR1 | Bethyl Laboratories | A300-408A | WB |
| Anti-NCOR1 | Bethyl Laboratories | A301-145A | WB |
| Anti-HDAC3 | Bethyl Laboratories | A300-464A | WB |
| Anti-CETN2 | Proteintech | 15877-1-AP | WB |
| Anti-USP44 | Santa Cruz | Sc-292324 | WB |
| Anti-USP22 | Home made | 3933-1 | WB |
| Anti-GAL4 | Millipore | 06-262 | ChIP |
| Anti-GAL4 | Santa Cruz | Sc-510 | WB |
| Anti- FLAG beads | Sigma | A2220 | IP |
| Anti-HA beads | Roche | 11815016001 | IP/ChIP |
| Anti-TBL1X | Santa Cruz | Sc-11391 | WB |
| Anti-beta-Tubulin | Cell signaling | 2146 | WB |
| Anti-beta-actin | Santa Cruz | Sc-47778 | WB |
| Anti-FLAG (M2) | Sigma | F3165 | WB |
| Anti-HA (12CA5) | Roche | 11583816001 | WB |
| Anti-H3 | Millipore | 06-755 | WB/ChIP |
| Anti H2A | Millipore | 07-146 | WB |
| Anti-H2B | Millipore | 07-371 | WB/ChIP |
| Anti-H2Bub (K120) | Millipore | 05-1312 | WB/ChIP |
| AntiH2Aub (K119) | Millipore | 05-678 | WB |
| Anti-H3K9/14ac | Millipore | 06-599 | WB/ChIP |
| Anti-Rabbit-HRP | GE Healthcare | NA934-1ML | WB |
| Anti-Mouse-HRP | GE Healthcare | NA931-1ML | WB |
| Anti-V5 | Invitrogen | 46-0705 | WB/IF |
| Anti-ATXN7L3 | (Zhao et al., 2008) | 2325 | IF |
| Alexa Fluor 488-conjugated Anti-rabbit | Life Technologies | A-11034 | IF |
| Alexa Fluor 594-conjugated Anti-mouse | Life Technologies | A-11005 | IF |

**Table 2: Antibodies used in this study**

### 2.4 Baculovirus expression system

Baculovirus transfection, infection, and maintenance were performed as previously described (Lan et al., 2015). In 60 mm plastic dishes, $2x10^6$ Sf21 cells were co-transfected with 3 µg of pBacPAK8.3 expression vectors, containing the indicated cDNAs, and 0.5µg of linearized baculovirus DNA (BestBac 1.0, Expression systems, Cat. # 91-001) using Lipofectamine 2000 or FuGENE® 6 (Promega, Cat. # E2691) following manufacturer's instructions. 3 days post the transfection, the medium containing the recombinant viral particles were collected. To increase the titer of the virus, this medium was further used (in 1:4 dilution) to infect new Sf21 cells for several times. For infection, exponentially growing Sf21 cells were seeded in 15 cm plastic dishes ($2x10^7$ cells/dish) and viral medium was added after the cells were attached to the dish (~15 min to attach). Cells were incubated in a humidity chamber (plastic box with wet paper towels at the bottom) for 3 days at 26-27°C. The viral medium was then collected, and stored in dark boxes at 4°C for several weeks, or at -80°C for longer periods. The expression level of each cDNA was monitored by western blot at the end of each round infection using WCL from the infected cells. For large-scale protein purification, $4x10^7$ cells were infected and maintained in flasks (50 mL final volume in 250 flask) in an orbital shaker for 3-6 days at 27°C, 120 rpm. Cells were then harvested by centrifugation and used to make protein lysates.

### 2.5 Protein purification from Baculovirus system

To purify the recombinant proteins, recombinant baculoviruses were used to infect Sf21 cells. For complex purification, different baculoviruses were used to co-infect Sf21 cells. After 3 to 5 days of infection, cells were harvested and resuspended in buffer C (50 mM HEPES [pH 7.9], 5 mM $MgCl_2$, 20% glycerol, 0.2% Triton X-100, 300 mM NaCl, 1

mM dithiothreitol [DTT], 1 mM phenylmethylsulfonyl fluoride [PMSF]) with a protease inhibitor cocktail (Roche). Then, the cells were homogenized by bead beating 3 times for 30 s each time on ice. The supernatant was recovered by centrifuging at 15,000 rpm for 10 min, and then the supernatant was further cleared by being centrifuged at 40,000 rpm for 1 h at 4°C. The supernatant was then incubated with the M2 anti-Flag–agarose (Sigma) or anti-HA matrix (Roche) equilibrated with washing buffer (10 mM HEPES [pH 7.9], 1.5 mM $MgCl_2$, 10 mM KCl, 0.1% Triton X-100, 300 mM NaCl, 1 mM DTT, 1 mM PMSF) with a protease inhibitor cocktail (Roche) overnight at 4°C. After being washed with washing buffer 3 times for 10 min each time, bound proteins were eluted with the Flag peptide (0.2 mg/ml) or HA peptide (0.4 mg/ml), respectively, for 2 to 4 h at 4°C or room temperature (RT) in elution base buffer (10 mM HEPES [pH 7.9], 100 mM NaCl, 1.5 mM $MgCl_2$, 0.05% Triton X-100, 0.2 mM EDTA, 10% glycerol, 1 mM DTT, 1 mM PMSF) (Lan et al., 2015). The eluted DUBm complexes were further purified through a gel filtration Superdex 200 column (GE Healthcare).

**2.6 Gel filtration**

The eluted complexes were loaded onto a Superdex 200 column equilibrated in elution base buffer. The column was eluted with 1.5 column volumes of buffer, and 40 fractions (each faction was 0.5 ml) were collected. Each fraction was concentrated to 30 μl by Amicon Ultra centrifugal filters (Millipore) and analyzed using Western blotting with anti-HA and anti-Flag antibodies. All these processes were performed at 4°C (Kuzmichev et al., 2002).

### 2.7 In vitro deubiquitination assay

Total histones were prepared from HEK293T cells using a histone purification minikit (Active Motif). Free histones or nucleosomes (Epicypher) were incubated with purified recombinant proteins or complexes in DUB buffer (100 mM Tris-HCl, pH 8.0, 5% glycerol, 1 mM EDTA, 3 mM DTT) for 2 h or the times specified below at 37°C as described previously (Lang et al., 2011). SDS loading buffer was added to stop the reaction, and then Western blotting was performed to analyze the products of the reaction using specific antibodies. For *in vitro* assays using ubiquitin vinyl sulfone (Ub-VS; Boston Biochem), the purified complexes were incubated with 1 μM or 5 μM Ub-VS in a reaction buffer (100 mM Tris-HCl, pH 8.0, 5% glycerol, 100 mM KCl, 3 mM DTT) for the times specified below at RT. Laemmli blue was added to stop the reactions, and then the reaction products were analyzed by immunoblotting. For reaction with ubiquitin–7-amido-4-methylcoumarin (Ub-AMC; Boston Biochem), the purified complexes were incubated in DUB buffer (50 mM HEPES, pH 7.9, 0.5 mM EDTA, 0.1 M NaCl, 1 mM DTT, 0.1 mg/ml bovine serum albumin) on ice for 30 min and then at RT for 5 min. Reactions were initiated by adding 0.5 μM ubiquitin-AMC in DUB buffer. The reactions were monitored continuously for 15 min by determination of the fluorescence at 25°C (excitation λ, 360 nm; emission λ, 528 nm; Biotek Synergy 2 apparatus) as described previously (Yao et al., 2008).

### 2.8 Preparation of cell lysates

Whole-cell extracts (WCEs) were prepared using radioimmunoprecipitation assay (RIPA) buffer or buffer C. The supernatants and pellets of WCEs from Sf21 cells or human astrocytes were separated after centrifuging at 15,000 rpm for 20 min at 4°C. Laemmli buffer was added to dissolve these pellets at 95°C for 5 to 10 min. Both the

supernatant and pellet fractions of whole-cell lysates were analyzed by Western blotting with the indicated antibodies. Or cell lysates were then sonicated for 10 min (30 sec on; 30 sec off) using Biorupter Twin (Diagenode, UCD-400) and then centrifuged at 15000 rpm for 20 min at 4°C. The clear supernatants were used as whole cell lysates (WCL) for Western blotting.

**2.9 Immunoprecipitation (IP)**

1-2 mg of whole cell lysate or nuclear extract and 3-5 µg antibodies were used for each IP. Specific antibodies and normal rabbit (or normal mouse) IgG were added to the protein lysates and incubated overnight on a rocking platform at 4 °C. 40-50 µL (50% slurry) of pre-washed (by wash buffer 150 - 10 mM Tris-HCl pH 7.9, 10-20% glycerol, 150 mM NaCl, 1.5 mM $MgCl_2$, 0.1% NP-40, 0.2 mM EDTA, 0.5 mM DTT, 0.2 mM PMSF, protease inhibitors)) protein–G agarose beads (Millipore cat. # 16-266) were added to each sample and incubated for another 2 hours on a rocking platform at 4 °C. Beads were then collected by centrifugation for 1 min at 1000 rpm at 4 °C. Precipitated complexes were washed by wash buffer 150 and incubate on a rocking platform for 10 min at 4 °C. Repeated once using wash 350 (10 mM Tris-HCl pH 7.9, 10-20% glycerol, 350 mM NaCl, 1.5 mM $MgCl_2$, 0.1% NP-40, 0.2 mM EDTA, 0.5 mM DTT, 0.2 mM PMSF, protease inhibitors) and 2 more times with wash buffer 150. Washed beads were then harvested by centrifugation, mixed with an equal volume of 1.5x SDS sample buffer and boiling for 10 min at 95°C (heating block). Boiled beads were then removed by centrifugation at 15000 rpm, 1 min and the supernatants (usually 1/3) were used for western blot. For FLAG or HA tagged proteins, anti-FLAG (M2) (Sigma cat. #A2220), or anti-HA (Roche cat. #11815016001) beads were used. These IPs beads were washed and boiled in the same way as protein-G beads. FLAG and/or HA precipitated

complexes were eluted in wash 150 buffer containing 200 µg/mL 1x FLAG peptide (Sigma cat. # F3290) or 400 µg/mL HA peptide (Roche cat. #11666975001) for 2-4 hours on a rocking platform at 4°C or RT.

**2.10 Western blot analyses**

20-30 µg of WCL or 1/3 of IP elutes were resolved on 4-12% NuPAGE gels (Life Technologies cat. # NW04122BOX). Proteins were transferred to 0.2 µm nitrocellulose membrane in Tris-Glycine buffer containing 10% Methanol for 75 min at a constant 100 volts at 4 °C after electrophoresis in SDS-PAGE, transferred nitrocellulose membrane was then blocked in 5% non-fat milk in TBS-T for 1 hour on an orbital shaker at RT and incubated with primary antibodies overnight on a rocking platform at 4°C. After washes in TBS-T 3x10 min, membranes were incubated with secondary-horseradish peroxidase (HRP) conjugated antibodies (GE Healthcare, Cat. # NA934V for Rabbit, NA931V for Mouse) for 1 hour on an orbital shaker at RT. Membranes were incubated with ECL Prime Western Blotting Detection Reagent (GE Healthcare Life Sciences, RPN2232) for 5 min and exposed after washes in TBS-T 3x(5-10) min.

**2.11 Nuclear extract preparation, affinity purification for gel filtration, deubiquitination assay or MudPIT analysis**

Sample preparations for MudPIT analysis were performed as previously described (Atanassov et al., 2016). 293T cells stably expressing pINTO-N-FH-hUSP44, pINTO-N-FH-hCETN2, pINTO-N-FH-hTBL1X or empty vector respectively were cultured in DMEM-H complete medium containing 100 µg/ml Zeocin. Cells were cultured in 15 cm plastic dishes (TPP cat. # 93150) at 37°C and 5% $CO_2$. (30-40) X15 cm dishes of ~80% confluent cells were used for each purification.

Cells were harvested by trypsinization, washed twice in ice cold PBS containing protease inhibitors (Sigma cat. # P8340) and pelleted by centrifugation for 5 min at 200g at 4 °C after each wash. Cell pellets were unpacked by flicking the tubes several times and resuspended in 10 pellet volumes of ice-cold hypotonic buffer (buffer A) (10 mM HEPES pH 7.5, 1.5 mM $MgCl_2$, 10 mM KCl, protease inhibitors, 1 mM DTT, 1 mM PMSF) and cell suspensions were incubated on ice for 20 min. The swollen cells was moved to a glass homogenizer (7 mL Wheaton) and homogenized with 10 strokes by loose pestle. The homogenized cell suspension was collected in a fresh 50 mL Falcon tube and incubated on ice for another 20 min, nuclei were harvested by centrifugation at 500g for 7 min at 4°C. The supernatant (cytoplasmic fraction) was carefully removed and nuclei were then lysed in 5 pellet volumes of buffer C (20 mM Tris-HCl pH 7.9, 20% glycerol, 420 mM NaCl, 1.5 mM $MgCl_2$, 0.1% NP-40, 0.2 mM EDTA, 0.5 mM DTT, 0.2 mM PMSF, protease inhibitors) and lysates incubated on ice for 30 min. Lysed nuclei were then moved to a glass homogenizer and homogenized with 15 strokes by a tight pestle. Homogenates were collected in fresh 50 mL falcon tubes and an equal volume of ice-cold buffer A (hypotonic buffer) containing DTT, PMSF and protease inhibitors. For pre-clearing, lysates were centrifuged at 5,000g for 15 min at 4°C. The supernatants were then moved to ice-cold ultra centrifuge tubes, balanced, and centrifuged for 1.5 hours at 45000 rpm at 4°C using a Beckman 50.2Ti rotor. After this centrifugation, the clear supernatants were moved to new Falcon tubes (without touching any pellets or clouds) and labeled as Nuclear Extract (NE). A small fraction was used as an input after measuring the protein concentration by Bradford assays (Bio-Rad, Cat. # 500-0006).

An equal amount of total protein for all samples were moved to 50 mL Falcon tubes and 200 μL of anti-FLAG (M2) beads (Sigma Cat. # A2220), pre-washed in wash buffer 150 (10 mM Tris-HCl pH 7.9, 20% glycerol, 150 mM NaCl, 1.5 mM $MgCl_2$, 0.1% NP-40,

0.2 mM EDTA, 0.5 mM DTT, 0.2 mM PMSF, protease inhibitors) were added to each tube, and then incubated for 4 hours or overnight on a rocking platform at 4°C. After incubation, the beads were spinned down at 1000 rmp, 1 min at 4 °C and then washed in wash buffer 150 1x10 min; wash buffer 350 (10 mM Tris-HCl pH 7.9, 10-20% glycerol, 350 mM NaCl, 1.5 mM $MgCl_2$, 0.1% NP-40, 0.2 mM EDTA, 0.5 mM DTT, 0.2 mM PMSF, protease inhibitors) 1x10 min and wash buffer 150 2x10 min on a rocking platform at 4°C.

Precipitated complexes were eluted by incubating the beads in 2-5 bed volumes of wash buffer 150 containing 200 µg/mL 1xFLAG peptide (Sigma cat. # F3290) for 30 min on a rocking platform at 4°C. Eluates were collected in 1.5 or 2 mL Falcon tubes and the elution was repeated one more time using the same volumes and conditions. 80-100 µL of pre-washed anti-HA beads (Roche cat. # 11815016001) were added to the FLAG eluates and mixtures were then incubated overnight on a rocking platform at 4°C. The beads were washed the same way as after the first IP. Precipitated complexes were eluted by 5 bed volumes of 100 mM glycine (pH 2.0) for 15 min on a rocking platform at 4°C or by 2 bed volumes of wash buffer 150 containing 400 µg/mL HA peptide (Roche cat. #11666975001) for 2-4 hours on a rocking platform at RT. The beads were removed using chromatography columns (Bio-Rad Poly-Prep Cat. # 7311550). The eluates (two time elutions) by HA peptide were collected and concentrated down to ~25-45 µL volume using centricons (Amicon Ultra, Millipore Cat. # UFC 501024 10K cut size) and then used for silver stain or western blots and gel filtration or DUB assay. For MudPIT analysis, the eluates by glycine (pH 2.0) were collected and neutralized by 1/10 eluate volumes of 1M Tris-HCl (pH 9.0). These elutes were then treated with Benzoase (Sigma cat. # E8263-5KU) 0.1U/tube on 37°C for 30 min. The volume of the elutes was brought to 400 µL by 100 mM Tris-HCl pH 8.5 and precipitated immediately by adding 100 µL of

ice-cold trichloroacetic acid (TCA) (Sigma) (final concentration 20% w/v). Elutes-TCA mixtures were incubated for precipitation at 4°C overnight. After the incubation, proteins were precipitated by centrifugation at 15,000 rpm for 30 min at 4°C followed by 2 immediate centrifugations at 15,000 rpm for 10 min at 4°C. Pellets were then washed twice with ice-cold acetone (carefully remove acetone), air-dried in a fume hood and submitted for MudPIT analysis.

### 2.12 *In vitro* binding assay

Recombinant HA-USP22 was incubated with recombinant Flag–ATXN7-24Q NT, Flag-ATXN7L3, or Flag-ENY2 at 16°C for 1 h. Then, the mixture was incubated with anti-Flag–agarose overnight at 4°C (Yao et al., 2006). After being washed 3 times with washing buffer, bound proteins were eluted with Flag peptide (0.2 mg/ml) (Sigma, cat. # F3290). The input and eluate were analyzed by immunoblotting with anti-Flag and anti-HA antibodies.

### 2.13 Histone purification from ATXN7 Wild-type and mutant adult mouse cerebellums

Atxn7$^{100Q}$ alleles carried naturally occurring contracted mutations of the coding sequence for the 266-Q tract in Atxn7 obtained when maintaining the Atxn7$^{266Q/5Q}$ mouse line (Yoo et al., 2003). Cerebellums from mice with all three different genotypes were collected and snap-frozen. Total histones from the cerebellums were prepared using a histone purification minikit (Active Motif). Laemmli buffer was added, and the lysates were analyzed by Western blotting. All procedures that involved animal handling were performed in accordance with the approved IACUC protocols at the M. D. Anderson Cancer Center.

### 2.14 Immunofluorescence microscopy

Astrocytes were cultured on Geltrex lactate dehydrogenase-elevating virus-free, reduced growth factor basement membrane matrix (Life Technologies)-coated glass coverslips in 12-well plates for 24 to 48 h and then fixed with 3% formaldehyde, washed in phosphate-buffered saline (PBS), blocked with 10% fetal calf serum in PBS, and stained using primary antibodies (Sigma) and then secondary antibodies (Life Technologies). Nuclei were stained with DAPI (4′,6-diamidino-2-phenylindole) in Vectashield mounting medium (Vector). Glass microslides with coverslips were allowed to set overnight to dry before coverslips were sealed with fingernail polish. Images were obtained using a laser scanning spectral confocal microscope (Leica STP6000).

### 2.15 Transfection and lentiviral infection

60%-70% confluent 293T cells were transfected in Opti-MEM® I (Life Technologies) using Lipofectamine® 2000 (Life Technologies cat. # 11668019) following manufacturer's instructions. The medium was changed to complete DMEM-H after Six to eight hours transfection. For lentiviral medium production, 293T cells were co-transfected with lentiviral (the shRNA expressing pGIPZ) and psPAX.2 and pMD2.G (Addgene). After 72 hours transfection, the DMEM-H medium containing the lentiviral particles were collected, filtered through 0.45 μm filters and used for infection. For cells infection, the lentiviral medium was diluted 1:2 with the culture medium containing 4-8 μg/ml polybrene (Sigma, Cat. # H9268), infecting for 24-48 hours.

### 2.16 Stable cell lines generation

293T cells stably expressing FLAG and HA-tagged hUSP44, hCETN2, or hTBL1X, were generated after transfection of 293T cells with pINTO-N-FH-hUSP44, pINTO-N-FH-

hCETN2, pINTO-N-FH-hTBL1X or pINTO-N-FH empty vector and subsequent selection in DMEM-H complete medium containing 300 µg/ml Zeocin™ (Life Technologies cat. # R25001) for 2-3 weeks. The same method was used to generate 293T-Rex-luciferase cells stably expressing pINTO-N-GAL4-hTBL1X, pINTO-N-GAL4-hTBL1XR1 or pINTO-N-GAL4 empty vector upon doxycycline induction. Stable 293T cell lines were maintained in medium containing 150 µg/ml Zeocin. Stable 293T-Rex-luciferase cells were maintained in medium containing 150 µg/ml Zeocin, 10 µg/ml blasticidin, and 400 µg/ml G418. Cells stably expressing pGIPZ shRNAs were generated by infecting cells with the indicated viral medium and selected with 3 µg/mL Puromycin (Calbiochem cat. # 540222) for 48 hours and maintained in a medium containing 2 µg/mL Puromycin.

**2.17 Subcellular fractionation**

Subcellular fractionations were performed as previously described (Mendez and Stillman, 2000). Briefly, 1 x$10^7$ Cells were lysed in 200 µl Buffer A (10 mM HEPES, pH 7.9, 10 mM KCl, 1.5 mM $MgCl_2$, 0.34 M sucrose, 10% glycerol, 0.1% Triton X-100, 1 mM DTT, 1 mM PMSF, protease inhibitor). Lysed cells were separated nuclei from a crude cytoplasmic fraction (S1), which was further clarified by high-speed centrifugation. The supernatant was marked as the cytoplasmic fraction (S2). Nuclei were washed twice in Buffer A and then lysed in 100 µl Buffer B (3 mM EDTA, 0.2 mM EGTA, 1 mM DTT, 1 mM PMSF, protease inhibitor) to separate insoluble chromatin in the pellet (P3) from soluble nuclear protein in the supernatant (S3). P3 was washed once in Buffer B and resuspended in 200ul of 2X SDS loading buffer, boiled for 10min, and sonicated for 15 sec 25% amplitude using EpiShear Probe Sonicator (Active Motif, Model CL-18). S2, S3 and P3 were used for western blot analysis.

### 2.18 Quantitative RT-PCR analysis

Equal number of 293T cells or MDA-MB-231 cells expressing either non-targeting shRNA or shRNA targeting USP44 were seeded in 60 mm dishes. Cells were harvested after 24 hours and Total RNA was isolated using an RNeasy purification kit (Qiagen cat# 74134) following the manufacturer's instructions. 25-50 ng of total RNA was used as a template in each RT-qPCR reaction. The RT-qPCRs were performed using a 7500 Fast Real-Time PCR System (Applied Biosystems) and the Power SYBR Green RNA-to-$C_T$ 1 step kit (Applied Biosystems cat.# 4389986). GAPDH was used as an internal control. Three technical replicates were used for each target per reaction.

### 2.19 ChIP-qPCR

Chromatin IP (ChIP) was performed as described (Atanassov et al., 2016). Equal number ($10x10^6$) of 293T-Rex-luciferase cells stably expressing GAL4-TBL1XR1 upon doxycycline induction were seeded in 10 cm dishes and then transfected with pCAG-USP44-C-FH. 24 hours post transfection, cells were treated with 100 ng/ml doxycycline. After 24 hours doxycycline induction, cells were cross-linked by adding Formaldehyde to the cultural medium (1% final concentration) and then incubated on an orbital shaker for 10-15 min at RT. The cross-linking reaction was stopped by adding glycine to the medium (final concentration 125mM) and incubation for 5 min. The medium was then aspirated and cells washed 2 times with ice-cold PBS containing protease inhibitors (PBS+PI). Cells were scraped into 4 ml ice cold PBS+PI, moved to 15 ml Falcon tubes and pelleted by centrifugation for 8 min at 3500g at 4°C. The cell pellets were resuspended in 2 ml PBS+PI, moved to two 1.5 ml tubes 1 ml in each and centrifuged again for 3 min at 2500g at 4°C. After aspiration of the supernatant, the cell pellets were resuspended in 1 ml of cell lysis buffer +PI and incubated on ice for 10 min. Tubes were

flipped every 3-4 minutes by hand to keep the cells in suspension. After this incubation, cells were pelleted by centrifugation at 2500g for 5 min and the supernatants removed. Each pellet was then resuspended in 300µL of nuclei lysis buffer+PI, moved to 1.5 ml TPX tubes (Diagenode cat# C30010010-1000) and incubated on ice for 5 min. Tubes were then assembled onto a Bioruptor sample rotor (Bioruptor Plus sonication device) and sonicated for 50 cycles (30sec on/30sec off) with 5 min interval between every 10 cycles with the temperature of the water in the sonication chamber kept between 4°C and 5°C. After the sonication, samples were centrifuged at 15000 rpm for 10 min at 4°C and supernatants carefully transferred to new 1.5 ml tubes. At this point, 5µL from each sample was used to check the DNA fragment size and concentration after reversion of the cross-links, following RNase treatment and purification of the DNA using a PCR purification kit (Qiagen). Equal amounts of chromatin (30 µg) was used for each ChIP reaction. The volume of the sonicated chromatin in each sample was justified with nuclei lysis buffer, and then diluted 10 times with ChIP dilution buffer (usually 2 mL final volume). The diluted chromatins were then pre-cleared by BSA-blocked protein-G agarose beads and incubating for 30 min using 360° rotor at 4°C (30 µl per antibody). After the pre-clearing step, the beads were spin down at 1000 rpm, 1 min at 4 °C and the clear supernatants were moved to new tubes, and 100µL (5%) were removed as an input (the inputs were kept at -20 °C until ready to be processed together with the ChIP reactions). Indicated antibodies (2-5 µg) or anti-HA beads were added to each tube and incubated on a 360° rotor overnight at 4°C. After this incubation, 50µL BSA-blocked protein–G agarose beads were added to each ChIP reaction, and mixtures were incubated on a 360° rotor for 1-2 hours at 4°C. After this incubation, beads were washed as follows (5 min on a rocking platform at 4 °C at each step): Low salt wash buffer (20mM Tric-Cl pH 8.0, 150mM NaCl, 2mM EDTA, 1% Triton X-100, 0.1% SDS) High salt

wash buffer (20mM Tris-Cl pH 8.0, 500mM NaCl, 2mM EDTA, 1% Triton X-100, 0.1% SDS), LiCl wash buffer (20 mM Tris-Cl pH 8.0, 250 mM LiCl, 1 mM EDTA, 1% NP-40, 1% Sodium deoxycholate), TE buffer (10 mM Tris-Cl pH 8.0, 1 mM EDTA). Beads were harvested by centrifugation at 1000 rpm, 1min and the supernatants were removed after each wash. Precipitated chromatin was eluted using 50µL of elution buffer (50 mM NaHCO3, 1% SDS, freshly made) to each tube and incubating for 15 min at room temperature, flicking the tubes every 2-3 min to keep the beads in suspension. After this incubation, the beads were spin down, and the clear elutes were moved to new tubes. The elution procedure was repeated one more time for a total of 100µL eluate for each ChIP reaction. For reversing the cross-links, 8 µl 4 M NaCl was added to each sample to final concentration 300 mM, and samples were incubated at 65°C in hybridization oven overnight. The volume of the inputs collected above was adjusted to 100µL with ChIP elution buffer, and these samples were processed in the same way, together with the ChIP reactions. After this incubation, 1µL of DNase free, RNase A (10mg/ml) (boiled for 10 min before use) was added to each sample and the samples were incubated at 37°C for 1 hour. The DNA in each sample was purified using a PCR purification kit (Qiagen, cat# 28106) and eluted in 50 µl (twice, 25 µL each time) nuclease-free water (Ambion, cat# AM9937). 1-2 µl eluted DNA of each antibody was used as template for qPCR with specific primers. 5% input was diluted to 1% with nuclease-free water and then use 1-2 µl for qPCR. The rest of eluted DNAs were stored at -20 °C.

**2.20 Luciferase activity assay**

Luciferase activity assay was performed as previously described (Gao et al., 2014). with modifications. Briefly, 293T-REx-luciferase cells (Vaquero et al., 2004) stably integrated with pINTO-GAL4 empty vector or with inserts of interest were treated

with100 ng/ml doxycycline. After 24 hours doxycycline induction, cells were lysed in passive lysis buffer and shaking for 15 min at RT. The cell lysate was centrifuged at 15000 rpm for 10 min and the protein concentration of the resulting supernatant was determined by Bradford assay. 10-25 µg of the supernatant was used for luciferase activity assay with luciferase assay substrate (Promega, cat# E1500) using GloMax-96 Microplate Luminometer (Promega).

**2.21 Transwell invasion assay**

Invasion assay was performed according to the manufacturer' s instructions (Corning, cat# 354480). Briefly, rehydrated Matrigel invasion chambers were placed in 24-well plates with normal culture medium. 50,000 of MDA-MB-231 cells suspended in DMEM containing 0.1% BSA were seeded on the upper layer of the chambers. After 48 hours incubation at 37°C with 5% $CO_2$, the membranes at the bottom of chambers were fixed with methanol for 3 min and stained with 0.5% crystal violet for 5-10 min. Then the cells above the membranes were removed using cotton swabs. Membranes were dried and cells attached below the membranes were imaged using microscope (ZEISS, Axiovert 40 CFL).

**2.22 Mice**

Mouse sperm harboring Usp22FloxFrt allele were obtained from the Knock Out Mouse Project (KOMP) and then sent to MD Anderson Cancer Center Genetically Engineered Mouse Facility for in vitro fertilization. Rosa-Flpase mice (stock no: 009086), Pcp2-Cre mice (stock no: 004146) and hGFAP-Cre mice (stock no: 004600) were purchased from the Jackson Laboratory. Mice were housed with same sex littermates and had free access to lab chow and water after weaning. Mice were maintained on a 12-h light/dark

cycle (lights on at 06:00). The laboratory temperature remained at 21 ± 1 °C. All behavioural experiments were started at 09:00 ± 1 h and performed under protocols approved by the M. D. Anderson Cancer Center IACUC and in accordance with NIH Principles of Laboratory Animal Care guidelines.

| Oligo Name | Sequence (5'-3') |
|---|---|
| HA-USP22-Mlu I-F | CGACGCGTCGGTAGCTTGGGGCCACCATGTACCCATACGATGTTCCAGAT TACGCTGTGTCCCGGCCAGAGCC |
| V5-USP22-Mlu I-F | CGACGCGTCGGTAGCTTGGGGCCACCATGGGTAAGCCTATCCCTAAC CCTCTCCTCGGTCTCGATTCTACG GTG TCC CGG CCA GAG CC |
| USP22-Nde I-R | GGAATTCCATATGGAATTCCCTACTCGTATTCCAGGAACTGTTTG |
| Flag-ATXN7L3-Mlu I-F | CGAACGCGTCGGTAGCTTGGGGCCACCATGGATTACAAG GATGACGAC GATAAGTCGCGAATG AAAATGGAGGAAATGTCTTTGTCTG |
| V5-ATXN7L3-Mlu I-F | CGACGCGTCGGTAGCTTGGGGCCACCATGGGTAAGCCTATCCCTAACC CTCTCCTCGGTCTCGATTCTACGAAAATGGAGGAAATGTCTTTGTCTG |
| ATXN7L3-Nde I-R | GGAATTC CATATG GAATTCC TCAGTTGATGTCATCATAGATGCTGGG |
| Flag-ENY2-Mlu I-F | CGAACGCGTCGGTAGCTTGGGGCCACCATGGATTACAAGGATGAC GACGATAAGTCGCGAATGGTGGTTAGCAAGATGAACAAAGATG |
| V5-ENY2-Mlu I-F | CGACGCGTCGGTAGCTTGGGGCCACCATGGGTAAGCCTATCCCTAACC CTCTCCTCGGTCTCGATTCTACG GTGGTTAGCAAGATGAACAAAGATG |
| ENY2-Nde I-R | GGAATTCCATATGGAATTCCTTAAAGGCTGGCATGCTGAGCAAG |

**Table 3: Primers used for PCR**

| Oligo Name | Sequence (5'-3') |
|---|---|
| **RT-qPCR Primers** | |
| qhUSP44-Fwd-Exon1 | GGGGAAAGACTGATTTTGAGG |
| qhUSP44-Rev-Exon2 | CATGTTTGCACGTATCCATTG |
| qhUSP44-Fwd-Exon4 | CCAGTTGTACTCACAGAAGCCC |
| qhUSP44-Rev-Exon5 | CCTGAATCGTTTGAGGTGCAG |
| hGAPDH-Fwd | ACCCACTCCTCCACCTTTGA |
| hGAPDH- Rev | CTGTTGCTGTAGCCAAATTCGT |
| **ChIP-qPCR Primers** | |
| GAL4-Fwd | CACCGAGCGACCCTGGATAAGC |
| GAL4-Rev | GCTTCTGCCAACCGAACGGAC |

**Table 4: Primers used for RT-qPCR and ChIP-qPCR**

## Chapter 3: PolyQ expansions in ATXN7 affect solubility but not activity of the SAGA deubiquitinating module

Contents of this chapter are based on Lan, X*., Koutelou, E*., Schibler, A.C., Chen, Y.C., Grant, P.A., and Dent, S.Y. (2015). Poly(Q) expansions in ATXN7 affect solubility but not activity of the SAGA deubiquitinating module. *Mol Cell Biol 35*, 1777-1787. (* Equal contribution authors)



### 3.1 Solubility of ATXN7 polyQ is increased by incorporation into the DUBm

ATXN7 is required for tethering of the DUBm to the SAGA complex (Figure 5A), and the N-terminal zinc finger domain in ATXN7 is necessary and sufficient for the assembly and activation of the DUBm (Kohler et al., 2008; Lang et al., 2011). The N-terminal part of the yeast ATXN7 homolog (Sgf73) has been used previously for biochemical and structural analysis of the DUBm, but the yeast protein lacks N-terminal sequences present in ATXN7 where polyQ expansions occur in SCA7 disease (Figure 5B). To determine the effects of polyQ expansion on ATXN7 functions, I tested the assembly and enzymatic activity of an *in vitro* reconstituted recombinant mammalian DUBm.

I purified full length USP22, ATXN7L3, ENY2 proteins along with two forms of the ATXN7 N-terminal domain containing either 24Qs (ATXN7-24Q NT (WT) or 92Qs (ATXN7-92Q NT (mutant) from insect cells. All of the DUBm components except for ATXN7-92Q NT were expressed efficiently as individual recombinant proteins in baculovirus and were readily purified using anti-FLAG (for ATXN7, ENY2, and ATXN7L3) or anti-HA (for USP22) immunoprecipitation (Figure 5C). Expression of

ATXN7-92Q NT was undetectable (Figure 5C, lane 5), so we initially focused on defining interactions of ATXN7-24Q NT with other DUBm components. Previous reports indicated that USP22 interacted with ATXN7L3 but not ENY2, as detected by immunoprecipitation after co-expression of USP22 and ATXN7L3 or USP22 and ENY2 in insect cells, respectively (Zhao et al., 2008). I found that USP22 directly interacted with ATXN7L3, as well as with ATXN7-24Q NT, but not with ENY2, using *in vitro* binding assays after mixing individually purified recombinant DUBm subunits (Figure 6). These results suggest ENY2 is incorporated into the DUBm through interactions with ATXN7L3 and/or ATXN7, which in turn interact with USP22.

The apparent lack of expression of ATXN7-92Q NT could reflect a defect in cDNA transcription, a defect in translation of the recombinant protein, a defect in the solubility of the protein, or a problem with protein stability. ATXN7-polyQ proteins form aggregates in mammalian cells (McCullough et al., 2012), so I re-examined our baculovirus supernatant and pellet fractions for expression of the ATXN7-24Q NT and ATXN7-92Q NT proteins. I found that ATXN7-24Q NT was soluble, as the main fraction of the protein was detected in the supernatant (Figure 5D, lanes 3 and 4), whereas the majority of ATXN7-92Q NT was insoluble and was detected mainly in the pellet (Figure 5D, lanes 5 and 6). Importantly, solubility of ATXN7-92Q NT was greatly increased upon co-expression with other DUBm components, as decreased levels of the insoluble protein were observed, with a corresponding increase in levels of the soluble form, in cellular extracts from cells expressing all four subunits (Figure 5D, lanes 7 and 8). I successfully isolated reconstituted DUBm complexes containing ATXN7-24Q NT or ATXN7-92Q NT using single affinity purification using HA agarose beads, and I verified the presence of all four subunits both by colloidal staining (Figure 5E) and by immunoblotting with anti-HA and anti-FLAG antibodies against the tagged subunits (Figure 5F). These results indicate that polyQ expanded forms of ATXN7 do not prevent

interactions with other DUB components, and that solubility and proper folding of ATXN7-92Q NT, which is prone to aggregate, were enhanced after the incorporation into the DUB complex.

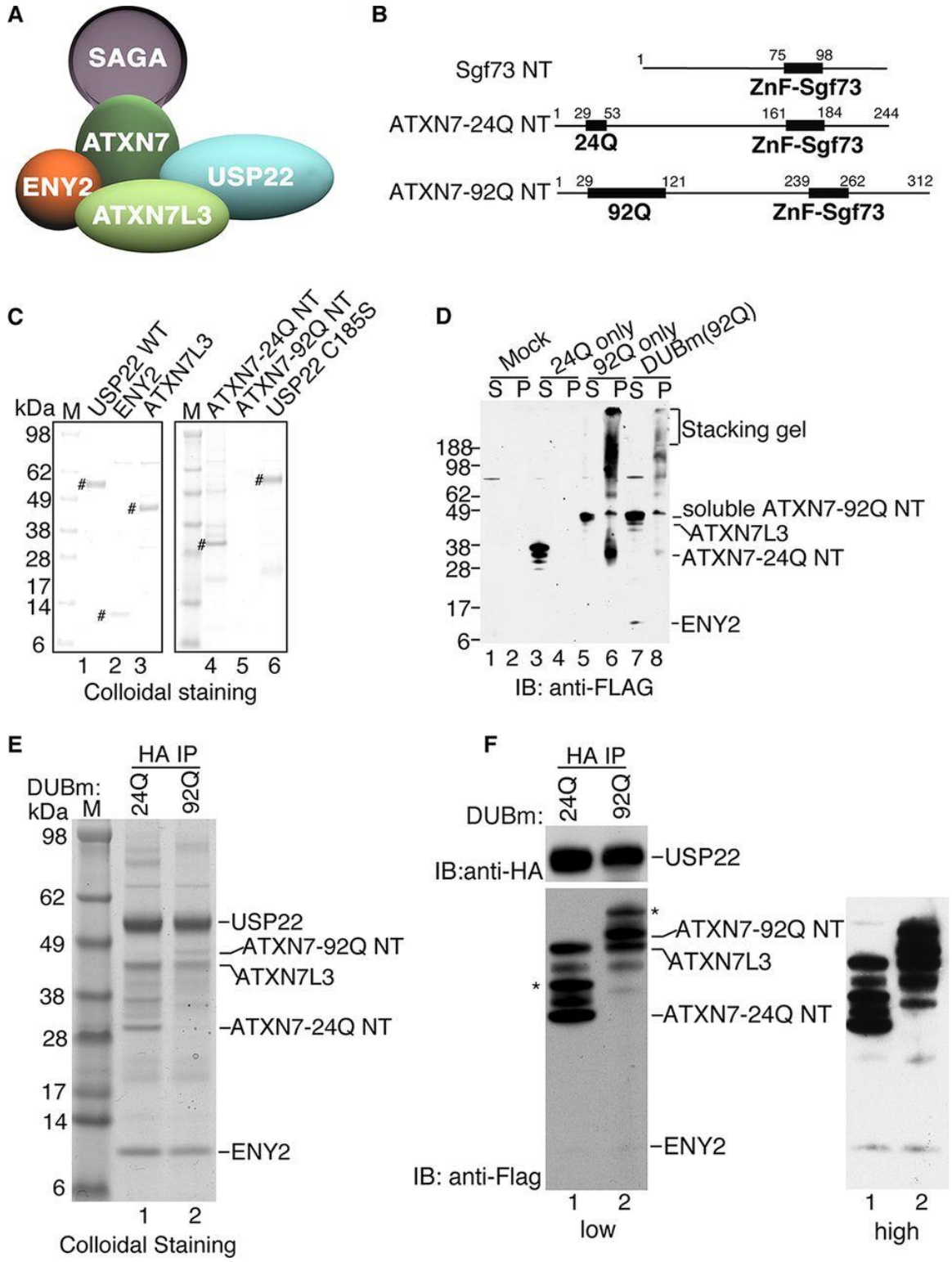


**Figure 5: Reconstitution of the mammalian DUBm.**

**Figure 5: Reconstitution of the mammalian DUBm.**

(**A**) Schematic of the mammalian SAGA DUBm. (**B**) Schematic representation of ATXN7 N-terminal fragments with 24 Q residues and 92 Q residues, where Q is glutamine. (**C**) Colloidal staining of DUBm subunits after elution with HA or Flag peptides from immunoaffinity agarose beads. The expression levels are similar for all the subunits analysed, with the exception of the expression level for ATXN7-92Q NT. #, purified DUBm subunits in each lane. (**D**) Expression of exogenous Flag-ATXN7 NT in WCEs from Sf21 insect cells after cellular fractionation at 3 days postinfection in order to assess the solubility of ATXN7-24Q NT and ATXN7-92Q NT. Lanes S, supernatant (soluble fraction); lanes P, pellet (insoluble fraction). Numbers on the left are molecular masses (in kilodaltons). (**E**) Colloidal staining of the reconstituted DUBm with ATXN7-24Q NT or ATXN7-92Q NT after anti-HA (USP22) immunoprecipitation. (**F**) Immunoblot analysis of the reconstituted DUBm for which the results are presented in panel E. ATXN7-24Q NT or ATXN7-92Q NT, ATXN7L3, and ENY2 are all Flag tagged and are detected with anti-Flag antibody; HA-USP22 is detected with anti-HA antibody. "*" modified forms of ATXN7-24Q NT or ATXN7-92Q NT due to ubiquitination (data not shown). Lanes M (C and E), molecular mass markers; IB, immunoblot analysis; IP, immunoprecipitation analysis.

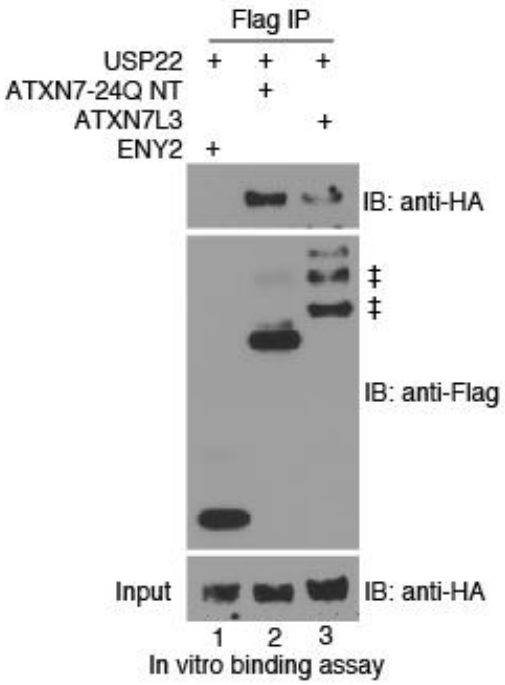


**Figure 6: In vitro binding assay shows USP22 directly interacts with ATXN7 or ATXN7L3, but not with ENY2.**

Purified recombinant USP22 was incubated with recombinant ATXN7-24Q, ATXN7L3 or ENY2 in elution base buffer at 16 $^{o}$C for 1 hr and precipitated with anti-FLAG agarose beads. After three washes with wash buffer, bound proteins were eluted with FLAG peptide and analyzed by immunoblotting with anti-HA and anti-FLAG antibodies. '‡' Daggers denote degradation products of ATXN7L3 due to its incubation at 16 $^{o}$C. USP22 was tagged with HA; ATXN7-24Q NT, ATXN7L3 and ENY2 were tagged with a FLAG epitope.

### 3.2 ATXN7 enhances DUB activity *in vitro*

The enzymatic activity of the SAGA DUB module requires the ATXN7 homolog in yeast (Kohler et al., 2008), but it has recently been shown to be dispensable in the drosophila DUB module (Mohan et al., 2014). A study with the mammalian components found that USP22 is partially activated *in vitro* upon interaction with ATXN7L3 and ENY2, and that full activity required additional interactions with ATXN7 (Lang et al., 2011), but those studies did not address the effects of polyQ expansions as their construct lacked the region that contains the polyQ repeats. I addressed the role of wild type and mutant ATXN7 in overall DUB assembly and activity *in vitro*. I first reconstituted subcomplexes by co-infecting various combinations of the three recombinant baculoviruses into Sf21 cells. I then purified the subcomplexes by immunoprecipitation using the HA epitope on USP22, and we used the catalytically inactive USP22 C185S mutant as a negative control (Figure 7A). I found that USP22 forms tripartite subcomplexes with ATXN7L3 and ENY2 (Figure 7B, lane 1, Figure 7C, lane 2), with ATXN7-24Q NT and ENY2 (Figure 7D, lane 1), or with ATXN7-24Q NT and ATXN7L3 (Figure 7D, lane 2). I tried to reconstitute subcomplexes by co-infecting combinations of two recombinant proteins in order to test the stability of these pairwise interactions, but we found that the USP22-ATXN7-24Q subcomplex was the only stable two-component complex formed (Figure 7D, lane 4). Although USP22 can interact with either ATXN7-24Q or ATXN7L3, the formation of stable subcomplexes requires the presence of more than two subunits of the DUBm, indicating that these interactions impact not only the enzymatic activity of the DUBm, but also the stability of the complex.

I next characterized the DUB activity of these subcomplexes using core histones (isolated from human 293T cells), which include H2Bub (Figure 8A, lane 1), as substrates. No H2Bub DUB activity was detected in the presence of USP22 alone (Figure 8A, lane 2) or with the USP22 C185S mutant (Figure 8A, lanes 3 and 5), as

expected. As previously reported, USP22 efficiently deubiquitinated H2Bub when in complex with ATXN7L3 and ENY2 within two hours of incubation (Figure 8B, lane 3), whereas DUBm subcomplexes that lacked ATXN7L3 or ENY2, did not (Figure 8B, lanes 2, 4, 5 and 6). These results are consistent with a recent report that the Drosophila SAGA DUBm is active without ATXN7 (Mohan et al., 2014). Importantly, a time course experiment reveals that ATXN7-24Q NT further stimulates the activity of the mammalian DUBm, as deubiquitination of both H2B (Figure 8C, compare lanes 5, 6, 7, and 8 to lanes 9, 10, 11 and 12) and H2A (Figure 8D, compare lanes 5, 6, 7 and 8 to lanes 9, 10, 11 and 12) is significantly more efficient in the presence of ATXN7. Deubiquitination of H2A and H2B in mononucleosomes is also more efficient in the presence of ATXN7-24Q NT (Figure 8E, compare lanes 5, 6, 7 and 8 to lanes 9, 10, 11 and 12 and data not shown).

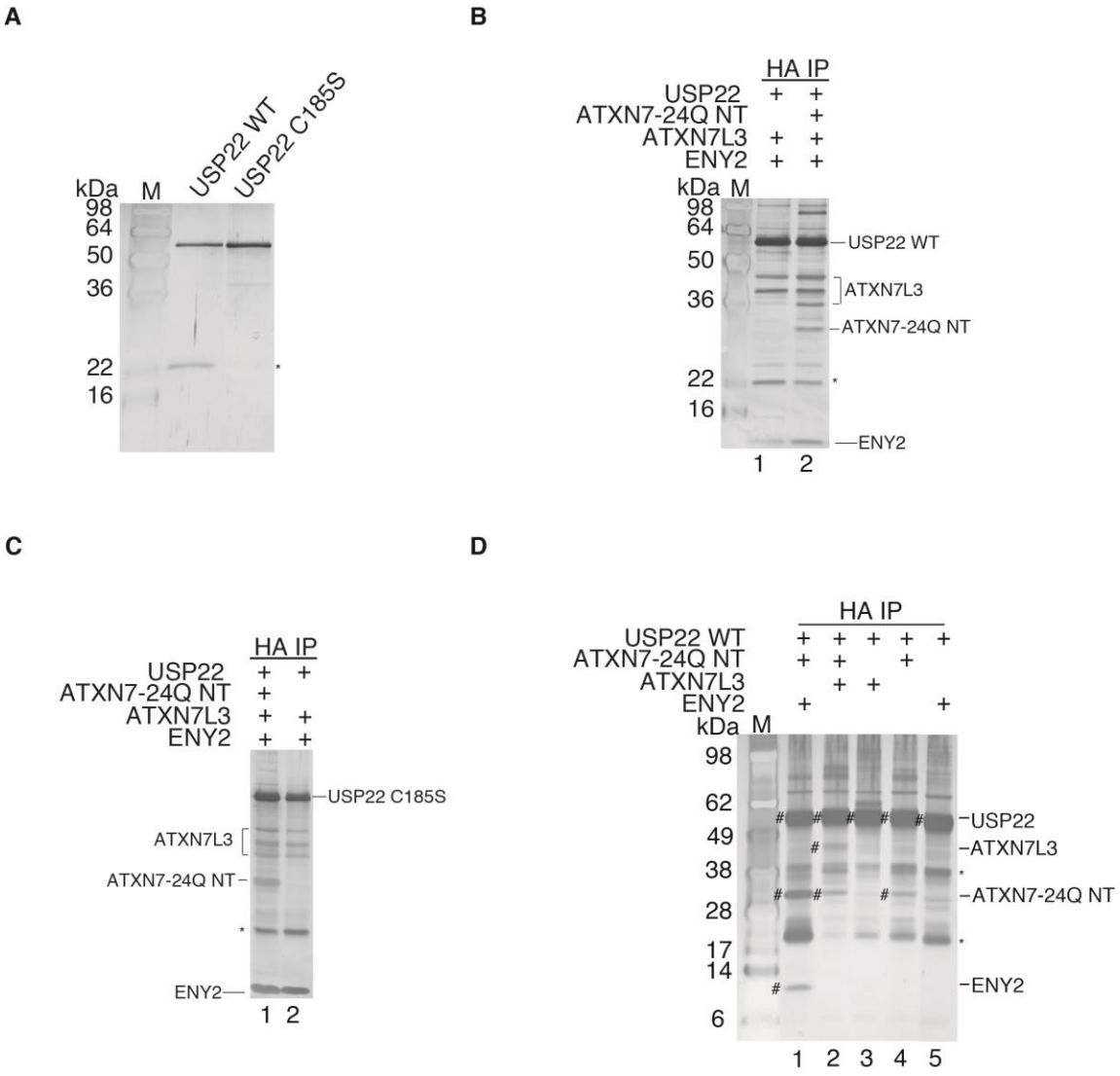


**Figure 7: Reconstitution of mammalian DUBm sub-complex.**

(A-D) Silver stainings of polyacrylamide gels displaying recombinant USP22 and different subcomplexes of DUBm eluted from HA agarose beads after USP22 affinity purifications to verify the expression of DUBm subunits and the purity of these recombinant proteins for control DUB assays. '*' denotes degradation products of ATXN7L3 or USP22. '#' on left of bands in (D) indicates the DUBm subunits purified in different combinations. USP22 WT or catalytic mutant was tagged with HA; ATXN7-24Q or 92Q NT, ATXN7L3 and ENY2 were tagged with FLAG.

To further assess the stimulation of DUB activity by ATXN7-24Q NT, I used a fluorescent substrate, ubiquitin C-terminal 7-amido-4-methylcounmarin (Ub-AMC), which provides a more quantitative assay for ubiquitin C-terminal hydrolase activity (Case and Stein, 2006). I confirmed the requirement of ATXN7-24Q NT for robust Ub-AMC hydrolyzing activity, whereas the reconstituted DUBm without ATXN7-24Q NT showed only minimal activity (Figure 9A). Similarly, the DUBm without ATXN7L3 or ENY2 had no detectable activity on Ub-AMC (Figure 9B). To extend these observations, I assayed the enzymatic activity of the different DUBm subcomplexes using ubiquitin vinyl sulfone (Ub-VS). Ub-VS is a DUB inhibitor, and it covalently attaches to the active site of the catalytic DUB subunit causing a shifted migration upon gel electrophoresis (Borodovsky et al., 2001). Although some shift of USP22 alone was observed when using higher concentrations of Ub-VS (1μM vs 5 μM) (Figure 9C, compare lane 1 with Figure 9D lane 1), both ATXN7L3 and ENY2 strongly promoted reactivity (Figure 9C-E), and this reactivity was further stimulated by ATXN7-24Q NT (Figure 9F). Altogether, these results demonstrate that ATXN7L3 and ENY2 are required for minimal activation of USP22, but ATXN7 significantly stimulates this enzymatic activity.

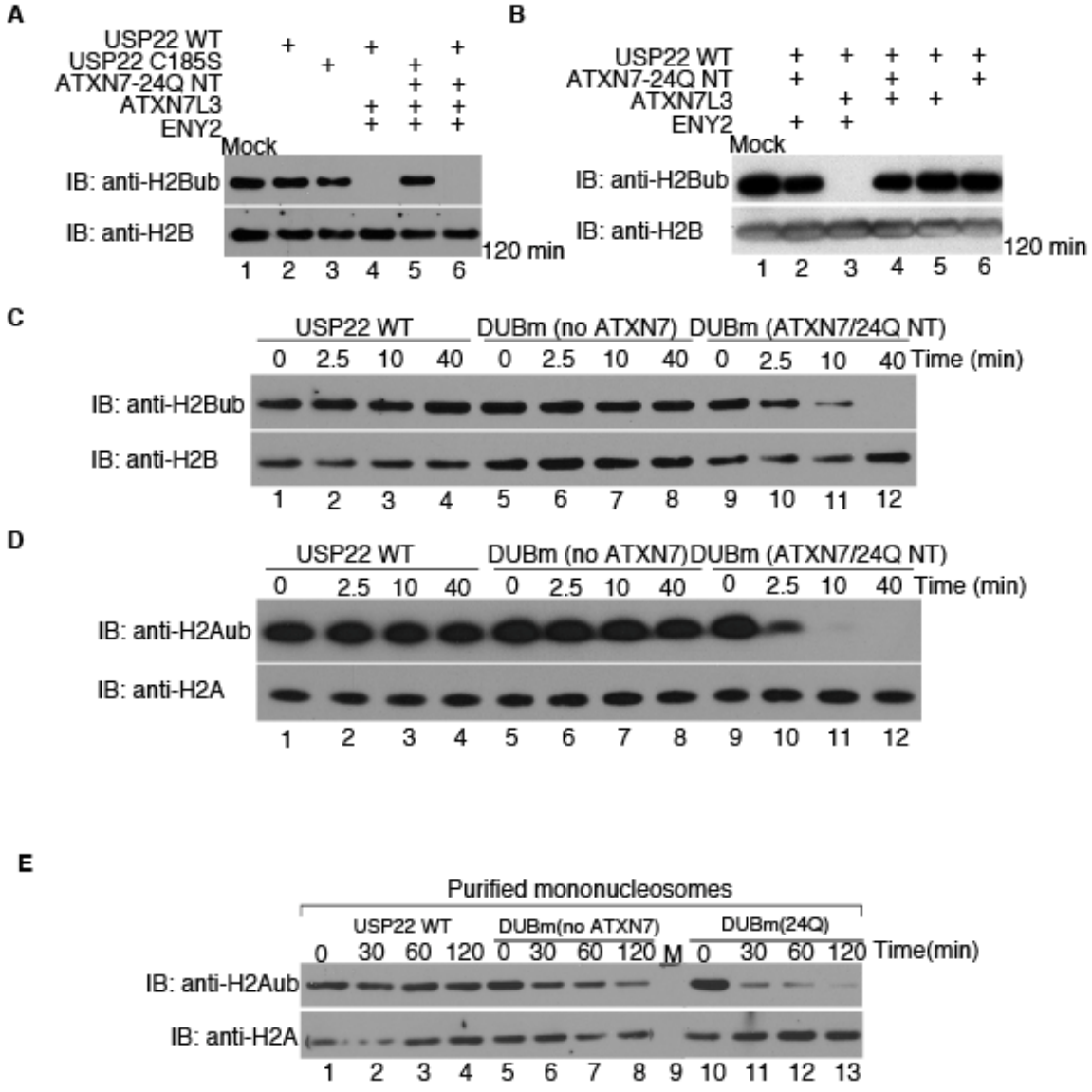


**Figure 8: ATXN7-24Q NT promotes robust DUB activity of the DUBm *in vitro*.**

**Figure 8: ATXN7-24Q NT promotes robust DUB activity of the DUBm *in vitro*.**

(A) *In vitro* deubiquitination assays using core histones as the substrates were performed with USP22 alone (lanes 2 and 3), trimeric DUBm (no ATXN7-24Q NT; lane 4), and tetrameric DUBm (with ATXN7-24Q NT, lanes 5 and 6). The USP22 C185S catalytically inactive mutant served as a negative control (lanes 3 and 5). The trimeric and tetrameric complexes had similar activities on ubiquitinated H2B after 2 h. (B) *In vitro* DUB assays using core histones were performed for different combinations of DUBm subunits coinfected in Sf21 insect cells, in order to test potential enzymatic activity. Similar amounts of USP22 in these complexes were incubated with core histones for 2 h. No activity was observed in any dimeric complex (lanes 5 and 6), and the only trimeric complex with obvious enzymatic activity contained USP22, ATXN7L3, and ENY2 (lane 3). (C and D) *In vitro* DUB assays using core histones were performed with USP22 alone (lanes 1 to 4), DUBm (no ATXN7-24Q NT; lanes 5 to 8), and DUBm (with ATXN7-24Q NT; lanes 9 to 12), and samples were collected for analysis at the indicated time points. H2A (D) and H2B (C) ubiquitination was monitored with antibodies specific for these modifications. In all assays (A to D), core histones were purified from HEK293T cells. (E) *In vitro* DUB assay for H2A of total mononucleosomes shows that ATXN7 promotes the DUB activity of DUBm.

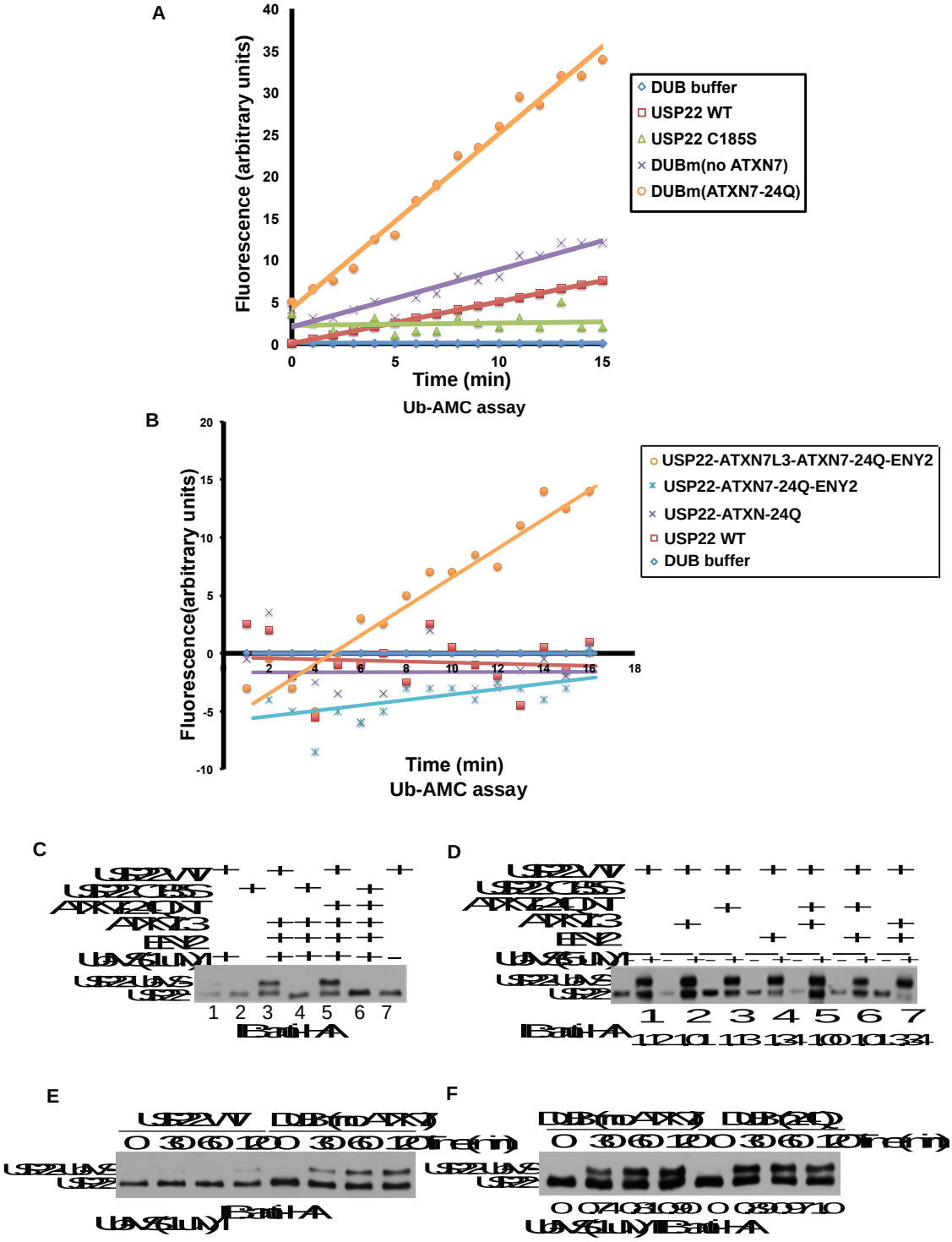


**Figure 9: Both ATXN7L3 and ENY2 are required for the activation of DUB activity of USP22 and ATXN7 further stimulates the DUB activity of DUBm.**

**Figure 9: Both ATXN7L3 and ENY2 are required for the activation of DUB activity of USP22 and ATXN7 further stimulates the DUB activity of DUBm.**

(A) Hydrolysis of ubiquitin-AMC (0.5 μM) alone or with similar amounts of recombinant USP22, DUBm (no ATXN7-24Q NT), and DUBm (with ATXN7-24Q NT). The release of AMC fluorescence was monitored by a spectrophotometer at 528 nm. The tetrameric DUBm with ATXN7-24Q NT showed the highest enzymatic activity. The USP22 WT or catalytic mutant was tagged with HA; ATXN7-24Q NT, ATXN7L3, and ENY2 were all tagged with Flag. (B) Ub-AMC hydrolysis assay using the indicated complexes. As a control, Ub-AMC was incubated with DUB buffer alone. USP22 WT or catalytic mutant was tagged by HA; ATXN7-24Q or 92Q NT, ATXN7L3 and ENY2 were tagged by Flag. C-F) Equal amounts of the different purified complexes were incubated with or without 1uM or 5 uM ubiquitin vinyl sulfone (Ub-VS), a suicide substrate of deubiquitinases at 37 $^{o}$C for 2 hrs. This compound can form a covalent bond only with active form of USP22, which is characterized by a ~7 kDa shift of the enzyme using immunoblot analysis with anti-HA antibody. The stronger activity the deubiquitinase possesses, the more shift it shows. USP22 alone shows poor activity. Quantitation of the HA-USP22-Ub-VS was normalized by HA-USP22 using ImageJ program.

### 3.3 PolyQ ATXN7 does not impair the assembly or activity of the DUBm *in vitro*

Due to the decreased solubility of ATXN7-92Q NT, it was difficult to isolate this protein as part of the DUBm complex *in vitro* (Figure 5E, lane 2). To determine whether I could increase ATXN7-92Q NT amounts to a more stoichiometric ratio in the complex, I first titrated increasing amounts of the ATXN7-92Q NT recombinant baculovirus relative to those expressing the other subunits, and then isolated the DUBm complex by immunoprecipitation using the HA epitope on USP22. I analyzed the isolated reconstituted DUBm complexes both by silver staining (Figure 10A) and by immunoblot using anti-HA and anti-FLAG antibodies against the tagged subunits (Figure 10B). Increasing amounts of ATXN7-92Q NT protein were detected after single step purification of USP22 associated proteins, but the silver stained gel indicated that this subunit was still present in sub-stoichiometric levels relative to other components, indicating ATXN7-92Q NT was incorporated into a minority of the isolated complexes. However, ATXN7-92Q NT greatly enhanced the activity of the DUBm, as showed by Ub-AMC assays and in vitro DUB assay (Figure 10C-D), even when present at sub-stoichiometric levels. To better assess the effects of the polyQ expansions on DUBm, I next performed a double affinity purification using sequential anti-HA and anti-FLAG immunoprecipitations. The components of the purified DUBm complex were again monitored by electrophoresis (colloidal staining; Figure 11A) and by immunoblot with anti-HA and anti-FLAG antibodies (Figure 11B). The amounts of DUBm subunits incorporated into the complexes containing ATXN7-24Q NT and ATXN7-92 NT were present in similar ratios (Figure 11B), so I performed Ub-AMC assays to directly compare their enzymatic activities I observed no difference between the ability of the two complexes to hydrolyze Ub-AMC (Figure 11C).

To further confirm these results, I repurified the DUBm using HA immunoprecipitation followed by gel filtration to remove free HA-USP22 as well as

partially formed complexes. Immunoblotting analysis of the column fractions indicated that the fully assembled DUB complex eluted with an apparent molecular weight of ~200 kDa (Figure 11D-E). The differences in solubility of the two ATXN7 polyQ proteins did not directly affect the assembly of DUB module as, once incorporated, ATXN7-24Q NT and ATXN7-92Q NT were both associated with similar amounts of the other DUBm subunits (Figure 11F). In order to assay equivalent amounts of the reconstituted DUB module, I normalized amounts of ATXN7-24Q NT with ATXN7-92Q NT collected from fractions 23 and 24, as confirmed by western blot (Figure 11F), and then carried out DUB assays using core histones or mononucleosomes as substrates. Importantly, I again found that ATXN7-92Q NT stimulated DUB activity to the same degree as ATXN7-24Q NT (Figure 11G-H). Our results demonstrate that a polyQ expansion in ATXN7 equivalent to those found in SCA7 patients does not affect the enzymatic activity of the SAGA DUBm *in vitro*.

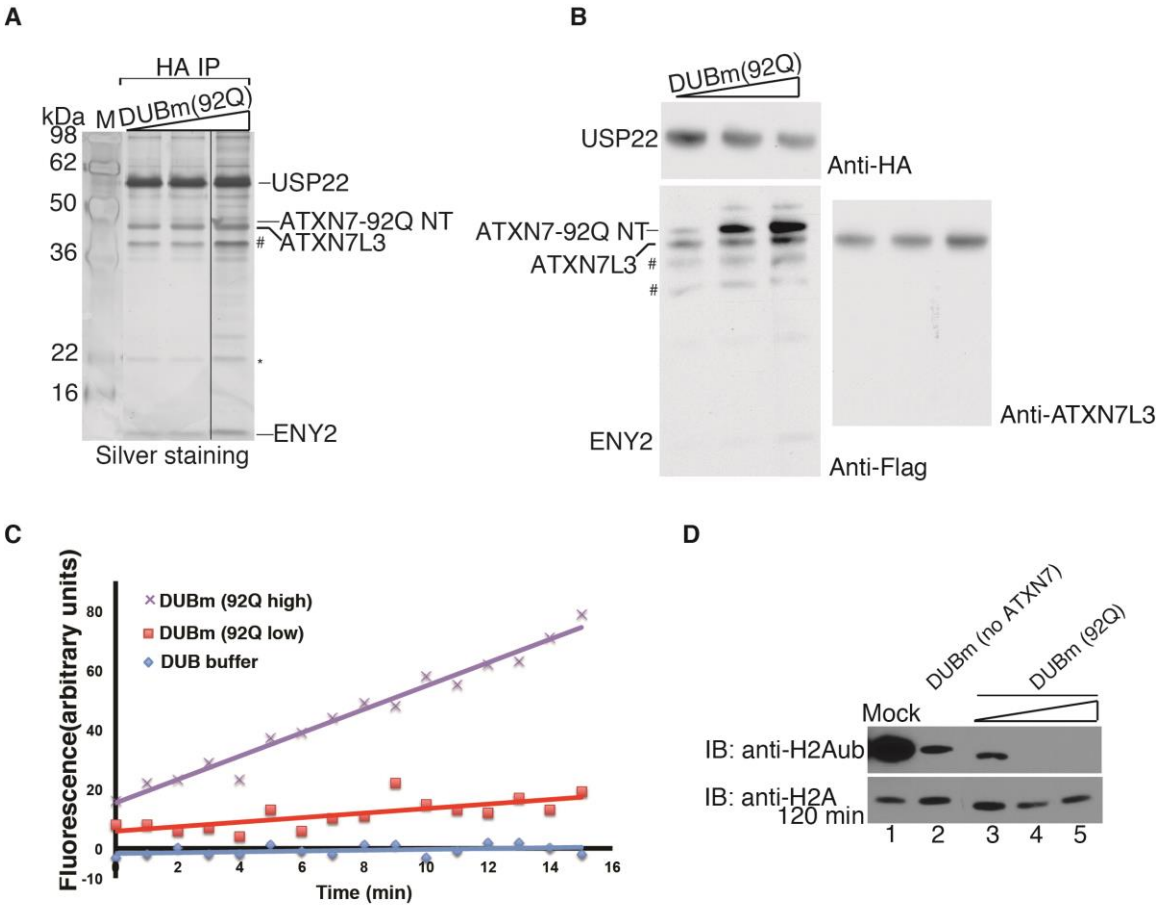


**Figure 10: Increased incorporation of ATXN7-92Q into DUBm promotes DUBm activity.**

**Figure 10. Increased incorporation of ATXN7-92Q into DUBm promotes DUBm activity.**

(A) Silver staining of DUBm with increasing amounts of subunit ATXN7-92Q NT after anti-HA (USP22) precipitation. Similar titers of USP22, ATXN7L3, ENY2 baculoviruses and increasing titers of ATXN7-92Q NT baculovirus were used to co-infect Sf21 cells, respectively. After 4-6 days of infection, anti-HA affinity matrix was used to purify these complexes. Increasing amounts of ATXN7-92Q NT protein incorporated into the DUBm are detected. (B) Immunoblot analysis of the reconstituted DUBm described in A, using anti-HA (USP22), anti-FLAG (ATXN7, ENY2, and ATNX7L3) and anti-ATXN7L3 antibodies. A tetrameric complex with all four subunits in the presence of ATXN7-92Q NT is observed. Degradation fragments are labeled with '#'. "*" Asterisk denotes modified forms of ATXN7-92Q NT due to ubiquitination (data not shown). (C) Comparative Ub-AMC hydrolysis assays using the reconstituted DUBm complexes with increasing amounts of ATXN7-92Q NT show that the more ATXN7-92Q NT incorporated into the complex, the more robust the enzymatic activity of the reconstituted DUBm (I used 1x (low) and 3x (high) amounts for the comparison). (D) In vitro DUB assays using purified total histones as the substrate were performed with DUB modules containing increased amounts of subunit ATXN7-92Q NT after anti-HA (USP22) precipitation, and H2A ubiquitination levels were monitored with antibodies specific for this modification. H2A served as a loading control.

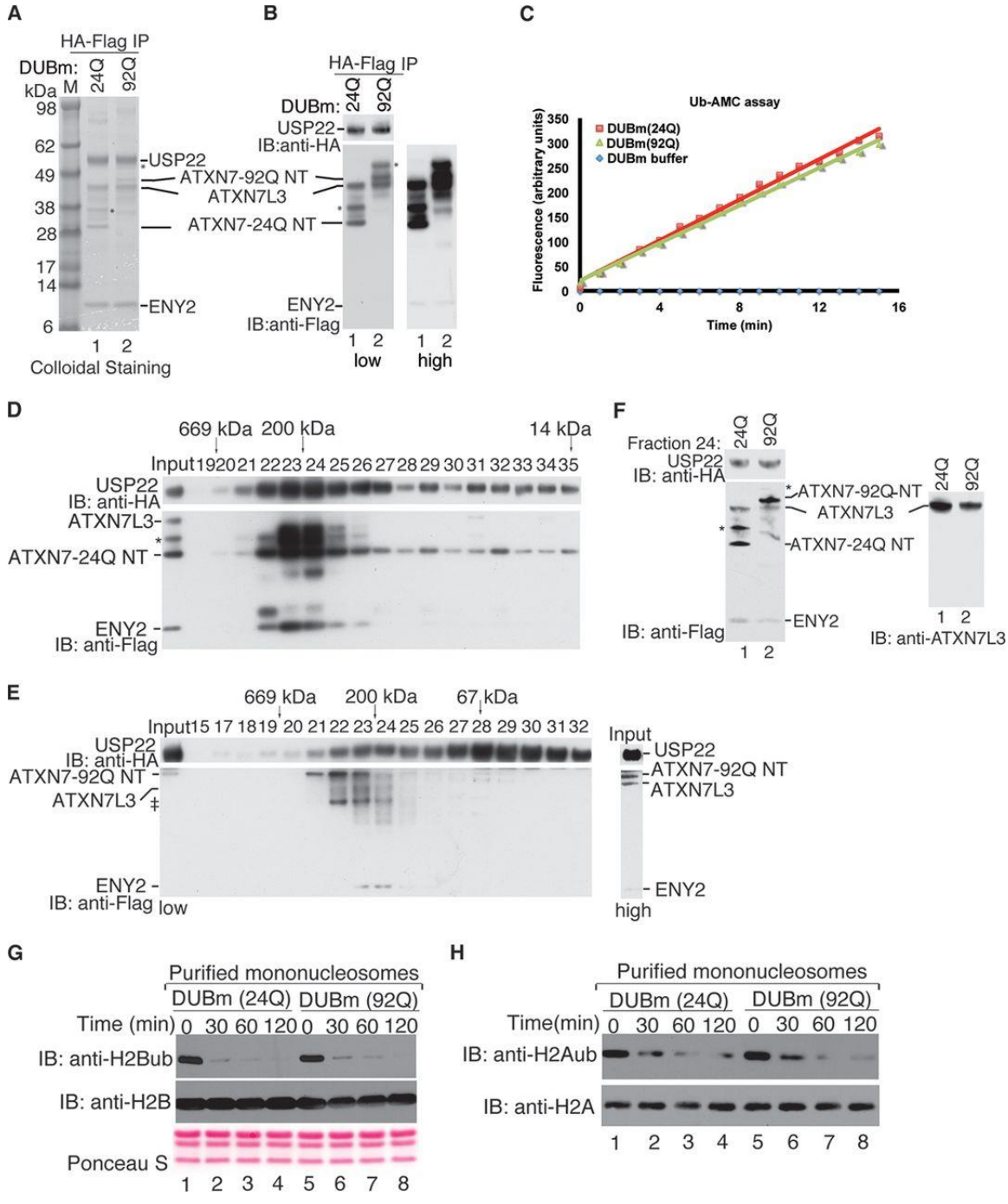


**Figure 11: ATXN7-92Q NT is not defective in promoting DUBm activity.**

**Figure 11: ATXN7-92Q NT is not defective in promoting DUBm activity.**

(A) Purification of the recombinant DUBm using two sequential affinity precipitations with anti-HA– and anti-Flag–agarose beads, respectively. Comparison of the two purified DUBm complexes containing ATXN7-24Q NT or ATXN7-92Q NT with colloidal staining shows very similar ratios of the DUBm subunits. Lane M, molecular mass markers. (B) Immunoblot analysis (low and high exposures are shown) of the DUBm after double-affinity purification (A) verifies the identities and the presence of similar amounts of DUBm components. The different subunits were detected with anti-HA and anti-Flag antibodies, as indicated. "*" modified forms of ATXN7-24Q NT or ATXN7-92Q NT due to ubiquitination (data not shown). (C) Comparative Ub-AMC hydrolysis assays using the reconstituted DUBm complexes with either ATXN7-24Q NT or ATXN7-92Q NT after the double-affinity purification confirm the very similar deubiquitinating activities between the two complexes. (D and E) Purification of reconstituted DUBm containing ATXN7-24Q NT (C) or ATXN7-92Q NT (D) by size exclusion chromatography using Superdex 200 gel filtration. Column fractions (numbers above the blots) were analyzed by immunoblotting with anti-HA (USP22) and anti-Flag (ATXN7, ATXN7L3, and ENY2) antibodies, and band positions for these components are as indicated. The elution profile of protein markers is indicated at the top of the blots. A complex containing all four subunits, including either ATXN7-24Q NT or ATXN7-92Q NT, is present in fractions 23 and 24 of both purifications and corresponds to the expected molecular mass for the DUBm. A darker exposure of the input lane for the ATXN7-92Q NT purification (labeled high) is provided to confirm the presence of all components in the starting material. ‡, degradation fragments. (F) Comparison of the integrity and stoichiometry of fraction 24 of the gel filtration from panels D and E was performed by immunoblotting with anti-HA and anti-Flag antibodies. Note that the amounts of the different subunits between the two reconstituted DUBm complexes are very similar. *, modified form of ATXN7-24Q NT

or ATXN7-92Q NT due to ubiquitination (data not shown). (G and H) *In vitro* DUB assays using purified mononucleosomes as the substrate were performed with both DUB modules, and H2A and H2B ubiquitination levels were monitored with antibodies specific for these modifications. Both reconstituted complexes showed very similar enzymatic activities toward both ubiquitinated histone H2A and H2B incorporated into nucleosomes at the time points analyzed. H2A or H2B immunoblotting or Ponceau S staining served as a loading control.

### 3.4 ATXN7-92Q aggregates sequester DUBm components *in vivo*

Nuclear aggregation of polyQ proteins is a hallmark of CAG expansion disorders (Todd and Lim, 2013). Aggregates associated with ATXN7-polyQ mutant proteins also include transcriptional regulators, ubiquitin/proteasome proteins, cell death associated proteins, chaperones and protein partners (Lebre and Brice, 2003). Previous work indicates that expression of ATXN7-92Q, but not ATXN7-24Q, leads to formation of aggregates and that GCN5, the catalytic subunit of HAT module in SAGA, is sequestered into these aggregates in human astrocytes (McCullough et al., 2012). I reconfirmed aggregate formation in the presence of ATXN7-92Q (Figure 12A) and then asked whether other DUBm components were also present within the aggregates observed in astrocytes. Double immunofluorescence staining with anti-FLAG to detect ATXN7-92Q and anti-ATXN7L3 antibodies demonstrated that endogenous ATXN7L3 was present in nuclear inclusions in astrocytes (n=86) containing ATXN7-92Q aggregates (Figure 12A, middle panel and data not shown). Since the solubility of ATXN7-92Q was improved in baculovirus cells upon co-expression of other DUBm subunits (Figure 5D), I asked whether such co-expression would also increase solubility and decrease aggregation in mammalian cells. Indeed, immunoblot analyses of human astrocyte extracts showed that co-overexpression of ATXN7L3 and ENY2 promoted the solubility of ATXN7-92Q and greatly inhibited its aggregation (Fig.12B, compare lanes 3 and 4). Increased solubility of ATXN7-92Q in transfected astrocytes was also indicated by immunofluorescence, as co-overexpression of ATXN7L3 and ENY2 clearly suppressed formation of ATXN7-92Q aggregates (Figure 12A, bottom panel). I further quantified this effect by counting cells showing no aggregates (N=0), 1 or 2 aggregates (N≤2), or more than 2 aggregates (N>2). Co-overexpression of ATXN7L3 and ENY2 greatly decreased the number of cells with more than 2 aggregates per nucleus (N>2, ~10% vs ~40% when ATXN7-92Q is expressed alone) (Figure 12C). Consistent with

these results, co-localization of ATXN7L3 with nuclear inclusions also decreased upon co-overexpression of ATXN7L3 and ENY2 (Figure 12A and Figure 12D ~35% vs ~5%; n=86). Overexpression of USP22, ATXN7L3 or ENY2 alone with ATXN7-92Q did not cause any obvious decrease in aggregation of ATXN7-92Q (data not shown). These results indicate that aggregates caused by ATXN7-polyQ mutants may be cytotoxic due to sequestration of important DUBm components and that co-overexpression of ATXN7L3 and ENY2 may oppose this toxicity through suppressing aggregate formation.

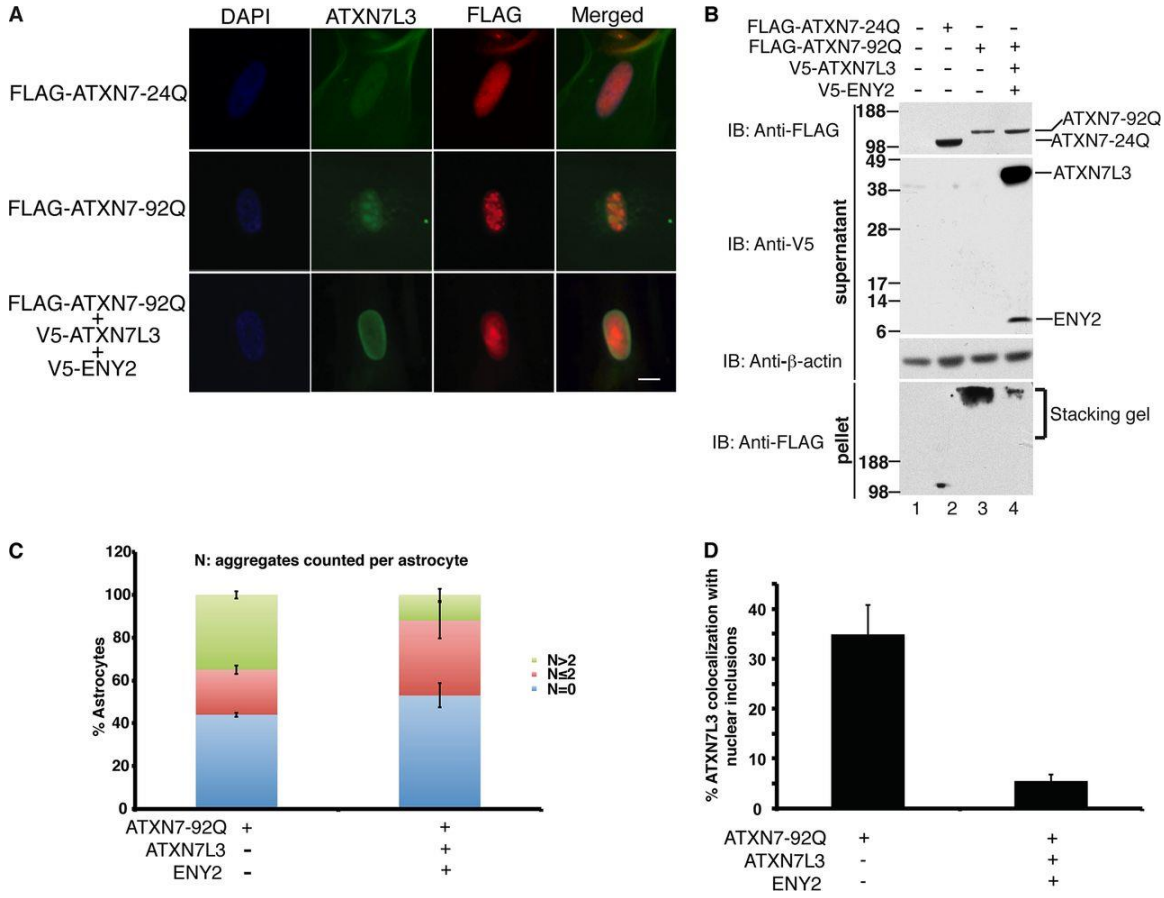


**Figure 12: Overexpression of ATXN7L3 and ENY2 prevents sequestration of ATXN7L3 into aggregates with ATXN7-92Q in vivo.**

**Figure 12: Overexpression of ATXN7L3 and ENY2 prevents sequestration of ATXN7L3 into aggregates with ATXN7-92Q in vivo.**

(A) Exogenous expression of ATXN7-92Q, but not that of ATXN7-24Q, causes aggregate formation in human astrocytes. ATXN7L3 colocalization with nuclear inclusions in ATXN7-92Q-expressing astrocytes was observed by immunofluorescence staining using anti-Flag and anti-ATXN7L3 antibodies. Co-overexpression of ATXN7L3 and ENY2 reduces this colocalization by inhibiting ATXN7-92Q aggregation. Nuclei were stained with DAPI (blue). Bar, 10 μm. (B) Upon co-overexpression of ATXN7L3 and ENY2 with ATXN7-92Q, the amount of soluble ATXN7-92Q in the supernatant fraction increased, whereas the amount of SDS-insoluble ATXN7-92Q aggregates in the pellet (trapped in the stacking gel) dramatically decreased compared to the amount obtained with overexpression of ATXN7-92Q alone. ATXN7-24Q is highly soluble. Anti-β-actin immunoblotting served as a loading control. ATXN7-24Q and ATXN7-92Q were tagged with Flag. ATXN7L3 and ENY2 were tagged with a V5 epitope. (C) Quantification of astrocytes containing nuclear inclusions. One hundred cells from multiple fields were counted and then sorted by the number of nuclear inclusions per cell (N). Three independent experiments were performed, and a two-tailed Student *t* test was used for statistical analysis; error bars represent ±SDs. (D) Quantification of astrocytes with endogenous ATXN7L3 co-localization with nuclear inclusions. Three independent experiments were performed, and a two-tailed Student *t* test was used for statistical analysis; error bars represent SDs.

### 3.5 Increased solubility of ATXN7-92Q rescues DUB activity *in vivo*

Given that depletion of ATXN7L3 caused robust increases in global H2Bub levels (Lang et al., 2011), sequestration of ATXN7L3 into ATXN7-92Q aggregates might affect global H2Bub levels. Consistent with previous work (McCullough et al., 2012), which indicated that global H2Bub levels were increased in astrocytes overexpressing ATXN7-92Q compared to those in wild type astrocytes, I found that H2Bub levels were increased in astrocytes upon over expression of ATXN7-92Q (Figure 13A). Interestingly, acetylation of H3 K9 and K14 was not altered in the ATXN7-92Q overexpressing cells, even though Gcn5 is also associated with aggregates in ATXN7 polyQ cells (McCullough et al., 2012). Importantly, co-overexpression of ATXN7L3 and ENY2 together with ATXN7-92Q opposed the increase in global H2Bub (Figure 13B, compare lane 2 to lane 4), suggesting that compromised DUB activity caused by aggregation of DUBm components can be rescued by co-overexpression of ATXN7L3 and ENY2. Together with our biochemical data that indicate ATXN7L3 and ENY2 are required to activate USP22 activity, these findings suggest that aggregates caused by ATXN7-polyQ mutant likely contribute to neuronal toxicity by impairing DUB activity through sequestering important DUBm components away from their substrates and that increased solubility of ATXN7 polyQ mutant by co-overexpression of DUBm components can counteract this toxicity.

Accumulation of ubiquitinated proteins is observed in SCA7 and other polyQ diseases in association with nuclear aggregation of the polyQ proteins, indicating that the polyQ expansions influence processing of ubiquitinated proteins *in vivo* (Ansorge et al., 2004; Cummings et al., 1998; Davies et al., 1998). To determine if sequestration of DUBm components influences H2Bub in a mouse model of SCA7 (Chen et al., 2012; Yoo et al., 2003), I extracted histones from the cerebellums of mice bearing one or two alleles of ATXN7-100Q, and compared H2Bub levels relative to histones extracted from

age matched wild type, ATXN7-5Q, mice. I found a slight increase in H2Bub levels in histones isolated from mice heterozygous for the expanded ATXN7 allele (ATXN7 100Q/5Q), and an even greater increase in H2Bub levels in ATXN7-100Q homozygous mice (Figure 13C, lanes 2 and 3). These results further indicate that DUB activity is indeed impaired by the ATXN7 polyQ expansions in a SCA7 mouse model.

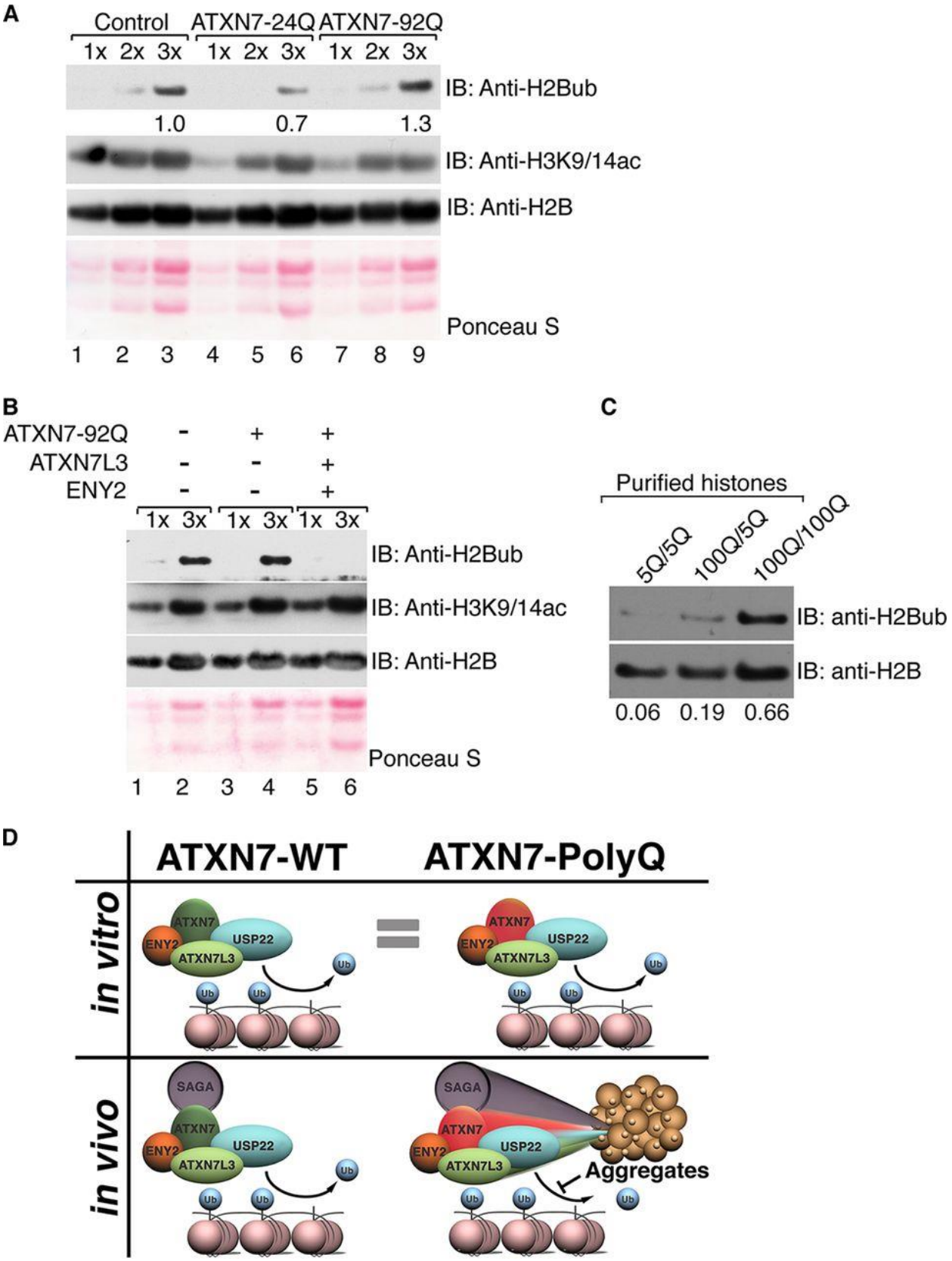


**Figure 13: Solubility of ATXN7-92Q *in vivo* correlates with DUB activity.**

**Figure 13: Solubility of ATXN7-92Q *in vivo* correlates with DUB activity.**

(A) Core histones were purified from human astrocytes infected with empty vector (lanes 1 to 3), ATXN7-24Q (lanes 4 to 6), or ATXN7-92Q (lanes 7 to 9) and were analyzed by electrophoresis of increasing sample amounts (1× to 3×), and the levels of H2Bub were monitored with antibodies specific for this modification. The levels of H2B ubiquitination increased in astrocytes expressing ATXN7-92Q, indicating impaired deubiquitination. Quantification of H2Bub levels was normalized to H2B levels using ImageJ software. (B) Cooverexpression of ATXN7L3 and ENY2 enhances global H2Bub deubiquitination in astrocytes expressing ATXN7-92Q, whereas H3K9/14ac levels are not altered. Different sample amounts (1× and 3×) were analyzed. H2B immunostaining or Ponceau S staining served as a loading control. (C) Core histones were purified from the cerebellums of 4-month-old mice bearing wild-type (5Q) or mutant (100Q) alleles of the ATXN7 gene. Both ATXN7$^{100Q/100Q}$ and ATXN7$^{100Q/5Q}$ mice exhibit SCA7 symptoms over time, but disease progression in ATXN7$^{100Q/100Q}$ mice was faster and more severe than that in ATXN7$^{100Q/5Q}$ mice. Immunoblot analysis was used to detect H2Bub levels with anti-H2Bub antibody. Samples from both ATXN7$^{100Q/100Q}$ and ATXN7$^{100Q/5Q}$ mice show increased H2B ubiquitination, with the effect being more severe in the samples from ATXN7$^{100Q/100Q}$ mice. H2Bub levels were normalized to H2B levels using ImageJ software. Representative results chosen from more than three independent experiments are shown. (D) Model of the contribution of ATXN7-poly(Q) to SCA7 disease in humans. *In vitro*, soluble DUBm with ATXN7-92Q exhibits DUB activity comparable to that of the DUBm with ATXN7-24Q. However, *in vivo* ATXN7-poly(Q) tends to form aggregates that sequester DUBm components away from their substrates. Incorporation into DUBm can help solubilize ATXN7-poly(Q) *in vitro* and *in vivo*, partially alleviating the formation of the poly(Q)-containing aggregates in astrocytes. Impaired DUB activity in the cerebellums of SCA7 patients expressing ATXN7-poly(Q) likely leads to increased global

H2Bub levels, as well as the deregulation of other DUBm substrates, contributing to SCA7 disease. *Model in figure 13D was made by Andria C. Schibler (a previous graduate student from Dr. Sharon Dent's lab, UT M.D. Anderson Cancer Center).*

### 3.6 Conclusions

In this study, we confirm that ATXN7 strongly stimulates DUB activity. Importantly, we demonstrate that ATXN7 with 92 Q residues at the N terminus (ATXN7-92Q NT) does not directly impair DUBm activity *in vitro* but that ATXN7-92Q NT is highly insoluble when not assembled into the DUBm. Co-overexpression of other DUBm subunits inhibits ATXN7-92Q aggregation *in vitro* and in human astrocytes. In addition, aggregates initiated by overexpression of ATXN7-92Q sequester ATXN7L3 and lead to increased global levels of H2Bub. Co-overexpression of ATXN7L3 and ENY2 with ATXN7-92Q ameliorates this effect. Consistent with these findings, H2Bub levels were elevated in the cerebellums of mice in a SCA7 mouse model, indicating that the impairment of DUBm activity might contribute to SCA7 disease. In conclusion, our findings suggest that ATXN7-poly(Q) causes SCA7 not by reducing USP22 activity *per se* but by forming aggregates that sequester DUBm components away from their substrates.

### 3.7 Discussion

The role of hallmark nuclear aggregates caused by polyQ expansions in the pathogenesis of neurodegenerative diseases is still under debate (Todd and Lim, 2013). Some studies suggest that nuclear inclusions are cytotoxic, while others indicate that they might be cytoprotective by functioning to sequester the misfolded disease proteins (Arrasate et al., 2004; Takahashi et al., 2008; Yang et al., 2002). Our data demonstrate that although polyQ expansions in ATXN7 have no effect on the assembly and enzymatic activity of the SAGA DUBm *in vitro*, they promote aggregation *in vivo*, further sequestering crucial activators of USP22 activity away from H2Bub and other substrates. Our data, then, indicate that the nuclear aggregates cause a loss of effective function of

ATXN7-polyQ and associated proteins *in vivo*, favoring a cytotoxic rather than a cytoprotective role for the nuclear inclusions observed in SCA7 disease (Figure 13D).

### 3.7.1 Nuclear aggregates caused by polyQ expansions are cytotoxic

Our findings are consistent with previous studies that indicate that aggregates induced by ATXN7 polyQ and other polyQ proteins cause cytotoxicity, whereas soluble forms of these proteins do not. For example, ATXN7 and soluble ATXN7-polyQ similarly associate with and equally stabilize microtubules, indicating that polyQ expansions that do not affect solubility do not affect cytoplasmic functions of ATXN7 (Nakamura et al., 2012).

At least two parameters affect ATXN7-polyQ solubility. SUMOylation attenuates the cellular toxicity of ATXN7-polyQ and promotes solubility (Janer et al., 2010). In addition, chaperone proteins, such as Hsp70 and Hsp40, promote polyQ protein solubility through assisting refolding of denatured and aggregated proteins in an ATP-dependent fashion (Hartl and Hayer-Hartl, 2002). Overexpression of Hsp70 and Hdj1/Hsp40 also significantly promote solubility and suppress the neurotoxicity of polyQ-expanded proteins in a SCA3 fly model (Chan et al., 2000).

Protein misfolding and aggregation can trigger autophagy, a process that plays essential, protective roles in neurons (Wong and Cuervo, 2010a, b). Emerging evidence indicates that autophagy may be dysfunctional in polyQ diseases (Cheung and Ip, 2011). Aggregation of ATXN7-polyQ impairs p53 driven autophagy by sequestering p53-FIP200 complexes, leading to accumulation of neuronal protein inclusions and neurodegeneration (Yu et al., 2013). Sequestration of CREB binding protein (CBP) into polyQ aggregates contributes to neuronal toxicity in Huntington's disease by interfering with CBP-mediated transcription (McCampbell et al., 2000; Nucifora et al., 2001). Also,

DnaJB1 is sequestered into nuclear inclusions of polyQ Ataxin3 in SCA3 (Seidel et al., 2012), and Huntingtin polyQ inclusions sequester the Sis1p/DnaJB1 chaperone to interfere with nuclear degradation of cytosolic proteins (Park et al., 2013). All of these studies point to the importance of preventing or reversing polyQ-induced aggregations in neurodegenerative diseases.

### 3.7.2 Associations with other subunits of DUBm improves the solubility of ATXN7-92Q

Interestingly, we observe that the solubility of ATXN7-92Q in insect cells is improved upon incorporation into the DUBm. Consistent with these findings, co-overexpression of ATXN7L3 and ENY2 in human astrocytes suppressed ATXN7-92Q aggregation, indicating that imbalances in the levels of the polyQ protein relative to the levels of the other DUB components may contribute to disease development. Samara et al (Samara et al., 2010) proposed that ATXN7 polyQ expansions would either disrupt interactions with other DUBm subunits and compromise the deubiquitinating activity, or would cause ATXN7 to aggregate, consequently preventing association with the other DUBm subunits. Despite the fact that the position of polyQ in yeast Sgf73 is different from that in mammalian ATXN7, our experiments favor the latter hypothesis, as we show that the presence of polyQ expansions do not affect the assembly or the activity of the DUBm *in vitro*. An intriguing interaction between the N-terminal portion of Sgf73, Sgf11 and Sus1 in yeast stabilizes the assembly of the DUB module and could explain how over expression of the mammalian counterparts of Sgf11 and Sus1, ENY2 and ATXN7L3, promote the solubility of polyQ ATXN7 (Kohler et al., 2010). The interaction of Ubp8 with Sgf73 does not require the N-terminal tail of Sgf73 that contains only a few residues upstream of the H1 helix in yeast. This part of the protein is, however,

fundamental in generating a three-protein junction between the N-terminal H1 helix of Sgf11, the C-terminal H5 helix of Sus1 and the N-terminal H1 helix of Sgf73, through the coordination of hydrophobic residues that come into close proximity (Kohler et al., 2010). Although structural information for mammalian ATXN7 is lacking, the N-terminal tail of the protein could be involved in similar interactions with ATXN7L3 and ENY2, and the subsequent aggregation caused by the presence of the polyQs might be prevented when these associations are formed. Although the degree of structural and functional conservation is significantly high between the yeast and the mammalian DUB module (Lang et al., 2011), the crystal structure of the mammalian DUB module would greatly enhance our understanding of the actual interfaces between the different subunits, and how they contribute to the function and solubility of the module.

PolyQ ATXN7 has also been reported to have an extended half-life relative to non-expanded ATXN7 (Yvert et al., 2001). Over time, accumulation of ATXN7-polyQ likely promotes aggregation and sequestration of DUBm components. This process might explain the delayed onset of SCA7 and also the inverse relationship between polyQ length and age of disease onset. Limiting amounts of DUBm subunits in neural or retinal cells could also explain why these specific cell types selectively degenerate in SCA7.

### 3.7.3 Nuclear aggregates caused by ATXN7-polyQ sequester both enzymatic subunits of SAGA complex

We have previously shown that that loss of Gcn5 functions contributes to SCA7 progression in a SCA7 mouse model (Chen et al., 2012) and Gcn5 is present in aggregates formed by ATXN7-92Q (McCullough et al., 2012). Our analysis of global histone levels purified from human astrocytes is in agreement with that of McCullough et al, in that H2Bub levels increase in the presence of the ATXN7-92Q overexpression with

no change in global levels of H3K9/K14ac. The fact that ATXN7L3, a crucial activator of USP22 activity, is also sequestered into aggregates in the presence of ATXN7-polyQ mutant can explain the defect in the deubiquitinating activity of the complex and the increased levels of H2B ubiquitination observed both globally (present study), as well as on specific promoters (McCullough et al., 2012). Although the fact that Gcn5 is also sequestered into nuclear foci, the lack of change in levels of H3K9/K14 acetylation might be explained by functional compensation through other HATs existed in human astrocytes, like PCAF. Interestingly, treatment of the human astrocytes with the HDAC inhibitor TSA rescued the DUB activity defect, but also increased the number of nuclear foci. McCullough et al, suggested that TSA treatment induces the aggregation of mutant ATXN7 into nuclear foci, making room for the endogenous wild type form of the protein to work more efficiently towards H2B deubiquitination. Our current results propose a different mechanism, wherein TSA might enhance expression of other DUB module components, thereby enhancing solubility of ATXN7 polyQ. Our data clearly show that overexpression of ATXN7L3 and ENY2 promotes the solubility of ATXN7-polyQ, possibly facilitating its incorporation in the SAGA complex, and restoring DUB activity.

Sequestration of both enzymatic centers in SAGA into nuclear aggregates upon ATXN7-polyQ expansion likely plays a key role in SCA7 progression and development. However, our findings strongly suggest that therapies designed to improve the acetyltransferase or the deubiquitinating activity of SAGA may have limited success in curing the symptoms of SCA7 disease unless they also inhibit polyQ expanded ATXN7 aggregation.

## Chapter 4: Defining the role of *Usp22* in SCA7 disease through establishing a *Usp22* conditional knockout mouse model

### 4.1 Establishment of *USP22* conditional knockout mouse

Our published data demonstrated that loss of Gcn5 accelerates cerebellar Purkinje cell and retinal degeneration in a SCA7 mouse model (Chen et al., 2012). Moreover, our latest results above showed that polyQ expansion in ATXN7 does not affect the assembly or enzymatic activity of the SAGA DUBm in vitro. However, in vivo, ATXN7-polyQ mutant impairs DUB activity reflected by increase of global H2Bub through forming aggregates to sequestrate DUBm components away from their substrates (Lan et al., 2015), indicating that ATXN7-polyQ mutant likely contributes to SCA7 by indirectly impairing DUB activity. Alternatively, the polyQ expansion itself might be toxic, irregardless of its affects on USP22 activity. Here, I propose to define the role of Usp22 in SCA7 through deletion of Usp22 in Purkinje cells and/or Bergman glia, both of which are involved in SCA7 pathogenesis (Bellamy, 2006; Custer et al., 2006; Garden et al., 2002).

To establish a *Usp22* conditional knockout mouse model, we obtained sperm from a mouse line generated by the Knockout Mouse Project (KOMP) (https://www.komp.org/). This mouse line contains the *Usp22*FloxFRT allele, in which exon2 of *Usp22* is flanked by loxP sites, and FRT cassette is inserted into the intron 1 of *Usp22*, terminating the transcription of *Usp22* (Figure 14A). We sent these sperm to the MDACC Genetically Engineered Mouse core facility in Houston, where in vitro fertilization was performed. We obtained 12 mice by in vitro fertilization. 6 out of the 12 mice contain the *Usp22*FloxFRT allele (named *Usp22*FloxFRT/+ mouse), as genotyped by PCR with the specific primers provided by the KOMP (Figure 14A and B). We further crossed these *Usp22*FloxFRT/+ mice with Flpase mice obtained from the Jackson Lab

and then examined the deletion of FRT cassette in their pups (Figure 14C). We identified that 24 out of 36 pups are positive for the recombined allele by PCR genotyping, indicating the deletion of FRT cassette (Figure 14A and C). These positive pups are hereafter named Usp22Flox/+ mice. Then we intercrossed Usp22Flox/+ mice and examined the frequencies of their pups with WT, Flox/+ and Flox/Flox genotypes. We obtained 41 pups (WT : Flox/+ : Flox/Flox is 8: 24: 9) as F1. At the same time, we crossed Usp22Flox/+ mice with two specific Cre lines (Pcp2-Cre and hGFAP-Cre). Crossing with Pcp2-Cre and hGFAP-Cre mice will cause the specific deletion of *Usp22* in Purkinje cells and Bergmann glia, respectively. Finally, these mice with specific loss of Usp22 will be monitored and identified for SCA7 linked "Ataxia" phenotypes (Chen et al., 2012). Pcp2-Cre mediated recombination is fully established by 2-3 weeks after birth (Barski et al., 2000), so mice with *Usp22* deletion in Purkinje cells will be monitored for "Ataxia" phenotype since 3 weeks after birth; hGFAP-Cre mediated recombination is fully established after birth (Zhuo et al., 2001), mice with *Usp22* deletion in Bergmann glia will be monitored for "Ataxia" phenotype since 2-3 weeks after birth. Currently, this project is still ongoing.

**4.2 Future directions**

We will examine whether or not Purkinje cell-specific and Bergmann glia-specific *Usp*22 deletion affect lifespan by performing survival analysis using these mice. Moreover, we will perform footprint analyses (Carter et al., 1999) and rotorod analyses (Jafar-Nejad et al., 2011) to examine whether these cell type-specific *Usp22* null mice exhibit "Ataxia" phenotype compared with WT mice (Chen et al., 2012). To validate the deletion of *Usp22*, we will carry out immunohistochemistry and in situ hybridization experiments. If we observe SCA7 related "Ataxia" phenotypes in these cell type-specific

*Usp22* null mice, we will further perform *hematoxylin and eosin Y* (H&E) *staining* to examine the histological structure of their cerebellums. To further characterize the potential Purkinje cell and Bergmann glia pathology, we will also perform immunofluorescence experiments using the cerebellar sections by anti-calbindin (Purkinje cell marker) and anti-GFAP (Bergmann glia marker) antibodies. To identify the related molecular pathways, we will examine the potential transcriptional change of well-documented target genes involved in SCA7 by qRT-PCR. Finally, since our lab have generated *Usp22* conditional overexpression mouse model, we can use this mouse model to rescue the potential SCA7 phenotypes caused by the specific *Usp22* loss in Purkinje cell and/or Bergmann glia. On the other hand, if we do not observe any SCA7 related phenotypes in these cell type-specific *Usp22* null mice, this could be explained be several reasons: 1) Other Usps compensate the loss of *Usp*22; 2) Defective Usp22 DUB activity is a passive rather than a causative effect in SCA7 disease. 3) PolyQ stretch itself is cytotoxic.

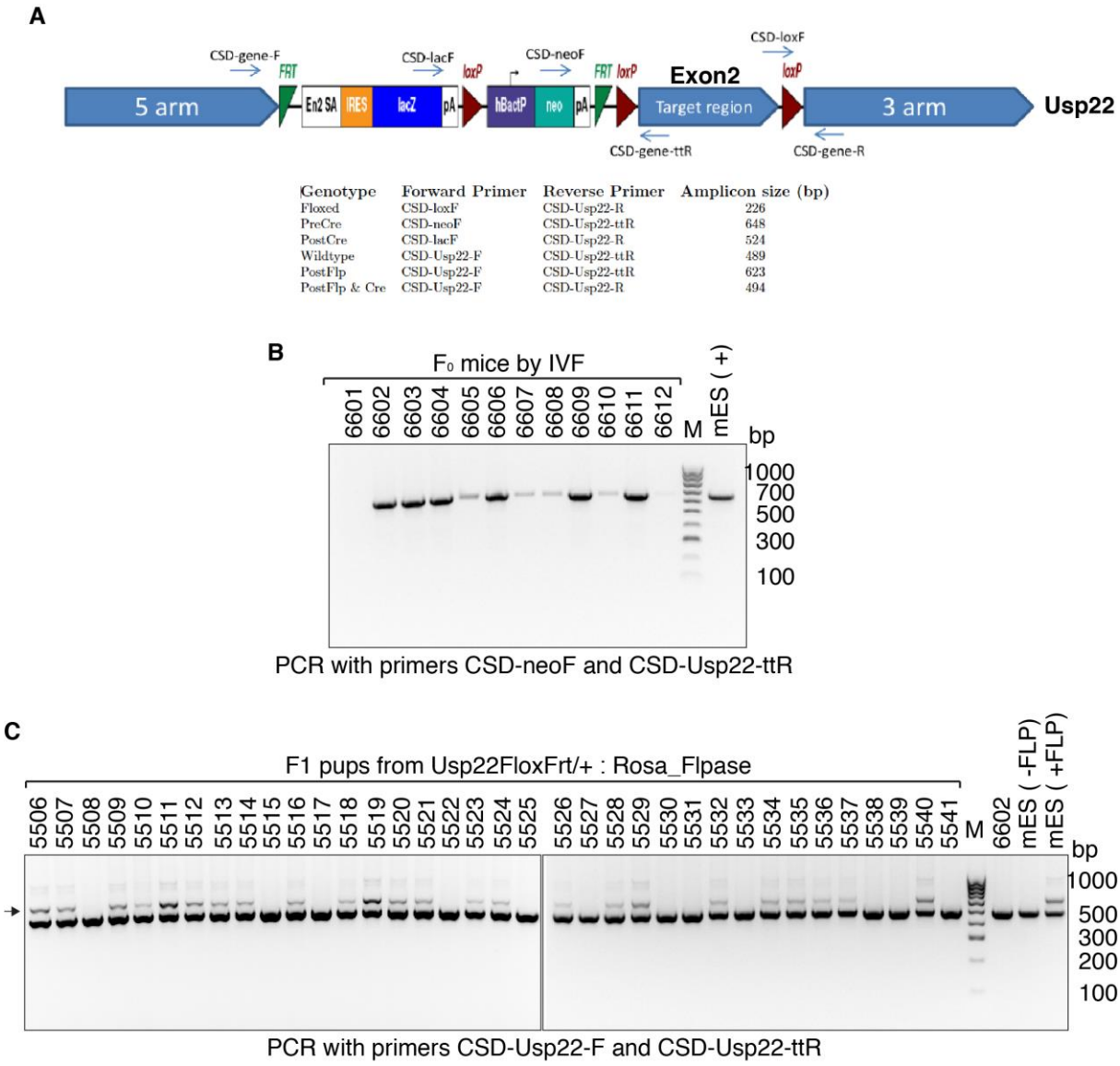


| Genotype | Forward Primer | Reverse Primer | Amplicon size (bp) |
|---|---|---|---|
| Floxed | CSD-loxF | CSD-Usp22-R | 226 |
| PreCre | CSD-neoF | CSD-Usp22-ttR | 648 |
| PostCre | CSD-lacF | CSD-Usp22-R | 524 |
| Wildtype | CSD-Usp22-F | CSD-Usp22-ttR | 489 |
| PostFlp | CSD-Usp22-F | CSD-Usp22-ttR | 623 |
| PostFlp & Cre | CSD-Usp22-F | CSD-Usp22-R | 494 |

**Figure 14: Establishment of *Usp22* conditional knockout mouse.**

**Figure 14: Establishment of *Usp22* conditional knockout mouse.**

(A) Diagram of an *Usp22* knockout first allele, this knockout first allele is initially a null form, but can be converted to a conditional allele via Flpase recombination. The specific primers for genotyping are indicated. To obtain the *Usp22* conditional allele, the mice containing this allele are crossed with Flpase mice to delete the FRT cassette, resulting in floxed mice. The Exon2 of *Usp22* gene, which encodes part of ZnF domain of Usp22 protein required for the activation of Usp22 DUB activity, will be deleted after Cre recombination. (B) Genotyping of the *Usp22*FloxFRT/+ mice (generated by in vitro fertilization) by PCR with the indicated primers. The band of 648 bp represents the PCR product of *Usp22*FloxFRT mice, and no band corresponds to the WT mice. mES cells containing the *Usp22*FloxFRT allele serves as positive control. (C) Validation of FRT cassette deletion after Flpase recombination (cross with Flpase mice) by PCR with the indicated primers. The band of 489 bp represents the PCR product of WT allele, and the slow migrating band of 623 bp indicated by "arrow" corresponds to *Usp22*Flox/+ mice. mES cells containing the *Usp22*FloxFRT allele without and with Flpase treatment serve as negative control and positive control, respectively. An *Usp22*FloxFRT/+ mouse (named 6602) serves as negative control. *Amanda M Martin (Technician), and Andrew P Salinger (lab manager) from Dr. Sharon Dent's lab (UT M.D. Anderson Cancer Center) help me set up the mouse breeders and make mouse genomic DNA. I did the genotyping by PCR.*

## Chapter 5: USP44 is an integral component of N-CoR that contributes to target gene repression by modulating H2Bub1 levels

Contents of this chapter are based on Xianjiang Lan, Boyko S. Atanassov, Wenqian Li, Ying Zhang, Laurence Florens, Ryan D. Mohan, Michael P. Washburn, Jerry L. Workman, and Sharon Y. R. Dent* USP44 is an integral component of N-CoR that contributes to target gene repression by modulating H2Bub1 levels. In revision for publication.

### 5.1 USP44 is a subunit of the N-CoR complex

USP44 is implicated in ES cell differentiation, DNA damage repair, and cancer development (Fuchs et al., 2012; Liu et al., 2015; Mosbech et al., 2013; Stegmeier et al., 2007; Zhang et al., 2012). As a deubiquitinating enzyme, decreased USP44 levels were used to account for a global increase in H2Bub levels during ES cell differentiation (Fuchs et al., 2012). However, USP44 alone is not active, whether USP44 can directly deubiquitinate histone H2B and what the other partners required for the activation of its DUB activity are not known.

To further define USP44 functions, I tested the ability of recombinant USP44 to deubiquitinate H2Bub1 in vitro. Like most other H2B DUBs identified to date (USP22, USP27x, USP49 and USP51), I found that recombinant USP44 is not active by itself and association with CETN2 is also not active (Figure 15). The protein domain structure of USP44 is very similar to that of the other DUBs (Figure 16A), all of which require association with partner proteins for full enzymatic activity (Lang et al., 2011; Zhang et al., 2013), I reasoned that USP44 might also require partners to acquire enzymatic activity toward H2Bub1. To test this idea, I used a proteomic approach to identify USP44

interacting proteins. I isolated nuclear extracts from 293T cells that stably express USP44 fused with N-terminal FLAG and HA affinity tags (FH-USP44), and then performed tandem affinity purification (TAP) followed by MudPIT analysis to uncover USP44 associated proteins. As expected, CETN2 (centrin2), the only known USP44 interacting protein (Zhang et al., 2012), was one of the major proteins we identified (Figure 16B). Surprisingly, the majority of the other USP44-associated proteins we identified are subunits of the N-CoR complex, including TBL1X, TBL1XR1, HDAC3, NCOR1 and NCOR2 (also called SMRT) (Yoon et al., 2003). Moreover, a number of proteasomal subunits, including PSMC1, PSMC2, PSMC4 and PSMC5, which associate with N-CoR for its degradation (Perissi et al., 2004), were also identified as USP44 interacting proteins, none of these USP44 partners were detected in the FH-vector control purified in parallel (Figure 16B).

To further explore possible connections between CETN2, USP44, and N-CoR, we performed TAP of FH-tagged CETN2 followed by MudPIT analysis. Consistent with our results above, USP44 was detected as a CETN2 interacting protein. Moreover, RAD23B and XPC, both of which are known to form a complex with CETN2 in the nucleus (Nishi et al., 2005), were also detected in the CENT2 precipitated fractions. However, N-CoR complex subunits were not detected in the CETN2 purification, and XPC and RAD23B were not found in USP44 precipitated fractions (Figure 16B). Thus, these data indicate that USP44 is likely part of two separate complexes, associated with either CETN2 or N-CoR.

To validate our MudPIT results, I immunoprecipitated ectopically expressed USP44 from 293T nuclear extracts and blotted the precipitated fractions for TBL1X, TBL1XR, NCOR1 or HDAC3. These experiments confirmed interactions between endogenous N-CoR complex subunits and FH-USP44, but not another H2Bub1 DUB, USP22 (Figure 16C). Reciprocal immunoprecipitation using a TBL1X antibody pulled down FH-tagged

USP44 (anti-HA blot), as well as other N-CoR complex subunits (Figure 16D). To further determine whether USP44 is an integral component of the N-CoR complex, I performed gel filtration using FLAG and HA purified USP44 eluates. Immunoblots of column fractions showed that USP44 co-purifies with N-CoR subunits (fractions 16 and 17), corresponding to the expected molecular weight of the N-CoR complex (1.5-2 MDa) (Yoon et al., 2003). Importantly, CETN2 was found mostly in fractions that contained little or no N-CoR subunits (fractions 18-23) (Figure 16E), again indicating that USP44 forms separate complexes with these proteins. Further cell fractionation experiments confirmed associations of USP44 and N-CoR complex components with chromatin (Figure 17). Collectively, these results demonstrate that USP44 associates with the N-CoR complex independently of CETN2 in the nucleus, indicating that this DUB likely functions in multiple processes.

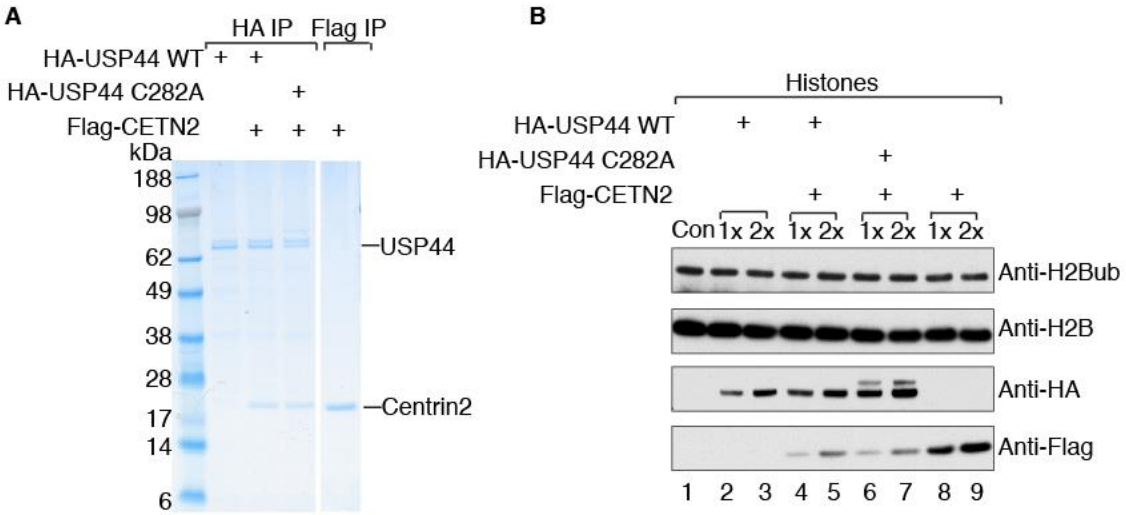


**Figure 15: Recombinant USP44 alone is not active and interaction with CETN2 or TBL1X and/or TBL1XR1, and/or PSMC5 does not affect the DUB activity of USP44.**

(A) Colloidal Coomassie staining of purified USP44 (WT and catalytic mutant) and USP44-CETN2 complex from bacurovirus infected insect cells. (B) Purified USP44 alone or together with CETN2 were used for in vitro DUB assay with purified core histones as substrate. Total H2B was used as a loading control. USP44 was HA-tagged and CETN2 was FLAG-tagged. 1x and 2x indicate the amount of purified enzymes used in the assay. All components were probed with indicated antibodies.

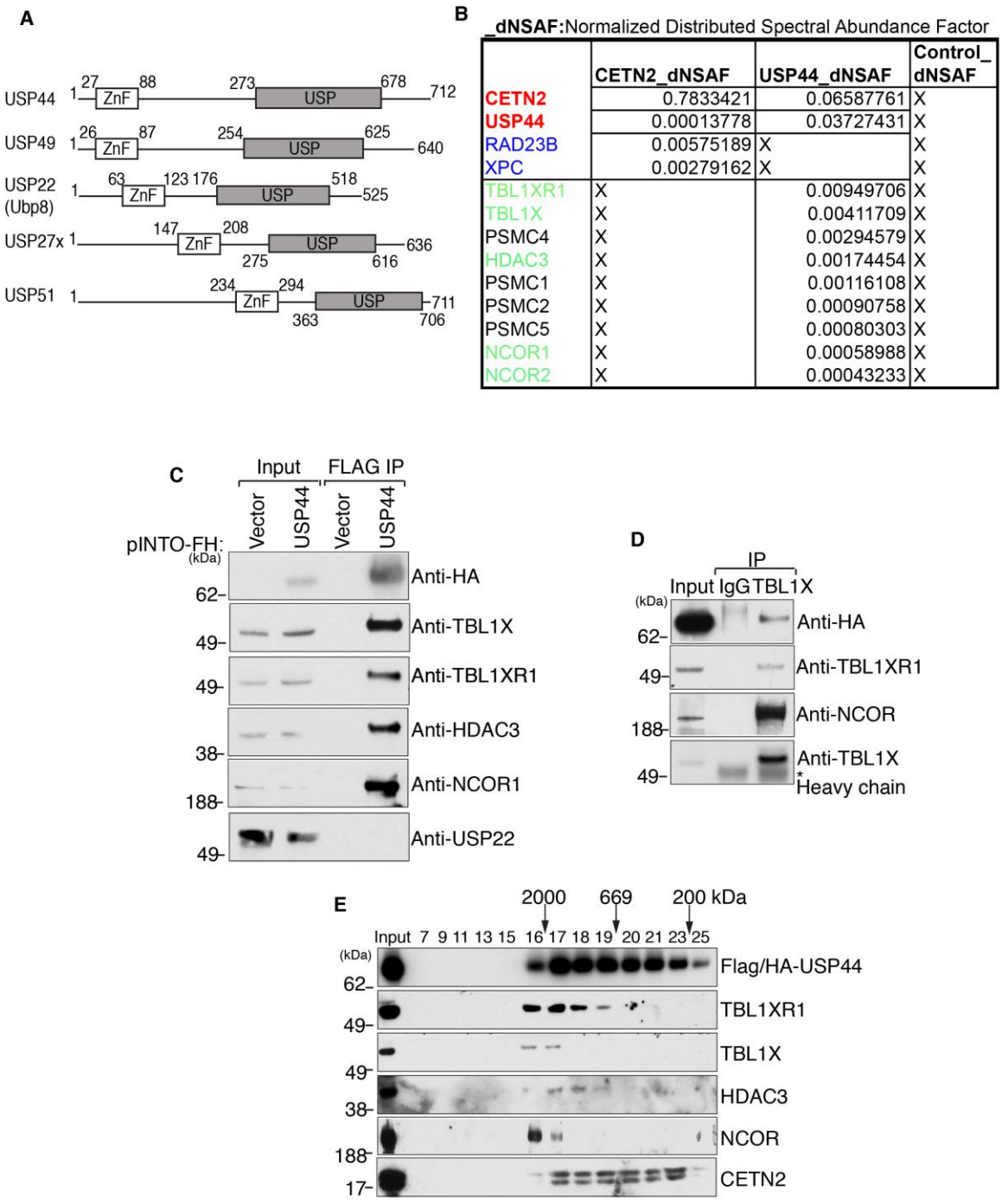


| | CETN2_dNSAF | USP44_dNSAF | Control_ dNSAF |
|---|---|---|---|
| CETN2 | 0.7833421 | 0.06587761 | X |
| USP44 | 0.00013778 | 0.03727431 | X |
| RAD23B | 0.00575189 | X | X |
| XPC | 0.00279162 | X | X |
| TBL1XR1 | X | 0.00949706 | X |
| TBL1X | X | 0.00411709 | X |
| PSMC4 | X | 0.00294579 | X |
| HDAC3 | X | 0.00174454 | X |
| PSMC1 | X | 0.00116108 | X |
| PSMC2 | X | 0.00090758 | X |
| PSMC5 | X | 0.00080303 | X |
| NCOR1 | X | 0.00058988 | X |
| NCOR2 | X | 0.00043233 | X |

**Figure 16: USP44 associates with N-CoR complex.**

**Figure 16: USP44 associates with N-CoR complex.**

(A) Schematic representation of protein domain structure of USP44, USP49, USP22, USP27x, and USP51 (B). Normalized Distributed Spectral Abundance Factor (dNSAF) of partial CETN2 associated polypeptides and USP44 associated polypeptides identified by MudPIT analysis. Bait proteins are highlighted in red, components of CETN2-XPC complex are highlighted in blue, and components of N-CoR comlex are in green and dark. (C) Immunoprecipitation (IP) from nuclear extract (NE) of NFH-USP44 293T cells using FLAG beads. (NFH, N-terminal FLAG and HA tags). pINTO-NFH vector cells serves as negative control. Bound proteins were resolved on SDS-PAGE and analyzed by western blot with indicated antibodies. (D) Immunoprecipitation (IP) from nuclear extract (NE) of NFH-USP44 293T cells using TBL1X antibody, followed by western blot with inidicated antibodies. (E) Gel filtration analysis of tandem FLAG and HA-purified NFH-USP44 complexes. Fractions were resolved on SDS-PAGE followed by immunoblot with indicated antibodies. *Multidimensional Protein Identification Technology (MudPIT) analysis in Figure 17B was performed by Ying Zhang, Laurence Florens from Dr. Michael P. Washburn lab (Stowers Institute for Medical Research, Kansas City, Missouri, USA).*

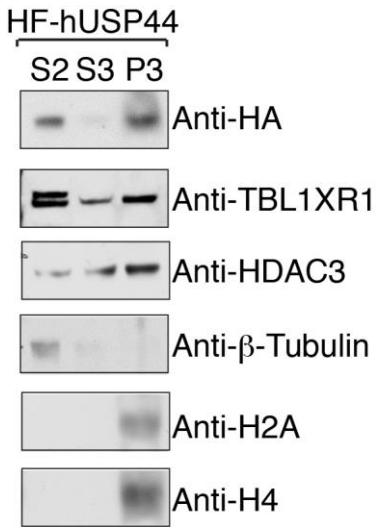


**Figure 17: USP44 mainly associates with chromatin in the nucleus, together with N-CoR subunits.**

Cytoplasmic, soluble nuclear, and chromatin fractions were isolated from NFH-USP44 293T cells. Fractions were resolved on SDS-PAGE and blotted with the indicated antibodies.β-tubulin serves as a marker for cytoplasmic fraction, H2A and H4 serves as markers for chromatin fraction. S2: cytoplasmic fraction; S3: soluble nulcear fraction; P3: chromatin fraction.

### 5.2 USP44 interacts directly with WD40 repeats in TBL1X and TBLXR1

Several USPs interact with WD40-containing proteins (Villamil et al., 2013). For example, WDR48 interacts with USP1, USP12 and USP46 to activate their DUB activity (Cohn et al., 2009) (Yin et al., 2015). Interestingly, two N-CoR components, TBLX and TBL1XR1, contain WD40 repeats (Figure 18A). Moreover, TBL1X and TBL1XR1 were the top non-CETN2 USP44 interacting proteins detected in our MudPIT analyses (Figure 18B). To determine whether USP44 interacts directly with TBLX1 or TBLXR1, I performed immunoprecipitation (IP) experiments using recombinant HA-USP44 and FLAG-TBL1X/TBL1XR1 from baculovirus infected insect cells. Both TBL1X and TBL1XR1 interacted with USP44, alone and together (Figure 18B). TBL1X and TBL1XR1 contain multiple domains, including LisH domains, F-box domains, and WD40 repeats (Figure 18A). Previous studies demonstrated that the N-terminal of LisH and F-box domains bind to histones H2B and H4 and are also required for assembly of the N-CoR complex (Oberoi et al., 2011; Yoon et al., 2003). To determine whether these domains or the C-terminal WD40 repeats of TBL1X/TBL1XR1 are required for interaction with USP44, I created expression constructs for truncated forms of TBLXR1 that contained either the N-terminal LisH and F-box motifs (F1) or the C-terminal WD40 repeats (F2) fused to Gal4 (Figure 18A). Introduction of these constructs into 293T cells expressing FH-USP44 and subsequent FLAG-immunoprecipotations revealed that full length TBLXR1 and the C-terminal fragment interacted with USP44, but the N-terminal TBL1XR1 construct did not (Figure 18C). These results indicate that the WD repeats in TBXLR1 are both necessary and sufficient for USP44 interaction. Nevertheless, an in vitro reconstituted USP44, TBL1X and TBLXR1 containing complex did not show obviously different DUB activity toward H2Bub1 relative to USP44 alone (Figure 19), indicating that the interactions with TBL1X and TBLXR1 are required for USP44 association with N-CoR but are not sufficient for USP44 activation.

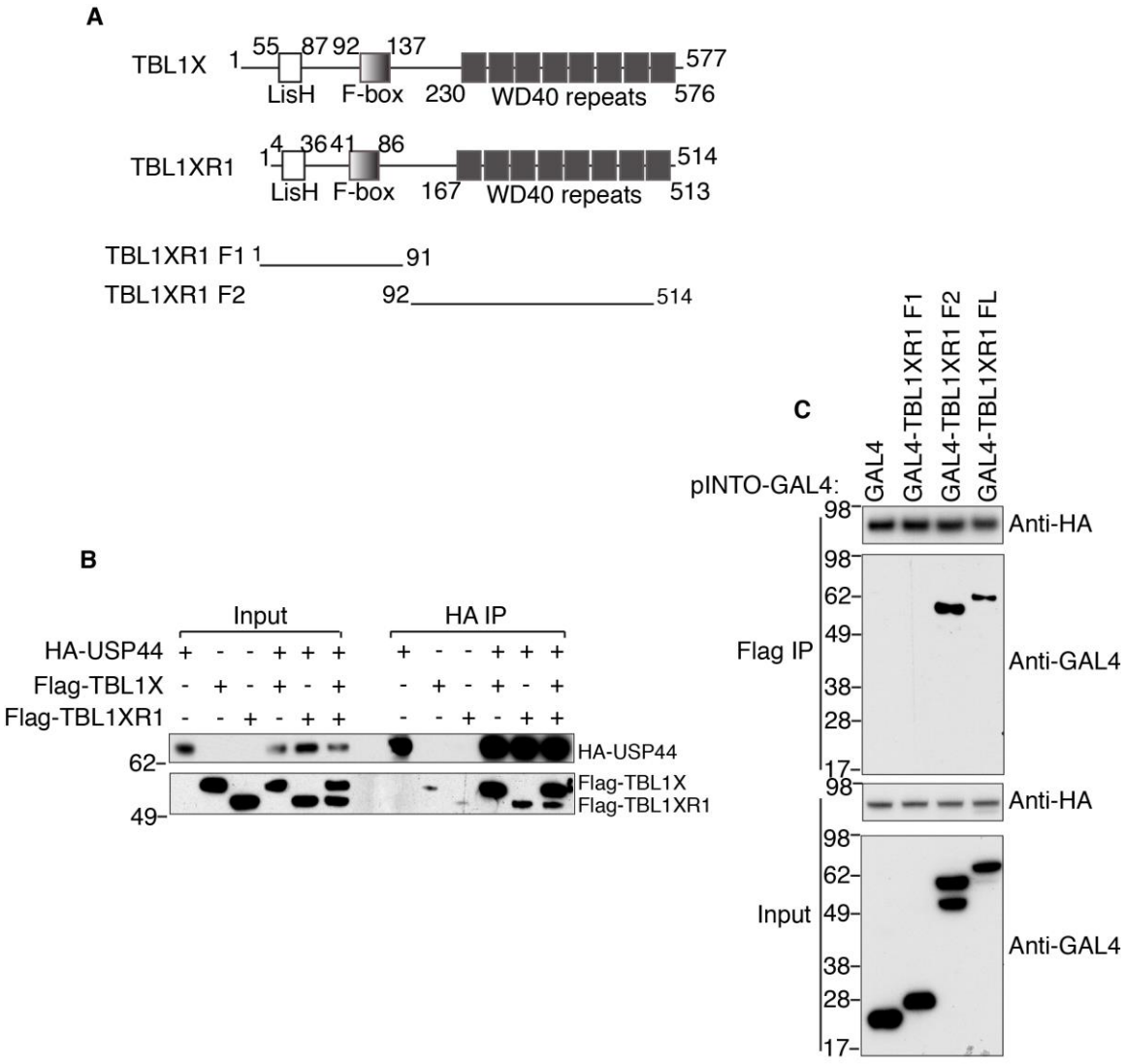


**Figure 18: WD40 repeats of TBL1X/R1 are required for the association of USP44 with N-CoR complex.**

(A) Schematic of TBL1X and TBL1XR1 domains. The deletion constructs of TBL1XR1 were as indicated. (B). Immunoprecipitations using lysates from Sf21 cells expressing the proteins indicated, using HA beads followed by western blot using HA or FLAG antibodies. (C). NFH-USP44 cells were transiently transfected with the indicated GAL4-TBL1XR1 truncations. Immunoprecipitations using the cell lysates using FLAG beads followed by western blot using HA or GAL4 antibodies.

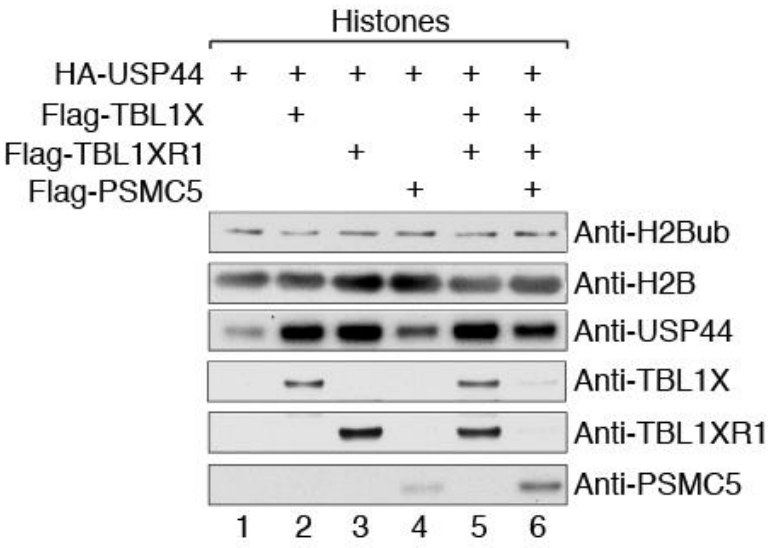


**Figure 19: Recombinant USP44 interaction with TBL1X and/or TBL1XR1, and/or PSMC5 does not affect the DUB activity of USP44.**

Purified USP44 alone or together with TBL1X, and/or TBL1XR1, and/or PSMC5 were used for in vitro DUB assay with purified core histones as substrate. Total H2B was used as a loading control. All components were probed with indicated antibodies.

### 5.3 USP44 deubiquitinates H2Bub1 as part of N-CoR

To determine whether USP44 is active towards H2Bub1 in vivo, I depleted USP44 in 293T cells using shRNAs (Figure 20A). Consistent with previous reports using ES cells (Fuchs et al., 2012), depletion of USP44 led to noticeable (~2 fold) increase in H2Bub1 levels in 293T cells (Figure 20A and B). To further address USP44 effects on H2Bub1, I overexpressed either wild type (WT) or a catalytic mutant (C282A) of USP44 (Figure 20C). Overexpression of WT USP44 led to an obvious decrease H2Bub1 levels, whereas overexpression of the C282A mutant did not (Figure 20C and D).

To more directly test the ability of USP44 to deubiquitinate H2Bub1, I utilized our TAP purified FH-USP44-N-CoR complex for in vitro DUB assays using purified core histones as substrate (Figure 20E). H2Bub1 immunoblots indicate that relative to a FH-vector control purified in parallel, increased amounts of FH-USP44-N-CoR in the reaction led to decreased H2Bub1. To further test whether DUB activity is associated with the N-CoR complex, I repeated these experiments using TAP-purified N-CoR from 293T cells stably expressing FH-TBL1X (Figure 21). Incubation of the FH-TBL1X-N-CoR complex with purified histones again led to decreased levels of H2Bub1 (Figure 20F). Moreover, association with CETN2 did not affect the DUB activity of USP44 in vitro. These experiments indicate that USP44 is an active deubiqutinase when associated with the N-CoR complex.

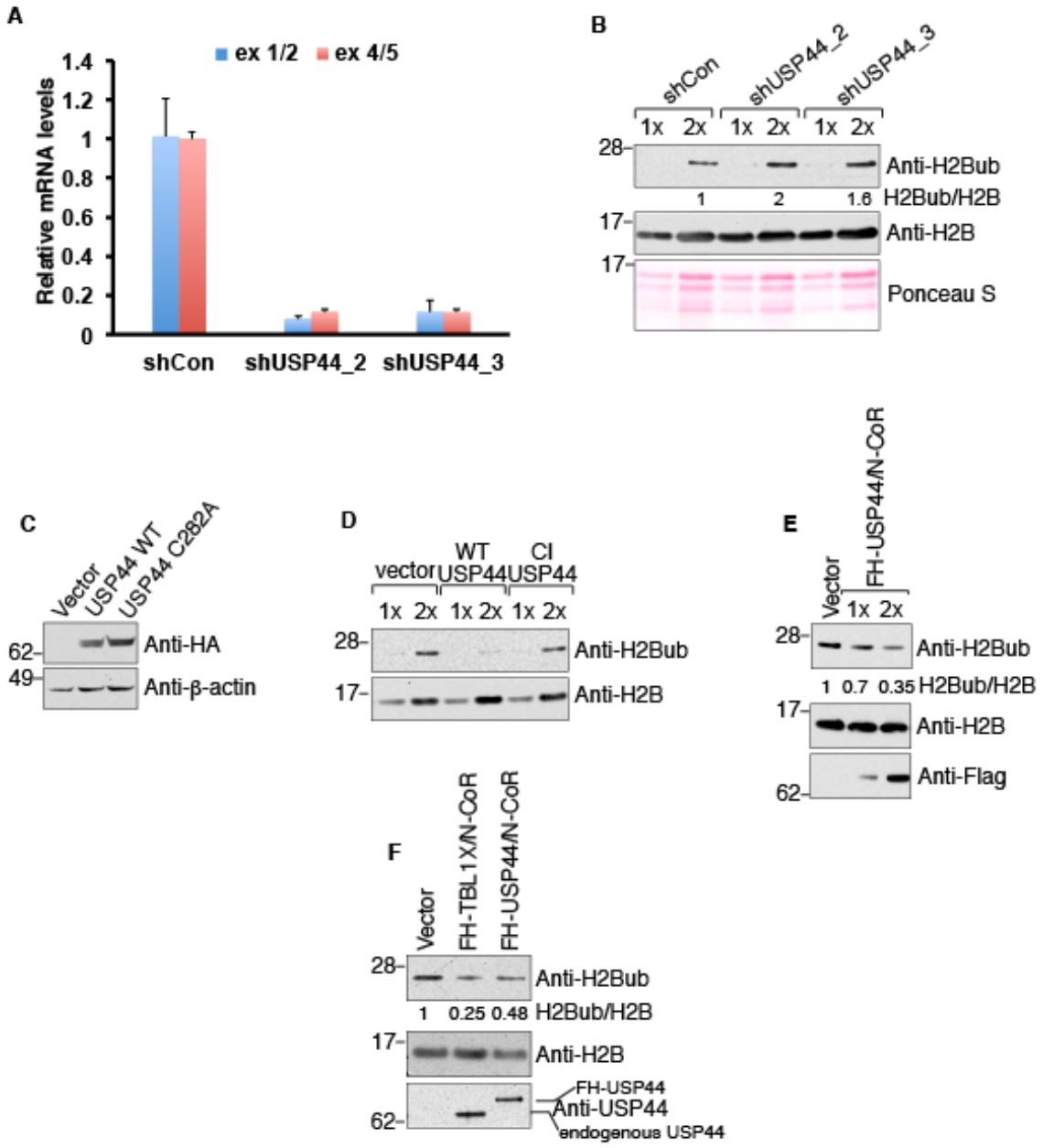


**Figure 20: USP44-N-CoR complex deubiquitinates H2B in vivo and in vitro.**

**Figure 20: USP44-N-CoR complex deubiquitinates H2B in vivo and in vitro.**

(A) 293T cells were infected with pGIPZ shControl or shUSP44 lentivirus. After 48 hours infection, the knockdown efficiency of USP44 was detected by quantitative real-time PCR with two different pairs of USP44 primers. GAPDH was used as internal control for normalization. Each value is the mean of three technical replicates with error bars representing the standard deviation. (B) Depletion of USP44 leads to marked increase of global H2Bub1. H2B and Ponceau serve as the loading control. Different sample amounts (1× and 2×) were analyzed (C) Expression levels of WT or catalytically inactive USP44 proteins in 293T cells. (D) Expression of WT USP44, rather than catalytic inactive USP44 reduces global levels of H2Bub1 in 293T cells. Different sample amounts (1× and 2×) were analyzed (E, F) Sequential FLAG and HA purified USP44 complex or TBL1X complex from 293T cells was used for in vitro DUB assay using histones as substrate. Both complexes show moderate activity towards H2Bub in vitro. Different amounts of USP44/N-CoR complex (1× and 2×) were used for the assay. Blots were quantified using ImageJ software in this and all other figures in this article.

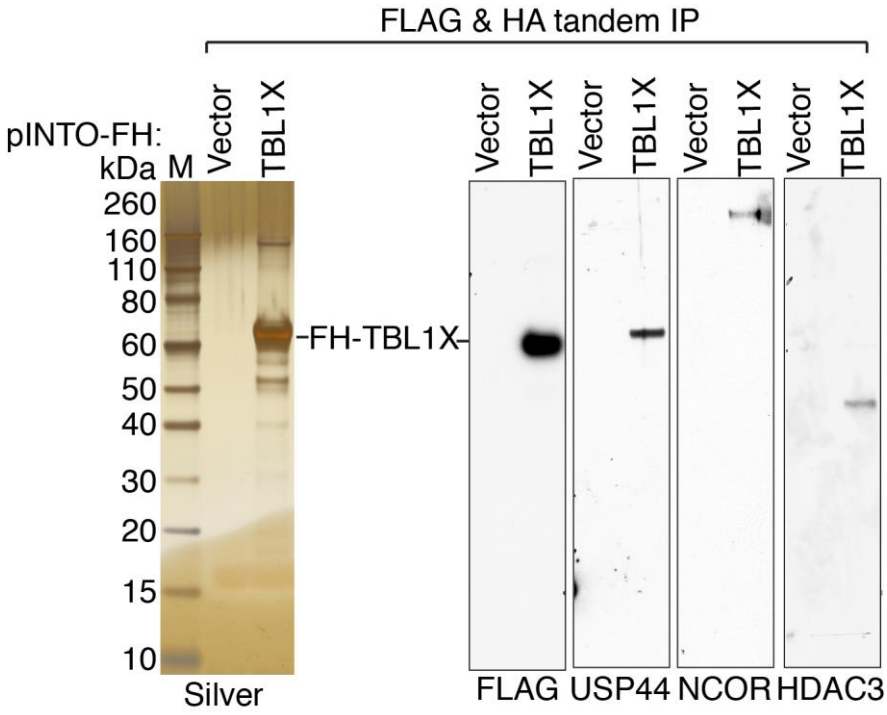


**Figure 21: FH-TBL1X-N-CoR complex purification from 293T cells.**

Silver stain and immunoblot analyses to confirm the subunits of N-CoR complex. FH-TBL1X bait protein is indicated by black line. USP44, NCOR and HDAC3 were probed by specific antibody, respectively.

### 5.4 USP44 enhances the repressive activity of N-CoR

Given that N-CoR functions as a transcriptional repressor through recruitment of the histone deacetylase HDAC3 (Wong et al., 2014), I next determined whether USP44 also contributes to N-CoR functions using a genome integrated luciferase reporter system as previously described (Vaquero et al., 2004) (Figure 22A). I generated stable 293 T-Rex cells (Vaquero et al., 2004) containing doxycycline-inducible expression constructs for GAL4-TBL1X, GAL4-TBL1XR1 or GAL4 alone. As expected, luciferase expression and activity was repressed upon induction of GAL4-TBL1X or GAL4-TBL1XR1 (Figure 22B). I next examined the contribution of USP44 and TBL1XR1 to the repressive activity of GAL4-TBL1XR1. Quantitative real-time PCR (qRT-PCR) and immunoblot analyses confirmed the knockdown (KD) efficiency of USP44 and GAL4-TBL1XR1 (Figure 22C and D). As expected, depletion of TBL1XR1 led to a marked increase of luciferase activity (Figure 22E). Interestingly, depletion of USP44 also led to a moderate increase of luciferase activity (Figure 22E). As GAL4-TBL1XR1 is required for recruitment of both USP44 and HDAC3, the enhanced effect of TBLXR1 KD likely reflects loss of both HDAC3 and USP44.

I next confirmed promoter recruitment of USP44 together with the N-CoR complex by ChIP-qPCR. As expected, upon doxycycline induction, GAL4-TBL1XR1 and FLAG-HA-USP44 were both recruited to the TK promoter that drives the luciferase reporter (Figure 22F). In addition, histone H3 acetylation at lysines 9 and 14 (H3K9/14ac), the main substrate of HDAC3 (Bhaskara et al., 2010), was reduced, consistent with HDAC3/N-CoR recruitment (Figure 22G). Moreover, H2Bub1 was also reduced (Figure 22H), consistent with USP44/N-Co-R recruitment at this locus. Collectively, these results suggest that USP44-N-CoR complex creates a compact chromatin environment by removing histone acetylation and H2Bub1, further exerting repressive activity for transcription.

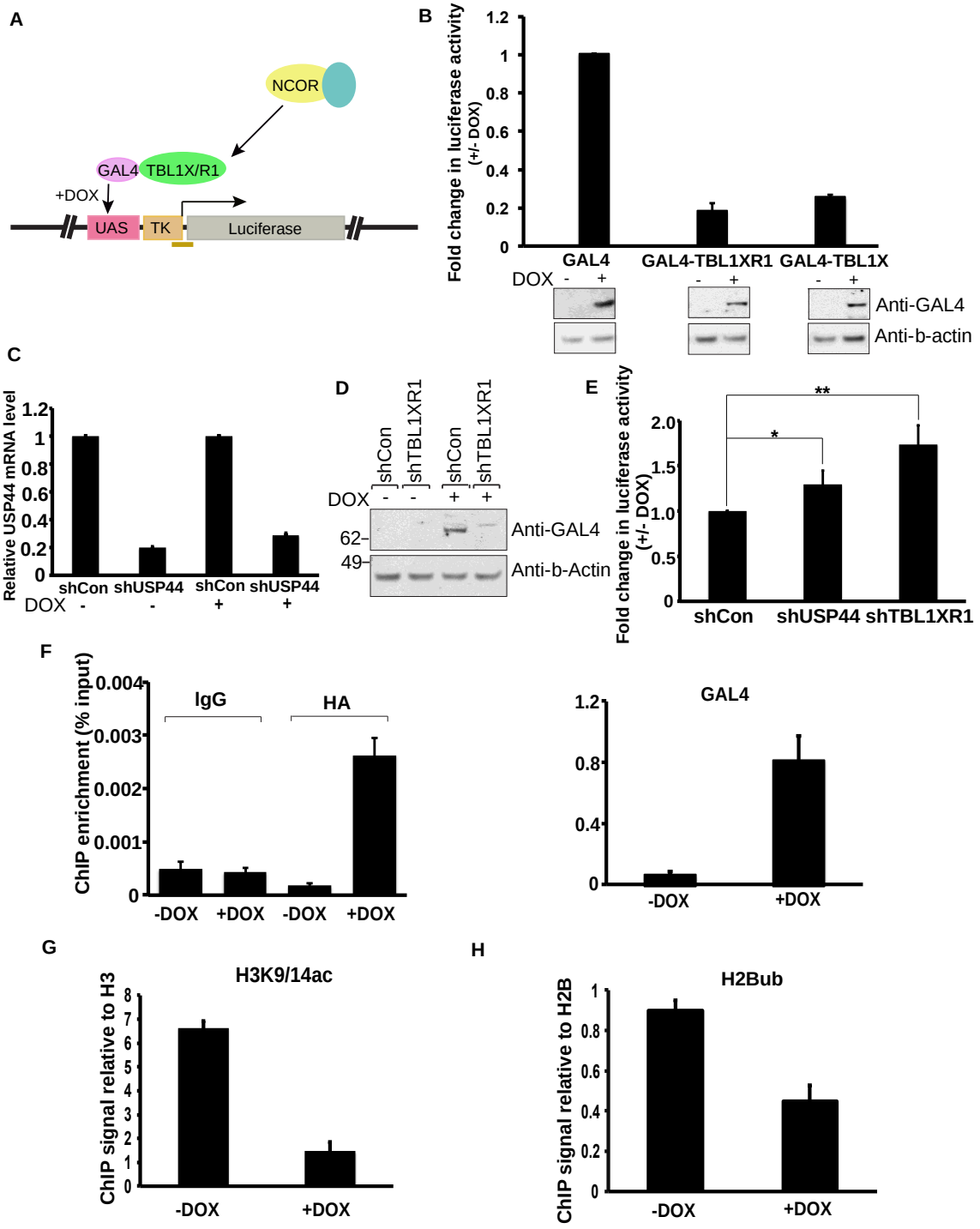


**Figure 22: USP44 facilitates the repressive activity of N-CoR complex through deubiquitinating H2B.**

**Figure 22: USP44 facilitates the repressive activity of N-CoR complex through deubiquitinating H2B.**

(A) Schematic of the luciferase reporter system. (B) Fold change in luciferase activity in cells expressing GAL4, GAL4-TBL1XR1, and GAL4-TBL1X, after 24 hours doxycycline (100 ng/ml) induction. Each value is the mean of three independent measurements with error bars representing the standard deviation. Expression levels of all GAL4-tagged proteins are shown at the *bottom* without (−) and with (+) induction. qRT-PCR (C) and immunoblots (D) demonstrating the efficient silencing of USP44 and TBL1XR1 in GAL4-TBL1XR1 cells with or without induction. (E) Fold change in luciferase activity in GAL4-TBL1XR1 cells upon knockdown of USP44 or TBL1XR1. Cells were infected by pGIPZ shcontrol, shUSP44 or shTBL1XR1 lentivirus for two days and then 100 ng/ml doxycycline was used to induce GAL4-TBL1XR1 expression. After 24 hours induction, luciferase activity was measured. Each value is the mean of three independent measurements with error bars representing the standard deviation. * $p$-value < 0.05 and ** $p$-value < 0.01 by two-sided $t$-test, compared with pGIPZ shcontrol. (F-H) ChIP followed by qRT-PCR using the antibodies indicated and GAL4-TBL1XR1 cells without or with doxycycline induction after transfection with pCAG-USP44-C-FH vector. ChIP enrichment is shown as percentage of input, histone H3 or histone H2B. All values represent the average of three technical replicates with error bars indicating standard deviation.

### 5.5 USP44-N-CoR complex links H2Bub1 to invasiveness of triple negative breast cancer cells

USP44 (protein level) is highly expressed in breast cancer stem cells, and it may contribute to breast cancer aggressiveness (Liu et al., 2015). TBL1XR1 (protein level) is overexpressed and involved in aggressiveness of malignant breast cancer cells, including MDA-MB-231 triple negative cells (Li et al., 2014). Interestingly, I find that USP44 mRNA level is significantly higher, and H2Bub1 levels are lower (but H2Aub1 levels are similar) in MDA-MB-231 cells compared to MCF10A normal breast epithelial cells (Figure 23A and B). Depletion of USP44 significantly impaired the invasiveness of MDA-MB-231 cells in vitro and led to an increase of global H2Bub1 levels (Figure 23C, D and E). Our results showed depletion of TBL1XR1 impaired the invasiveness of breast cancer cells (Figure 24), which are consistent with a previous study (Kadota et al., 2009). Accordingly, I found that depletion of TBL1XR1 also led to increased levels of H2Bub1 and moderately increased levels of H3K9/14ac, but no obvious change of H2Aub1 levels (Figure 23F and G). Together our results indicate that USP44 contributes to N-CoR functions in regulating gene expression and in modulating the invasiveness of triple negative breast cancer cells.

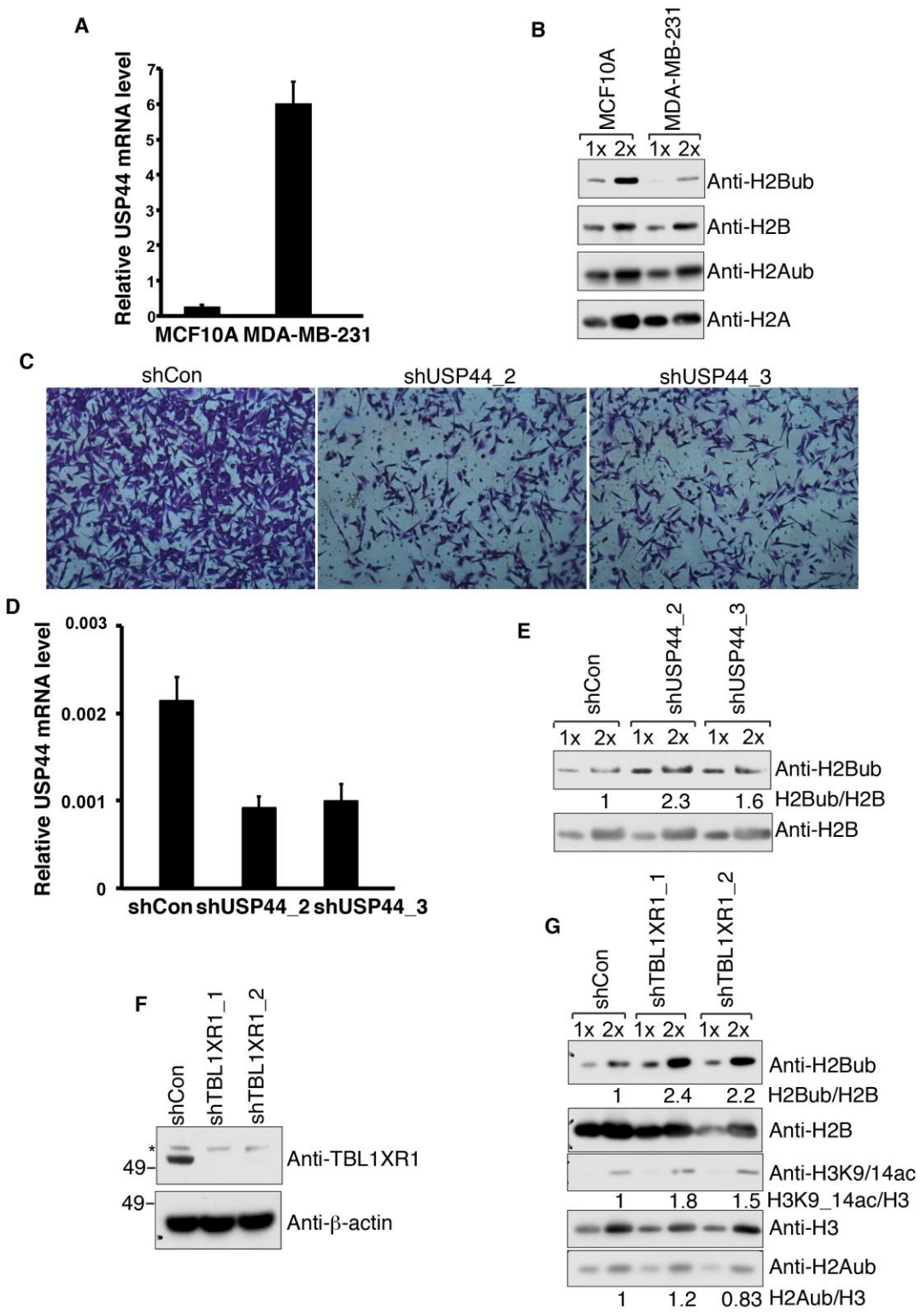


**Figure 23: USP44 regulates the invasiveness of breast cancer cells.**

**Figure 23: USP44 regulates the invasiveness of breast cancer cells.**

(A) qRT-PCR analysis of USP44 mRNA in MCF10A cells and MDA-MB-231 cells. GAPDH serves as internal control. (B) Histones was purified from MCF10A and MDA-MB-231 cells, and resolved on SDS-PAGE and blotted with anti-H2Bub or anti-H2Aub antibody. Total H2B or H2A blots were used as loading control. (C) MDA-MB-231 cells stably infected with pGIPZ shcontrol or two different shUSP44 lentiviruses were used to perform transwell invasion assay. After 48 hours incubation, cells invading to the bottom of Matrigel chambers were stained with crystal violet. (D) qRT-PCR to demonstrate efficient silencing of USP44 in MDA-MB-231 cells. (E) Histones purified from MDA-MB-231 cells stably infected with pGIPZ shcontrol or shU SP44 lentiviruses were resolved on SDS-PAGE and blotted with indicated antibodies. (F) Immunoblots to demonstrate silencing efficiency of TBL1XR1 in MDA-MB-231 cells. Two different TBL1XR1 shRNAs were used. (G) Histones purified from MDA-MB-231 cells stably infected with pGIPZ shcontrol or shTBL1XR1 lentiviruses were resolved on SDS-PAGE and blotted with indicated antibodies. Total H2B, H3 or H2A serves as loading control, Different sample amounts (1× and 2×) were analyzed.

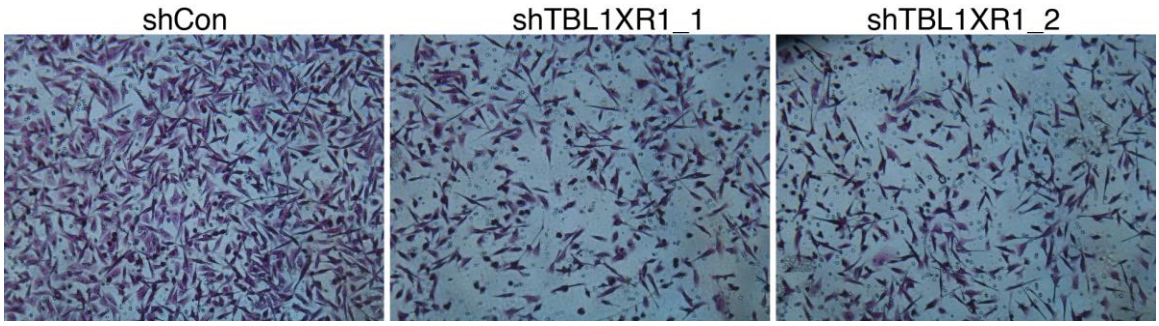


**Figure 24: Ablation of TBL1XR1 impairs the invasiveness of MDA-MB-231 cells.**

MDA-MB-231 cells stably infected with pGIPZ shcontrol or two different shTBL1XR1 lentiviruses were used to perform transwell invasion assay. After 48 hours incubation, cells invading to the bottom of Matrigel chambers were stained with crystal violet and imaged. Three independent experiments were performed and representative views are showed above.

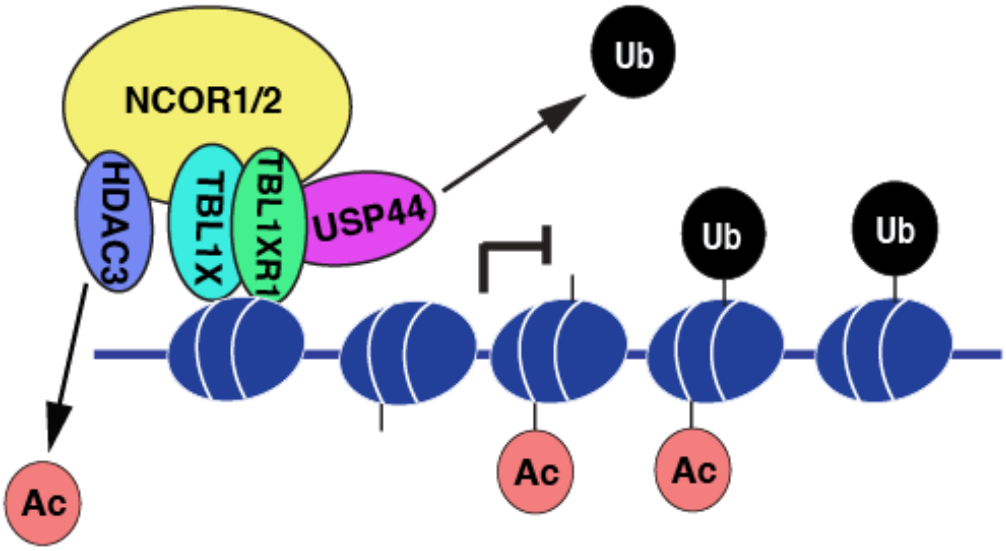


**Figure 25: Model of the function of USP44-N-CoR complex in cells.**

On the gene promoters, N-CoR complex bind chromatin through TBL1X/TBL1XR1, and directly recruits USP44 to deubiquitinate histone H2B and HDAC3 to deacetylate histone H3K9/14, both of which work together to repress transcription.

## 5.6 Conclusions

Here we report use of tandem affinity purification and Multidimensional Protein Identification Technology (MudPIT) to identify USP44 interacting proteins. We found that USP44 interacts with several components of the Nuclear receptor co-repressor complex (hereafter N-CoR complex). As part of N-CoR, USP44 deubiquitinates H2B both in vivo and in vitro, and it contributes to N-CoR mediated repression in vivo.

USP44 has been reported to be a marker for breast cancer stem cells (Liu et al., 2015). We find that USP44 expression is highly increased in triple negative, MDA-MB-231 breast cancer cells relative to MCF10-A cells. Importantly, depletion of USP44 markedly impairs the invasiveness of MDA-MB-231 cells and leads to increased global H2Bub1 levels. Consistently, depletion of another N-CoR component, TBL1XR1, known to be highly expressed in breast cancer cells (Kadota et al., 2009; Li et al., 2014), also leads to increased global H2Bub1 levels. Overall, our study demonstrates that USP44 associates with the N-CoR complex to regulate H2Bub1 levels and impacts the invasiveness of breast cancer cells.

## 5.7 Discussion and future directions

The N-CoR complex functions as co-repressor for various transcription factors including nuclear receptors through recruitment of HDACs (Wong et al., 2014). Here we report that USP44 functions as a second enzymatic subunit of the N-CoR complex and that this complex can deubiquitinate histone H2B in vivo and in vitro. Our results indicate that both the deubiquitination of histone H2B by USP44 and deacetylation of histone H3 by HDAC3 contribute to N-CoR mediated transcriptional repression (Figure 25).

### 5.7.1 USP44-NCOR1 complex is a multiple enzymatic subunits containing complex

Several chromatin modifying complexes contain multiple activities, as we describe here for the USP44-N-CoR complex. The SAGA complex, a well-characterized histone modifying complex, contains two enzymes, the histone acetyltransferase Gcn5 and the histone deubiquitinase USP22 (Koutelou et al., 2010). Moreover, the MOF-MSL complex is composed of the MOF histone acetyltransferase and the MSL E3 ubiquitin ligase (Wu et al., 2011). These multiple enzymatic subunits containing complexes reflect how complicated networks of chromatin modifying enzymes function coordinately in transcription regulation (Workman, 2016).

The N-terminal domains of TBL1X and TBL1XR were previously reported to bind histone H2B and H4 (Yoon et al., 2003). Here we found that the C-terminal WD40 repeat domains of TBL1X and TBL1XR1 are required to recruit USP44. Given that USP44 functions as a histone DUB, interaction with TBL1X and TBL1XR1 could help USP44 target its substrate for deubiquitination. However, association with TBL1X and TBL1XR1 is not enough to activate the DUB activity of USP44 in vitro, indicating that additional partners may be required. Future work will determine which other subunits of N-CoR are needed for USP44 activity and the structural basis for its activation.

A previous report of global proteomic analyses identified interacting proteins for 75 human DUBs, including USP44 in whole cell lysates (Sowa et al., 2009). The major USP44 interacting proteins identified were CETN2 and a number of mitochondrial proteins, such as MRPL40, MRPL23 and MRPL53. The USP44-CETN2 complex is known to play an important role in preventing chromosome segregation errors during mitosis (Zhang et al., 2012). The function of USP44 in association with mitochondrial proteins is not yet clear. However, no subunits of the N-CoR complex were identified, which might reflect the use of whole cell extracts rather than nuclear extracts as used in our study. Indeed, none of the mitochondrial proteins identified in the previous study

were found in our MudPIT analyses. Together, these data suggest that USP44 plays multiple roles in different cellular compartments by forming complexes with distinct partners.

Genome-wide ChIP-seq analyses in human cells show that H2Bub1 is generally associated with highly expressed genes, being enriched at 5' beginning of transcribed regions and also broadly distributed throughout gene bodies (Jung et al., 2012; Minsky et al., 2008). Several studies have highlighted the important roles of H2Bub1 in transcriptional elongation (Fleming et al., 2008; Pavri et al., 2006; Zhang and Yu, 2011). However, the role of H2Bub1 at gene promoters is less lucid. It is still an open debate whether relatively low H2Bub1 signals at gene promoters reflect enhanced deubiquitination activity at this region or low ubiquitination of promoter nucleosomes. In yeast, cycles of H2B ubiquitination and deubiquitination are needed for a productive switch from transcription initiation to elongation (Henry et al., 2003). Recent studies indicate a direct link between H2B deubiquitination at promoter regions and decreased transcription in *Drosophila* and mammalian cells (Kessler et al., 2015; Sussman et al., 2013). In addition, in vitro analyses using chemically defined nucleosome arrays containing recombinant H2Bub1 (Fierz et al., 2011) demonstrated that H2Bub1 can disrupt higher-order chromatin architectures, facilitating more open, accessible conformations needed for transcription. Our data indicate that USP44-N-CoR complex likely represses transcription by removing H2Bub1 via USP44 and histone acetylation via HDAC3 at the promoter.

### 5.7.2 USP44-NCOR1 complex is involved in the regulation of breast cancer development

Reduced global H2Bub1 levels have been observed in multiple advanced cancers including breast cancer, lung cancer, colorectal cancer and seminoma (Fuchs and Oren, 2014), raising the possibility that high levels of H2Bub1-specific DUBs could play a causal role in tumor formation or progression. In support of this notion, USP22, a well-known H2Bub1 DUB (Zhang et al., 2008), is highly expressed in various aggressive cancers and is part of an 11 genes “death from cancer signature” that defines tumors with cancer stem cell phenotypes of aggressive growth, metastasis and resistance to therapy (Glinsky, 2006). USP44 was reported to be overexpressed in human T cell leukemias (Zhang et al., 2011). We report here that USP44 is highly expressed in aggressive breast cancer MDA-MB-231 cells, leading to low global H2Bub1 levels and contributing to the invasiveness of these cells. Consistent with these findings, another essential subunit of the N-CoR complex, TBL1XR1, is also highly expressed in advanced breast cancer cells and contributes to their aggressiveness (Li et al., 2014). Although N-CoR complex is well documented as a co-repressor for unliganded nuclear receptors, we were unable to detect an effect of USP44 KD on the transcription of estrogen receptor (ER) target genes in MCF7 cells (data not shown). However, the mRNA levels of USP44 in MCF7 cells are very low (data not shown), as they are in MCF10-A cells (Figure 23A). The USP44-N-CoR complex, then, may function as co-repressor for other types of transcription factors in MDA-MB-231 cells that drive metastatic behavior. We also cannot rule out the possibility that USP44 has non-histone substrates that are important for aggressive cancer phenotypes.

Overall, our results suggest that USP44-N-CoR complex may contribute to the aggressiveness of triple negative breast cancers through regulating the transcription of target genes by modulating the H2Bub1 levels and H3K9/14ac levels at the promoters.

However, due to the lack of ChIP grade antibody for USP44, currently, we are not able to identify these specific target genes of USP44-N-CoR complex. Additional efforts on identifying these target genes likely provide new insights for therapeutic purpose of breast cancer.

## Chapter 6: Discussion

Histones undergo multiple posttranslational modifications, which play important roles in regulating various DNA-templated biological processes including DNA repair, DNA replication, and gene expression (Zhou et al., 2011). H2B monoubiquitination (H2Bub1) is very conserved from yeast to mammals and plays important roles in modulating various genome functions (Smith and Shilatifard, 2010). Dysregulation of H2Bub1 is correlated with multiple serious human diseases including neurodegenerative diseases and cancers (Weake and Workman, 2008).

USP22 of DUBm in SAGA complex is an important H2Bub1 regulator and its DUB activity contributes to crucial roles of SAGA complex in regulating gene expression (Weake et al., 2008). However, USP22 alone is not active, appropriate structural organization of the DUBm is required for activating its DUB activity (Kohler et al., 2010). We demonstrated that ATXN7 polyQ mutant indirectly impairs the DUB activity of USP22 through forming nuclear inclusions to sequester USP22 and other SAGA components away from its targets, further contributing to neurodegenerative disease, SCA7. More importantly, we discovered that co-overexpression of other DUBm subunits significantly promotes the solubility of ATXN7-polyQ mutant and further restores the DUB activity. Given that there is still no known cure for SCA7 disease, our data suggest that therapies designed to prevent aggregation of ATXN7-polyQ mutant should achieve good effect for treating SCA7 and other nuclear inclusions-formed polyQ diseases.

Similar to USP22, USP44 is associated with H2Bub1 regulation and is not active by itself. Several literatures reported that USP44 is involved in various biological processes including DNA damage response, ES differentiation and cancer development (Fuchs et al., 2012; Liu et al., 2015; Mosbech et al., 2013; Stegmeier et al., 2007; Zhang et al., 2012), however, what the other partners required for its DUB activity are and how these

partners may dedicate its roles in these biological processes remains to be known. I discovered here that USP44 functions as an integral subunit of N-CoR complex and contributes to N-CoR-mediated transcriptional repression through deubiquitinating H2Bub1, regulating breast cancer aggressiveness.

Genome-wide analysis by ChIP-seq in human cells shows that H2Bub1 is broadly distributed through the whole gene and associated with highly expressed genes (Jung et al., 2012; Minsky et al., 2008), but this modification is involved in both gene repression and activation (Shema et al., 2008). My data further highlight the importance of H2Bub1 regulation via USP22, which is involved in neurodegenerative disease and cancer, and via USP44, which is associated with breast cancer progression. Despite the fact that both USP22 and USP44 deubiquitinate H2Bub1, they likely regulate distinct target genes by occupying different gene loci to remove H2Bub1. In addition to USP22 and USP44, a number of other USPs are also involved in regulating H2Bub1 levels to modulate different biological processes including USP3, USP27X, USP42, USP49 and USP51. Given that around 95 DUBs exist in human genome, more and more H2Bub1 DUBs, I believe, will be identified. There are at least two ways for these H2Bub1 DUBs to play roles in distinct biological processes. One is that the same USP forms different complexes with different partners like USP44-Centrin2 complex and USP44-N-CoR complex. The other is that different USPs forms different complexes with different partners like USP22-SAGA complex and USP44-N-CoR complex. In this regard, my data indicate that more effort for therapies should be put on specific targeting of USPs in terms of USP-related diseases.

# Chapter 7: Future studies

## 7.1 Identifying the role of Usp22 in SCA7 disease using *Usp22* conditional knock-out mouse

Our published data suggest that impairment of SAGA DUB activity contributes to SCA7 development (Lan et al., 2015). To further dissect the molecular mechanism underlying defective Usp22 DUB activity in the pathogenesis of SCA7, we decided to specifically delete *Usp22* in the Purkinje cells or Bergmann glia using *Usp22* conditional knockout mouse model.

As I mentioned in Chapter 4, we have successfully generated Usp22 conditional knockout mouse model. Two specific Cre mouse lines will be used to study SCA7 disease, Pcp2-Cre line and hGFAP-Cre line. Crossing with Pcp-2-Cre mouse line and hGFAP-Cre mouse line will lead to specific deletion of *Usp22* in Purkinje cells and in Bergmann glia, respectively. The cell bodies of Bergmann glial cells are around Purkinje cells. Both of Purkinje cells and Bergmann glia locate in the cerebellum and are involved in the pathogenesis of SCA7 disease (Custer et al., 2006; Furrer et al., 2011). If we detect the SCA7 related phenotype-Ataxia, which can be examined by several behavior study approaches and histological methods (Chen et al., 2012; Jafar-Nejad et al., 2011), this result will be consistent with our published work, indicating that defective USP22 DUB activity in cerebellum at least contributes to SCA7 development. On the other hand, if SCA7 related phenotypes are not detected in these Usp22 specific null mice, this will indicate that other USPs may compensate for the loss of *Usp22* in the cerebellum. In this regard, we need to generate double or triple USPs specific null mice if other Usps conditional knockout mice are available. Another alternative possibility is that defective Usp22 DUB activity is a resulting rather than a causative effect in SCA7 disease due to the cytotoxicity of polyQ stretch. Consistent with this hypothesis, Adachi et al reported

that transgenic mice with an expanded CAG repeat display polyQ nuclear inclusions and neuronal dysfunction (Adachi et al., 2001). Dissecting the molecular mechanism of SCA7 will help therapeutic design of drugs for targeting impaired DUB activity or polyQ stretch.

### 7.2 Identifying the USP44-N-CoR complex gene targets involved in breast cancer aggressiveness

My data indicate that the USP44-N-CoR complex contributes to the aggressiveness of triple negative breast cancer cells through repressing the transcription of target genes by deubiquitinating H2Bub1 and deacetylating H3K9/14ac at their promoters. What the specific targets of Usp44 are in this context remains to be determined.

To identify the potential target genes of USP44-N-CoR complex, we need to generate a ChIP-grade USP44 antibody for ChIP-seq experiments using MDA-MB-231 cells. Since TBL1XR1 ChIP-grade antibody is available, we also need to do TBL1XR1 ChIP-seq analysis. Comparison of USP44 ChIP-seq and TBL1XR1 ChIP-seq data will show the common targets. In addition, RNA-seq analyses upon USP44 depletion and/or TBL1XR1 depletion in MDA-MB-231 cells will be performed as well. The common target genes with similar transcriptional change will be identified by comparing the USP44 and TBL1XR1 RNA-seq data. The direct target gene list of USP44-N-CoR complex will be identified through combining the ChIP-seq and RNA-seq data. We will validate several of the most confident targets by ChIP-qPCR using USP44, TBL1XR1, HDAC3, H2Bub1 and H3K9/14ac antibodies. To further confirm the potential roles of these targets in the aggressiveness of MDA-MB-231 cells, depletion of these targets followed by invasion assay and other aggressiveness related assays will be performed.

In summary, these work emphasize the importance of H2Bub1 regulation in normal cells. My work also set a good example on dissecting the molecular mechanism of diseases involved in the regulation of chromatin and transcription.

## 8. References


Adachi, H., Kume, A., Li, M., Nakagomi, Y., Niwa, H., Do, J., Sang, C., Kobayashi, Y., Doyu, M., and Sobue, G. (2001). Transgenic mice with an expanded CAG repeat controlled by the human AR promoter show polyglutamine nuclear inclusions and neuronal dysfunction without neuronal cell death. Hum Mol Genet *10*, 1039-1048.

Ansorge, O., Giunti, P., Michalik, A., Van Broeckhoven, C., Harding, B., Wood, N., and Scaravilli, F. (2004). Ataxin-7 aggregation and ubiquitination in infantile SCA7 with 180 CAG repeats. Ann Neurol *56*, 448-452.

Arrasate, M., Mitra, S., Schweitzer, E.S., Segal, M.R., and Finkbeiner, S. (2004). Inclusion body formation reduces levels of mutant huntingtin and the risk of neuronal death. Nature *431*, 805-810.

Atanassov, B.S., and Dent, S.Y. (2011). USP22 regulates cell proliferation by deubiquitinating the transcriptional regulator FBP1. EMBO Rep *12*, 924-930.

Atanassov, B.S., Evrard, Y.A., Multani, A.S., Zhang, Z., Tora, L., Devys, D., Chang, S., and Dent, S.Y. (2009). Gcn5 and SAGA regulate shelterin protein turnover and telomere maintenance. Mol Cell *35*, 352-364.

Atanassov, B.S., Mohan, R.D., Lan, X., Kuang, X., Lu, Y., Lin, K., McIvor, E., Li, W., Zhang, Y., Florens, L.*, et al.* (2016). ATXN7L3 and ENY2 Coordinate Activity of Multiple H2B Deubiquitinases Important for Cellular Proliferation and Tumor Growth. Mol Cell *62*, 558-571.

Barski, J.J., Dethleffsen, K., and Meyer, M. (2000). Cre recombinase expression in cerebellar Purkinje cells. Genesis *28*, 93-98.

Bellamy, T.C. (2006). Interactions between Purkinje neurones and Bergmann glia. Cerebellum *5*, 116-126.

Bhaskara, S., Knutson, S.K., Jiang, G., Chandrasekharan, M.B., Wilson, A.J., Zheng, S., Yenamandra, A., Locke, K., Yuan, J.L., Bonine-Summers, A.R.*, et al.* (2010). Hdac3 is essential for the maintenance of chromatin structure and genome stability. Cancer Cell *18*, 436-447.

Borodovsky, A., Kessler, B.M., Casagrande, R., Overkleeft, H.S., Wilkinson, K.D., and Ploegh, H.L. (2001). A novel active site-directed probe specific for deubiquitylating enzymes reveals proteasome association of USP14. Embo J *20*, 5187-5196.

Briggs, S.D., Xiao, T., Sun, Z.W., Caldwell, J.A., Shabanowitz, J., Hunt, D.F., Allis, C.D., and Strahl, B.D. (2002). Gene silencing: trans-histone regulatory pathway in chromatin. Nature *418*, 498.

Cao, J., and Yan, Q. (2012). Histone ubiquitination and deubiquitination in transcription, DNA damage response, and cancer. Front Oncol *2*, 26.

Carter, R.J., Lione, L.A., Humby, T., Mangiarini, L., Mahal, A., Bates, G.P., Dunnett, S.B., and Morton, A.J. (1999). Characterization of progressive motor deficits in mice transgenic for the human Huntington's disease mutation. J Neurosci *19*, 3248-3257.

Case, A., and Stein, R.L. (2006). Mechanistic studies of ubiquitin C-terminal hydrolase L1. Biochemistry *45*, 2443-2452.

Chan, H.Y., Warrick, J.M., Gray-Board, G.L., Paulson, H.L., and Bonini, N.M. (2000). Mechanisms of chaperone suppression of polyglutamine disease: selectivity, synergy and modulation of protein solubility in Drosophila. Hum Mol Genet *9*, 2811-2820.

Chen, Y.C., Gatchel, J.R., Lewis, R.W., Mao, C.A., Grant, P.A., Zoghbi, H.Y., and Dent, S.Y. (2012). Gcn5 loss-of-function accelerates cerebellar and retinal degeneration in a SCA7 mouse model. Hum Mol Genet *21*, 394-405.

Cheung, Z.H., and Ip, N.Y. (2011). Autophagy deregulation in neurodegenerative diseases - recent advances and future perspectives. J Neurochem *118*, 317-325.

Cohn, M.A., Kee, Y., Haas, W., Gygi, S.P., and D'Andrea, A.D. (2009). UAF1 is a subunit of multiple deubiquitinating enzyme complexes. J Biol Chem *284*, 5343-5351.

Cole, A.J., Clifton-Bligh, R., and Marsh, D.J. (2015). Histone H2B monoubiquitination: roles to play in human malignancy. Endocr Relat Cancer *22*, T19-33.

Cummings, C.J., Mancini, M.A., Antalffy, B., DeFranco, D.B., Orr, H.T., and Zoghbi, H.Y. (1998). Chaperone suppression of aggregation and altered subcellular proteasome localization imply protein misfolding in SCA1. Nat Genet *19*, 148-154.

Custer, S.K., Garden, G.A., Gill, N., Rueb, U., Libby, R.T., Schultz, C., Guyenet, S.J., Deller, T., Westrum, L.E., Sopher, B.L.*, et al.* (2006). Bergmann glia expression of polyglutamine-expanded ataxin-7 produces neurodegeneration by impairing glutamate transport. Nat Neurosci *9*, 1302-1311.

David, G., Durr, A., Stevanin, G., Cancel, G., Abbas, N., Benomar, A., Belal, S., Lebre, A.S., Abada-Bendib, M., Grid, D.*, et al.* (1998). Molecular and clinical correlations in autosomal dominant cerebellar ataxia with progressive macular dystrophy (SCA7). Hum Mol Genet *7*, 165-170.

Davies, S.W., Beardsall, K., Turmaine, M., DiFiglia, M., Aronin, N., and Bates, G.P. (1998). Are neuronal intranuclear inclusions the common neuropathology of triplet-repeat disorders with polyglutamine-repeat expansions? Lancet *351*, 131-133.

Fierz, B., Chatterjee, C., McGinty, R.K., Bar-Dagan, M., Raleigh, D.P., and Muir, T.W. (2011). Histone H2B ubiquitylation disrupts local and higher-order chromatin compaction. Nat Chem Biol *7*, 113-119.

Fleming, A.B., Kao, C.F., Hillyer, C., Pikaart, M., and Osley, M.A. (2008). H2B ubiquitylation plays a role in nucleosome dynamics during transcription elongation. Mol Cell *31*, 57-66.

Fuchs, G., and Oren, M. (2014). Writing and reading H2B monoubiquitylation. Biochim Biophys Acta *1839*, 694-701.

Fuchs, G., Shema, E., Vesterman, R., Kotler, E., Wolchinsky, Z., Wilder, S., Golomb, L., Pribluda, A., Zhang, F., Haj-Yahya, M.*, et al.* (2012). RNF20 and USP44 regulate stem cell differentiation by modulating H2B monoubiquitylation. Mol Cell *46*, 662-673.

Furrer, S.A., Mohanachandran, M.S., Waldherr, S.M., Chang, C., Damian, V.A., Sopher, B.L., Garden, G.A., and La Spada, A.R. (2011). Spinocerebellar ataxia type 7 cerebellar disease requires the coordinated action of mutant ataxin-7 in neurons and glia, and displays non-cell-autonomous bergmann glia degeneration. J Neurosci *31*, 16269-16278.

Gao, Z., Lee, P., Stafford, J.M., von Schimmelmann, M., Schaefer, A., and Reinberg, D. (2014). An AUTS2-Polycomb complex activates gene expression in the CNS. Nature *516*, 349-354.

Gao, Z., Zhang, J., Bonasio, R., Strino, F., Sawai, A., Parisi, F., Kluger, Y., and Reinberg, D. (2012). PCGF homologs, CBX proteins, and RYBP define functionally distinct PRC1 family complexes. Mol Cell *45*, 344-356.

Garden, G.A., Libby, R.T., Fu, Y.H., Kinoshita, Y., Huang, J., Possin, D.E., Smith, A.C., Martinez, R.A., Fine, G.C., Grote, S.K.*, et al.* (2002). Polyglutamine-expanded ataxin-7 promotes non-cell-autonomous purkinje cell degeneration and displays proteolytic cleavage in ataxic transgenic mice. J Neurosci *22*, 4897-4905.

Glinsky, G.V. (2006). Genomic models of metastatic cancer: functional analysis of death-from-cancer signature genes reveals aneuploid, anoikis-resistant, metastasis-enabling phenotype with altered cell cycle control and activated Polycomb Group (PcG) protein chromatin silencing pathway. Cell Cycle *5*, 1208-1216.

Hartl, F.U., and Hayer-Hartl, M. (2002). Molecular chaperones in the cytosol: from nascent chain to folded protein. Science *295*, 1852-1858.

Helmlinger, D., Hardy, S., Abou-Sleymane, G., Eberlin, A., Bowman, A.B., Gansmuller, A., Picaud, S., Zoghbi, H.Y., Trottier, Y., Tora, L.*, et al.* (2006). Glutamine-expanded ataxin-7 alters TFTC/STAGA recruitment and chromatin structure leading to photoreceptor dysfunction. PLoS Biol *4*, e67.

Helmlinger, D., Hardy, S., Sasorith, S., Klein, F., Robert, F., Weber, C., Miguet, L., Potier, N., Van-Dorsselaer, A., Wurtz, J.M.*, et al.* (2004). Ataxin-7 is a subunit of GCN5 histone acetyltransferase-containing complexes. Hum Mol Genet *13*, 1257-1265.

Henry, K.W., Wyce, A., Lo, W.S., Duggan, L.J., Emre, N.C., Kao, C.F., Pillus, L., Shilatifard, A., Osley, M.A., and Berger, S.L. (2003). Transcriptional activation via sequential histone H2B ubiquitylation and deubiquitylation, mediated by SAGA-associated Ubp8. Genes Dev *17*, 2648-2663.

Jafar-Nejad, P., Ward, C.S., Richman, R., Orr, H.T., and Zoghbi, H.Y. (2011). Regional rescue of spinocerebellar ataxia type 1 phenotypes by 14-3-3epsilon haploinsufficiency

in mice underscores complex pathogenicity in neurodegeneration. Proc Natl Acad Sci U S A *108*, 2142-2147.

Janer, A., Werner, A., Takahashi-Fujigasaki, J., Daret, A., Fujigasaki, H., Takada, K., Duyckaerts, C., Brice, A., Dejean, A., and Sittler, A. (2010). SUMOylation attenuates the aggregation propensity and cellular toxicity of the polyglutamine expanded ataxin-7. Hum Mol Genet *19*, 181-195.

Johansson, J., Forsgren, L., Sandgren, O., Brice, A., Holmgren, G., and Holmberg, M. (1998). Expanded CAG repeats in Swedish spinocerebellar ataxia type 7 (SCA7) patients: effect of CAG repeat length on the clinical manifestation. Hum Mol Genet *7*, 171-176.

Jung, I., Kim, S.K., Kim, M., Han, Y.M., Kim, Y.S., Kim, D., and Lee, D. (2012). H2B monoubiquitylation is a 5'-enriched active transcription mark and correlates with exon-intron structure in human cells. Genome Res *22*, 1026-1035.

Kadota, M., Sato, M., Duncan, B., Ooshima, A., Yang, H.H., Diaz-Meyer, N., Gere, S., Kageyama, S., Fukuoka, J., Nagata, T*., et al.* (2009). Identification of novel gene amplifications in breast cancer and coexistence of gene amplification with an activating mutation of PIK3CA. Cancer Res *69*, 7357-7365.

Karpiuk, O., Najafova, Z., Kramer, F., Hennion, M., Galonska, C., Konig, A., Snaidero, N., Vogel, T., Shchebet, A., Begus-Nahrmann, Y*., et al.* (2012). The histone H2B monoubiquitination regulatory pathway is required for differentiation of multipotent stem cells. Mol Cell *46*, 705-713.

Kessler, R., Tisserand, J., Font-Burgada, J., Reina, O., Coch, L., Attolini, C.S., Garcia-Bassets, I., and Azorin, F. (2015). dDsk2 regulates H2Bub1 and RNA polymerase II pausing at dHP1c complex target genes. Nat Commun *6*, 7049.

Kim, J., Hake, S.B., and Roeder, R.G. (2005). The human homolog of yeast BRE1 functions as a transcriptional coactivator through direct activator interactions. Mol Cell *20*, 759-770.

Kohler, A., Schneider, M., Cabal, G.G., Nehrbass, U., and Hurt, E. (2008). Yeast Ataxin-7 links histone deubiquitination with gene gating and mRNA export. Nat Cell Biol *10*, 707-715.

Kohler, A., Zimmerman, E., Schneider, M., Hurt, E., and Zheng, N. (2010). Structural basis for assembly and activation of the heterotetrameric SAGA histone H2B deubiquitinase module. Cell *141*, 606-617.

Koutelou, E., Hirsch, C.L., and Dent, S.Y. (2010). Multiple faces of the SAGA complex. Curr Opin Cell Biol *22*, 374-382.

Kouzarides, T. (2007). Chromatin modifications and their function. Cell *128*, 693-705.

Kuzmichev, A., Nishioka, K., Erdjument-Bromage, H., Tempst, P., and Reinberg, D. (2002). Histone methyltransferase activity associated with a human multiprotein complex containing the Enhancer of Zeste protein. Genes Dev *16*, 2893-2905.

Lan, X., Koutelou, E., Schibler, A.C., Chen, Y.C., Grant, P.A., and Dent, S.Y. (2015). Poly(Q) Expansions in ATXN7 Affect Solubility but Not Activity of the SAGA Deubiquitinating Module. Mol Cell Biol *35*, 1777-1787.

Lang, G., Bonnet, J., Umlauf, D., Karmodiya, K., Koffler, J., Stierle, M., Devys, D., and Tora, L. (2011). The tightly controlled deubiquitination activity of the human SAGA complex differentially modifies distinct gene regulatory elements. Mol Cell Biol *31*, 3734-3744.

Lebre, A.S., and Brice, A. (2003). Spinocerebellar ataxia 7 (SCA7). Cytogenet Genome Res *100*, 154-163.

Lee, K.K., Florens, L., Swanson, S.K., Washburn, M.P., and Workman, J.L. (2005). The deubiquitylation activity of Ubp8 is dependent upon Sgf11 and its association with the SAGA complex. Mol Cell Biol *25*, 1173-1182.

Li, X., Liang, W., Liu, J., Lin, C., Wu, S., Song, L., and Yuan, Z. (2014). Transducin (beta)-like 1 X-linked receptor 1 promotes proliferation and tumorigenicity in human breast cancer via activation of beta-catenin signaling. Breast Cancer Res *16*, 465.

Lin, Z., Yang, H., Kong, Q., Li, J., Lee, S.M., Gao, B., Dong, H., Wei, J., Song, J., Zhang, D.D.*, et al.* (2012). USP22 antagonizes p53 transcriptional activation by deubiquitinating Sirt1 to suppress cell apoptosis and is required for mouse embryonic development. Mol Cell *46*, 484-494.

Liu, T., Sun, B., Zhao, X., Li, Y., Liu, Y., Yao, Z., Gu, Q., Dong, X., Shao, B., Lin, X.*, et al.* (2015). USP44+ Cancer Stem Cell Subclones Contribute to Breast Cancer Aggressiveness by Promoting Vasculogenic Mimicry. Mol Cancer Ther *14*, 2121-2131.

McCampbell, A., Taylor, J.P., Taye, A.A., Robitschek, J., Li, M., Walcott, J., Merry, D., Chai, Y., Paulson, H., Sobue, G.*, et al.* (2000). CREB-binding protein sequestration by expanded polyglutamine. Hum Mol Genet *9*, 2197-2202.

McCullough, S.D., Xu, X., Dent, S.Y., Bekiranov, S., Roeder, R.G., and Grant, P.A. (2012). Reelin is a target of polyglutamine expanded ataxin-7 in human spinocerebellar ataxia type 7 (SCA7) astrocytes. Proc Natl Acad Sci U S A *109*, 21319-21324.

McMahon, S.J., Pray-Grant, M.G., Schieltz, D., Yates, J.R., 3rd, and Grant, P.A. (2005). Polyglutamine-expanded spinocerebellar ataxia-7 protein disrupts normal SAGA and SLIK histone acetyltransferase activity. Proc Natl Acad Sci U S A *102*, 8478-8482.

Mendez, J., and Stillman, B. (2000). Chromatin association of human origin recognition complex, cdc6, and minichromosome maintenance proteins during the cell cycle: assembly of prereplication complexes in late mitosis. Mol Cell Biol *20*, 8602-8612.

Minsky, N., Shema, E., Field, Y., Schuster, M., Segal, E., and Oren, M. (2008). Monoubiquitinated H2B is associated with the transcribed region of highly expressed genes in human cells. Nat Cell Biol *10*, 483-488.

Mohan, R.D., Dialynas, G., Weake, V.M., Liu, J., Martin-Brown, S., Florens, L., Washburn, M.P., Workman, J.L., and Abmayr, S.M. (2014). Loss of Drosophila Ataxin-7, a SAGA subunit, reduces H2B ubiquitination and leads to neural and retinal degeneration. Genes Dev *28*, 259-272.

Mosbech, A., Lukas, C., Bekker-Jensen, S., and Mailand, N. (2013). The deubiquitylating enzyme USP44 counteracts the DNA double-strand break response mediated by the RNF8 and RNF168 ubiquitin ligases. J Biol Chem *288*, 16579-16587.

Moyal, L., Lerenthal, Y., Gana-Weisz, M., Mass, G., So, S., Wang, S.Y., Eppink, B., Chung, Y.M., Shalev, G., Shema, E.*, et al.* (2011). Requirement of ATM-dependent monoubiquitylation of histone H2B for timely repair of DNA double-strand breaks. Mol Cell *41*, 529-542.

Nakamura, Y., Tagawa, K., Oka, T., Sasabe, T., Ito, H., Shiwaku, H., La Spada, A.R., and Okazawa, H. (2012). Ataxin-7 associates with microtubules and stabilizes the cytoskeletal network. Hum Mol Genet *21*, 1099-1110.

Ng, H.H., Xu, R.M., Zhang, Y., and Struhl, K. (2002). Ubiquitination of histone H2B by Rad6 is required for efficient Dot1-mediated methylation of histone H3 lysine 79. J Biol Chem *277*, 34655-34657.

Nicassio, F., Corrado, N., Vissers, J.H., Areces, L.B., Bergink, S., Marteijn, J.A., Geverts, B., Houtsmuller, A.B., Vermeulen, W., Di Fiore, P.P.*, et al.* (2007). Human USP3 is a chromatin modifier required for S phase progression and genome stability. Curr Biol *17*, 1972-1977.

Nijman, S.M., Luna-Vargas, M.P., Velds, A., Brummelkamp, T.R., Dirac, A.M., Sixma, T.K., and Bernards, R. (2005). A genomic and functional inventory of deubiquitinating enzymes. Cell *123*, 773-786.

Nishi, R., Okuda, Y., Watanabe, E., Mori, T., Iwai, S., Masutani, C., Sugasawa, K., and Hanaoka, F. (2005). Centrin 2 stimulates nucleotide excision repair by interacting with xeroderma pigmentosum group C protein. Mol Cell Biol *25*, 5664-5674.

Nucifora, F.C., Jr., Sasaki, M., Peters, M.F., Huang, H., Cooper, J.K., Yamada, M., Takahashi, H., Tsuji, S., Troncoso, J., Dawson, V.L.*, et al.* (2001). Interference by huntingtin and atrophin-1 with cbp-mediated transcription leading to cellular toxicity. Science *291*, 2423-2428.

Oberoi, J., Fairall, L., Watson, P.J., Yang, J.C., Czimmerer, Z., Kampmann, T., Goult, B.T., Greenwood, J.A., Gooch, J.T., Kallenberger, B.C.*, et al.* (2011). Structural basis for the assembly of the SMRT/NCoR core transcriptional repression machinery. Nat Struct Mol Biol *18*, 177-184.

Palhan, V.B., Chen, S., Peng, G.H., Tjernberg, A., Gamper, A.M., Fan, Y., Chait, B.T., La Spada, A.R., and Roeder, R.G. (2005). Polyglutamine-expanded ataxin-7 inhibits STAGA histone acetyltransferase activity to produce retinal degeneration. Proc Natl Acad Sci U S A *102*, 8472-8477.

Park, S.H., Kukushkin, Y., Gupta, R., Chen, T., Konagai, A., Hipp, M.S., Hayer-Hartl, M., and Hartl, F.U. (2013). PolyQ proteins interfere with nuclear degradation of cytosolic proteins by sequestering the Sis1p chaperone. Cell *154*, 134-145.

Pavri, R., Zhu, B., Li, G., Trojer, P., Mandal, S., Shilatifard, A., and Reinberg, D. (2006). Histone H2B monoubiquitination functions cooperatively with FACT to regulate elongation by RNA polymerase II. Cell *125*, 703-717.

Perissi, V., Aggarwal, A., Glass, C.K., Rose, D.W., and Rosenfeld, M.G. (2004). A corepressor/coactivator exchange complex required for transcriptional activation by nuclear receptors and other regulated transcription factors. Cell *116*, 511-526.

Pirngruber, J., Shchebet, A., Schreiber, L., Shema, E., Minsky, N., Chapman, R.D., Eick, D., Aylon, Y., Oren, M., and Johnsen, S.A. (2009). CDK9 directs H2B monoubiquitination and controls replication-dependent histone mRNA 3'-end processing. EMBO Rep *10*, 894-900.

Plass, C., Pfister, S.M., Lindroth, A.M., Bogatyrova, O., Claus, R., and Lichter, P. (2013). Mutations in regulators of the epigenome and their connections to global chromatin patterns in cancer. Nat Rev Genet *14*, 765-780.

Samara, N.L., Datta, A.B., Berndsen, C.E., Zhang, X., Yao, T., Cohen, R.E., and Wolberger, C. (2010). Structural insights into the assembly and function of the SAGA deubiquitinating module. Science *328*, 1025-1029.

Seidel, K., Meister, M., Dugbartey, G.J., Zijlstra, M.P., Vinet, J., Brunt, E.R., van Leeuwen, F.W., Rub, U., Kampinga, H.H., and den Dunnen, W.F. (2012). Cellular protein quality control and the evolution of aggregates in spinocerebellar ataxia type 3 (SCA3). Neuropathol Appl Neurobiol *38*, 548-558.

Shema, E., Tirosh, I., Aylon, Y., Huang, J., Ye, C., Moskovits, N., Raver-Shapira, N., Minsky, N., Pirngruber, J., Tarcic, G.*, et al.* (2008). The histone H2B-specific ubiquitin ligase RNF20/hBRE1 acts as a putative tumor suppressor through selective regulation of gene expression. Genes Dev *22*, 2664-2676.

Smith, E., and Shilatifard, A. (2010). The chromatin signaling pathway: diverse mechanisms of recruitment of histone-modifying enzymes and varied biological outcomes. Mol Cell *40*, 689-701.

Sowa, M.E., Bennett, E.J., Gygi, S.P., and Harper, J.W. (2009). Defining the human deubiquitinating enzyme interaction landscape. Cell *138*, 389-403.

Stegmeier, F., Rape, M., Draviam, V.M., Nalepa, G., Sowa, M.E., Ang, X.L., McDonald, E.R., 3rd, Li, M.Z., Hannon, G.J., Sorger, P.K.*, et al.* (2007). Anaphase initiation is regulated by antagonistic ubiquitination and deubiquitination activities. Nature *446*, 876-881.

Sun, Z.W., and Allis, C.D. (2002). Ubiquitination of histone H2B regulates H3 methylation and gene silencing in yeast. Nature *418*, 104-108.

Sussman, R.T., Stanek, T.J., Esteso, P., Gearhart, J.D., Knudsen, K.E., and McMahon, S.B. (2013). The epigenetic modifier ubiquitin-specific protease 22 (USP22) regulates embryonic stem cell differentiation via transcriptional repression of sex-determining region Y-box 2 (SOX2). J Biol Chem *288*, 24234-24246.

Takahashi, T., Kikuchi, S., Katada, S., Nagai, Y., Nishizawa, M., and Onodera, O. (2008). Soluble polyglutamine oligomers formed prior to inclusion body formation are cytotoxic. Hum Mol Genet *17*, 345-356.

Tan, M., Luo, H., Lee, S., Jin, F., Yang, J.S., Montellier, E., Buchou, T., Cheng, Z., Rousseaux, S., Rajagopal, N.*, et al.* (2011). Identification of 67 histone marks and histone lysine crotonylation as a new type of histone modification. Cell *146*, 1016-1028.

Todd, T.W., and Lim, J. (2013). Aggregation formation in the polyglutamine diseases: protection at a cost? Mol Cells *36*, 185-194.

Trujillo, K.M., and Osley, M.A. (2012). A role for H2B ubiquitylation in DNA replication. Mol Cell *48*, 734-746.

Vaquero, A., Scher, M., Lee, D., Erdjument-Bromage, H., Tempst, P., and Reinberg, D. (2004). Human SirT1 interacts with histone H1 and promotes formation of facultative heterochromatin. Mol Cell *16*, 93-105.

Villamil, M.A., Liang, Q., and Zhuang, Z. (2013). The WD40-repeat protein-containing deubiquitinase complex: catalysis, regulation, and potential for therapeutic intervention. Cell Biochem Biophys *67*, 111-126.

Weake, V.M., Lee, K.K., Guelman, S., Lin, C.H., Seidel, C., Abmayr, S.M., and Workman, J.L. (2008). SAGA-mediated H2B deubiquitination controls the development of neuronal connectivity in the Drosophila visual system. Embo J *27*, 394-405.

Weake, V.M., and Workman, J.L. (2008). Histone ubiquitination: triggering gene activity. Mol Cell *29*, 653-663.

Wetzel, R. (2012). Physical chemistry of polyglutamine: intriguing tales of a monotonous sequence. J Mol Biol *421*, 466-490.

Wong, E., and Cuervo, A.M. (2010a). Autophagy gone awry in neurodegenerative diseases. Nat Neurosci *13*, 805-811.

Wong, E., and Cuervo, A.M. (2010b). Integration of clearance mechanisms: the proteasome and autophagy. Cold Spring Harb Perspect Biol *2*, a006734.

Wong, M.M., Guo, C., and Zhang, J. (2014). Nuclear receptor corepressor complexes in cancer: mechanism, function and regulation. Am J Clin Exp Urol *2*, 169-187.

Workman, J.L. (2016). CHROMATIN. It takes teamwork to modify chromatin. Science *351*, 667.

Wu, L., Zee, B.M., Wang, Y., Garcia, B.A., and Dou, Y. (2011). The RING finger protein MSL2 in the MOF complex is an E3 ubiquitin ligase for H2B K34 and is involved in crosstalk with H3 K4 and K79 methylation. Mol Cell *43*, 132-144.

Xiao, T., Kao, C.F., Krogan, N.J., Sun, Z.W., Greenblatt, J.F., Osley, M.A., and Strahl, B.D. (2005). Histone H2B ubiquitylation is associated with elongating RNA polymerase II. Mol Cell Biol *25*, 637-651.

Yang, W., Dunlap, J.R., Andrews, R.B., and Wetzel, R. (2002). Aggregated polyglutamine peptides delivered to nuclei are toxic to mammalian cells. Hum Mol Genet *11*, 2905-2917.

Yao, T., Song, L., Jin, J., Cai, Y., Takahashi, H., Swanson, S.K., Washburn, M.P., Florens, L., Conaway, R.C., Cohen, R.E.*, et al.* (2008). Distinct modes of regulation of the Uch37 deubiquitinating enzyme in the proteasome and in the Ino80 chromatin-remodeling complex. Mol Cell *31*, 909-917.

Yao, T., Song, L., Xu, W., DeMartino, G.N., Florens, L., Swanson, S.K., Washburn, M.P., Conaway, R.C., Conaway, J.W., and Cohen, R.E. (2006). Proteasome recruitment and activation of the Uch37 deubiquitinating enzyme by Adrm1. Nat Cell Biol *8*, 994-1002.

Yin, J., Schoeffler, A.J., Wickliffe, K., Newton, K., Starovasnik, M.A., Dueber, E.C., and Harris, S.F. (2015). Structural Insights into WD-Repeat 48 Activation of Ubiquitin-Specific Protease 46. Structure *23*, 2043-2054.

Yoo, S.Y., Pennesi, M.E., Weeber, E.J., Xu, B., Atkinson, R., Chen, S., Armstrong, D.L., Wu, S.M., Sweatt, J.D., and Zoghbi, H.Y. (2003). SCA7 knockin mice model human SCA7 and reveal gradual accumulation of mutant ataxin-7 in neurons and abnormalities in short-term plasticity. Neuron *37*, 383-401.

Yoon, H.G., Chan, D.W., Huang, Z.Q., Li, J., Fondell, J.D., Qin, J., and Wong, J. (2003). Purification and functional characterization of the human N-CoR complex: the roles of HDAC3, TBL1 and TBLR1. Embo J *22*, 1336-1346.

Yu, X., Munoz-Alarcon, A., Ajayi, A., Webling, K.E., Steinhof, A., Langel, U., and Strom, A.L. (2013). Inhibition of autophagy via p53-mediated disruption of ULK1 in a SCA7 polyglutamine disease model. J Mol Neurosci *50*, 586-599.

Yvert, G., Lindenberg, K.S., Devys, D., Helmlinger, D., Landwehrmeyer, G.B., and Mandel, J.L. (2001). SCA7 mouse models show selective stabilization of mutant ataxin-7 and similar cellular responses in different neuronal cell types. Hum Mol Genet *10*, 1679-1692.

Zhang, F., and Yu, X. (2011). WAC, a functional partner of RNF20/40, regulates histone H2B ubiquitination and gene transcription. Mol Cell *41*, 384-397.

Zhang, X.Y., Varthi, M., Sykes, S.M., Phillips, C., Warzecha, C., Zhu, W., Wyce, A., Thorne, A.W., Berger, S.L., and McMahon, S.B. (2008). The putative cancer stem cell marker USP22 is a subunit of the human SAGA complex required for activated transcription and cell-cycle progression. Mol Cell *29*, 102-111.

Zhang, Y., Foreman, O., Wigle, D.A., Kosari, F., Vasmatzis, G., Salisbury, J.L., van Deursen, J., and Galardy, P.J. (2012). USP44 regulates centrosome positioning to prevent aneuploidy and suppress tumorigenesis. J Clin Invest *122*, 4362-4374.

Zhang, Y., van Deursen, J., and Galardy, P.J. (2011). Overexpression of ubiquitin specific protease 44 (USP44) induces chromosomal instability and is frequently observed in human T-cell leukemia. PLoS One *6*, e23389.

Zhang, Z., Jones, A., Joo, H.Y., Zhou, D., Cao, Y., Chen, S., Erdjument-Bromage, H., Renfrow, M., He, H., Tempst, P.*, et al.* (2013). USP49 deubiquitinates histone H2B and regulates cotranscriptional pre-mRNA splicing. Genes Dev *27*, 1581-1595.

Zhao, Y., Lang, G., Ito, S., Bonnet, J., Metzger, E., Sawatsubashi, S., Suzuki, E., Le Guezennec, X., Stunnenberg, H.G., Krasnov, A.*, et al.* (2008). A TFTC/STAGA module mediates histone H2A and H2B deubiquitination, coactivates nuclear receptors, and counteracts heterochromatin silencing. Mol Cell *29*, 92-101.

Zhou, V.W., Goren, A., and Bernstein, B.E. (2011). Charting histone modifications and the functional organization of mammalian genomes. Nat Rev Genet *12*, 7-18.

Zhuo, L., Theis, M., Alvarez-Maya, I., Brenner, M., Willecke, K., and Messing, A. (2001). hGFAP-cre transgenic mice for manipulation of glial and neuronal function in vivo. Genesis *31*, 85-94.

## 9. Vita

Xianjiang Lan was born in Nankang, Jiangxi, China on September 19, 1986, the son of Xiting Lan and Xiaolan Chen. He attended the South Central University of Nationality, where he obtained his Bachelors of Science in Biotechnology in 2008, Wuhan, Hubei, China. Then he attended the Sun-Yat Sen University, where he obtained his Masters of Science in Genetics in 2011, Guangdong, Guangzhou, China. In August of 2011, he joined Graduate School of Biomedical Sciences at The University of Texas M.D. Anderson Cancer Center, Houston, Texas, United States.